Dissertation

submitted to the

combined Faculties for Natural Sciences and Mathematics

of the Ruperto Carola University Heidelberg, Germany

for the degree of

Doctor of Natural Sciences

presented by

M.Sc. Thomas Johannes Roxlau

born in: Salzkotten, Germany

Day of oral examination: 08.07.2019

Investigation of the lipid environment of the mammalian transamidase complex

Referees:

Prof. Dr. Britta Brügger
Prof. Dr. Sabine Strahl

Declaration of Authorship

I hereby declare that I have authored this thesis independently, that I have not used other than the declared sources/resources, and that I have explicitly marked all material which has been quoted either literally or by content from the used sources. According to my knowledge, the content or parts of this thesis have not been presented to any other examination authority and have not been published.

Heidelberg, 26.02.2019 .....

Contents

1 Acknowledgments

Herewith I want to acknowledge the people without this thesis would not have been possible.

I want to express my gratitude to my wife **Elsa** and our beloved son **Joschuha**. Without the two of you, this would have never been possible. Thank you for the mental support, the encouragement and for just being there when needed. Furthermore, I want to thank my family for the support I received up to this point.

I thank all of the members of the Brügger group and especially

Prof. Dr. Britta Brügger for the chance I was given after my return from Sweden. Thank you for all of the support you have given me during my time in your lab. Thank you for the correction of my thesis and for being understandable with regards to the worries and needs of a young father.

Prof. Dr. Sabine Strahl and **Prof. Dr. Thomas Söllner** for being members of my thesis advisory committee and for providing valuable input during my doctoral work.

Dr. Rainer Beck and **Dr. Mathias Gerl** for the helpful and encouraging discussions, sharing of laboratory tips and tricks and help with some experiments. Thank you Rainer for your help with the CNBr-beads and the Äkta.

Markus Kurth, for the helpful discussions about cloning and for showing me the surface biotinylation assay. Thank you for sharing worries with us at the 2016 christmas retreat. But especial for being a person valuing my artistic side.

Hannah Olschowski, nee Wiedemann, for helping me with the click-reactions and the SMA experiments. And especially for having an open ear, being a good listener and a good friend. Without you, the time in the lab would have been way less entertaining.

Laura-Christin Förster, for the short western blot crash course and your knowledge about cloning. And for reminding me when my birthday is.

Daniela Ostkotte, for all your help in the click-experiments and the refreshing talks about sadly not existent animal species (they are cute though).

Alexia Herrmann, for having an open ear towards problems with experimental questions. For sharing cell culture freezing protocols, your chemically competent cells and for taking care of the cell culture facilities. And of course for the every day talk about everything.

Iris Leibrecht, **Christian Lüchtenborg**, **Timo Sachsenheimer** and **Katharina Wozny** for the help with lipid extractions, MS measurements of the SMA-extraction, refreshing talks about everything not lab related and especially to Katharina for all of the football discussions.

Dr. Doris Höglinger, your advice and support was very valuable for me during the inhibitor experiments.

Linda Boelsen and **Andrea Zuber** for all their encouragement, daily conversations and the astonish work that keeps the whole BZH running.

Ingeborg Reckmann for teaching me about ultracentrifuge maintenance and acknowledging the beautiful pronunciation of east-westphalians.

And last, but not the least important ones: **Martina Galvan**, **Sandra Martini** and **Rolf Lutz** at HBIGS for the all the help.

2 Summary/Zusammenfassung

2.1 Summary

The glycosylphosphatidylinositol (GPI) anchor is a lipid moiety attached to over 150 human proteins and plays a crucial role in cell surface display at the plasma membrane. The transamidase complex, consisting of the subunits PIGK/S/T/U and GPAA1, is localised to the endoplasmic reticulum (ER) and is responsible for attachment of the GPI-anchor to receiving proteins. Previously, interactions between the transamidase complex subunit GPAA1 and a sphingolipid have been shown. The aim of this thesis was to establish an experimental setup to analyse protein lipid interactions of the transamidase complex.
These interactions were assessed via in-gel fluorescence and western blot quantification through click chemistry with bifunctional sphingolipids combined with transient expression of transamidase subunits. Thin layer chromatography was used to verify the metabolic status of exogenously added photoactivatable and clickable sphingosine (pacSph) at given time points. Results confirmed the previous reported interaction of GPAA1. The validity of this outcome was limited to GPAA1 only due to uncertainty with regards to the transient expression, such as affecting the stoichiometry of the transamidase complex and mislocalisation of the transiently overexpressed GPAA1. To circumvent these limitations, CRISPR/Cas9-based gene editing was performed to insert a C-terminal tag in the genomic region of GPAA1. This allowed to establish a cellular model to study sphingolipid and cholesterol interactions with the endogenous transamidase complex. Gene edited tagging of GPAA1 did not interfere with synthesis and trafficking of GPI-anchor proteins to the cell surface. The analysis of the composition of the transamidase complex in this cell line by co-immunoprecipitation showed only PIGK/T/S to interact with GPAA1, but not PIGU. When styrene maleic anhydride (SMA) co-polymer was used to extract the transamidase complex and its native lipid environment, even PIGU was detected, suggesting that PIGU might be only loosely attached to the transamidase complex. Furthermore, first studies on mass spectrometric analysis of lipids extracted from an SMA-immunoprecipitation suggested that this approach allows to determine lipids in direct proximity of the transamaidase complex. Finally, GPAA1-pacSph metabolite interaction could be inhibited through the ceramide synthase inhibitor FB1, while the glucosylceramide synthase inhibitor PPMP did not interfere with the interaction. This suggested that ceramide or a metabolite upstream of this lipid is the interaction partner of GPAA1.
In summary, the established cellular model verified previously published results in an endogenous setting. For the future, this model lays the foundation for quantitative determination of the lipid environment of the transamidase complex. Furthermore, this system might also provide structural information via single particle cryo-electron microscopy of affinity purified GPAA1 complexes.

2.2 Zusammenfassung

Der Glycosylphosphatidylinositol (GPI)-Anker ist eine Lipidmodifikation, welche an über 150 verschiedenen menschlichen Proteinen gefunden wurde und eine wichtige Rolle in der Lokalisation von Oberflächenproteinen an der Plasmamembran spielt. Der Transamidasekomplex, bestehend aus den Untereinheiten PIGK/S/T/U und GPAA1, befindet sich im Endoplasmatischen Retikulum (ER) und ist verantwortlich für das Anfügen des GPI-Ankers an entsprechende Proteine. Das Ziel dieser Arbeit war die Entwicklung und Etablierung eines Versuchsaufbaues zur Analyse von Protein-Lipid-Interaktionen des heteropentameren Transamidasekomplexes.
Basierend auf photoaktivier- und kreuzvernetzbaren Sphingolipiden und transienter Expression von Transamidasekomplexuntereinheiten wurde ein Protokoll zur Untersuchung der Sphingolipidinteraktionen des Komplexes etabliert. Dünnschichtchromatographie wurde eingesetzt um die Verstoffwechselung des exogen hinzugefügten bifunktionalen Sphingosins (pacSph) zu verfolgen. Die Ergebnisse bestätigten bereits vorhandene Ergebnisse zur Sphingolipid-Interaktion von GPAA1. Durch die transiente Expression wurden jedoch eine Beeinflussung der Stöchiometrie des Transamidasekomplexes und Fehllokalisation von GPAA1 beobachtet, welche die Aussagekraft der Ergebnisse mindert. Um diese Limitierungen zu überkommen, wurde eine CRISPR/Cas9 Geneditierung im genomischen Lokus von GPAA1 mit dem Ziel der Insertion eines C-terminalen Tags durchgeführt. Dies führte zur Generierung einer Zelllinie, welche geeignet ist Interaktionen von Sphingolipiden und Cholesterin mit dem Transamidasekomplex zu studieren. Nach Geneditierung wurde keine Beeinflussung der Synthese oder des Transportes von GPI-Anker-Proteinen an die Zelloberfläche festgestellt. Bei der Analyse der Komposition des Transamidasekomplexes durch Co-Immunpräzipitation mit GPAA1 konnten nur PIGK/T/S nachgewiesen werden, während PIGU nicht detektierbar war. PIGU konnte jedoch nachgewiesen werden, wenn mit Styrol-Maleinsäureanhydrid (SMA)-Copolymer der Transamidasekompex in seiner nativen Lipidumgebung extrahiert wurde. Dies deutet auf eine eher transiente Assoziation von PIGU mit dem Transamidasekomplex hin. Weiterhin konnten bei einer massenspektrometrischen Analyse einer SMA-Immunpräzipitation Lipide detektiert werden, welches die Möglichkeit der quantitativen Analyse der nativen Lipidumgebung des Transamidasekomplexes anhand dieser Versuchsanordnung aufzeigt. Schlussendlich konnte die GPAA1-pacSph Interaktion durch die pharmakologische Hemmung der Ceramid-Synthase gestört werden, während ein Inhibierung der Glucosylceramid-Synthase keine Auswirkungen hatte. Dies ist ein Indiz dafür, dass Ceramid oder ein im Biosyntheseweg dem Ceramid nachgeschalteter Metabolit den Interaktionspartner von GPAA1 stellt.
Zusammenfassend konnten in dieser Arbeit mit dem neu etablierten Zellmodel bereits über einen alternativen Ansatz gewonnene Daten bestätigt werden. Darüber hinaus wurden die Grundlagen geschaffen, um in zukünftigen Experimenten die native Lipidumgebung zu untersuchen. Weiterhin dienen diese Vorarbeiten als Anknüpfungspunkt für weiterführende Experimente zur strukturelle Analyse des GPAA1-Komplexes durch Einzelpartikel-Kryo-Elektronenmikroskopie.

3 Introduction

3.1 Lipids and protein-lipid interactions

Membrane lipids are functionally characterised as compartmentalisation factors in cells, creating distinct cellular microenvironments and to serve as a matrix for membrane proteins[1]. To create distinct subcellular compartments, lipid bilayers are formed. Essential for the formation of this bilayer are amphipathic lipids, namely glycerophospholipids (GPLs), sphingolipids (SP) and sterols (ST), such as cholesterol (Chol), that contain a hydrophilic head group and a hydrophobic/lipophilic tail[2]. Containing a glucose-3-phosphate backbone esterified at the C-1 and C-2 position with fatty acids and varying groups at the phosphate, such as choline (PC), ethanolamine (PE), serine (PS), inositol (PI) or hydrogen (PA), GPLs form the major component of biological membranes[3]. The *de novo* synthesis of SPs (see figure 1) starts from a condensation reaction using serine and palmitoyl to form 3-ketodihydrosphingosine, which is sequentially reduced to dihydrosphingosine and acylated to form the ceramide precursor dihydroceramide[4]. Ceramide, the common hydrophobic core of all SPs is based on a sphingosine core, in mammalian membranes mainly a C18 amino alcohol containing a trans-double bond between C-4 and C-5, linked via an amide bond to a fatty acid[5]. The addition of different hydrophilic head groups results in sphingomyelins, cerebrosides or higher glycosphingolipids such as gangliosides[3]. The salvage pathway of long chain sphingoid bases leads to the re-generation of sphingolipids and has been estimated to contribute from 50% to 90% of sphingolipid biosynthesis and suggests a crucial role for sphingolipid breakdown in sphingolipid biosynthesis/turnover as well as in cellular signal transduction[6]. Manifold variations in the head groups, fatty acid chain length as well as saturation with and orientation of double bonds in GPLs and SPs give rise to an incredible high amount of possible combinations of lipid species. Analysis of the major structural membrane lipids (GPL, SP, ST), revealed an unequal distribution in different cellular membranes[7]. On top of this, some cellular organelles maintain an asymmetric lipid distribution between the cytosolic and luminal side of their membranes[8]. Interestingly, even though continuous vesicular transport from and to membranes takes place, the lipid distribution is stable and not altered over time[7]. As there are different lipid profiles for different subcellular membranes, variations between different cell types of one organism as well as different taxa should be no surprise[7].

Due to recent advances in technology, analysis of cellular lipidomes emerged as a feasible task and continuously provides new insights into the function of over thousands of different lipids in eukaryotic cells. Currently, the LIPID MAPS structure database counts 21118 manually curated lipids, as well as 21953 computational derived hypothesised lipids (time stamp: 29.08.2018)[9, 10]. This high complexity leads to the question of what is the rationale behind the need of the human body for such a huge amount of different lipid species within membranes. Identifications of protein amino acid sequences correlating with structural features of lipids or lipid classes lead to the term protein-lipid interaction motifs. For example, motifs are described for leaflet specific cholesterol interactions with the CARC ($L/VX_{1-5}YX_{1-5}K/R$) motif facing to the outer leaflet and the inverted CRAC ($K/RX_{1-5}Y/FX_{1-5}L/V$) motif facing the inner leaflet[11]. Recent reports indicate regulatory roles of individual lipid species by identifying specific protein-lipid interactions. For example the ganglioside GM3 has been shown to negatively regulate the autophosphorylation of the kinase domains of the epidermal growth factor receptor (EGFR)[12]. Another example is the necessity of cardiolipin for the supercomplex formation between the respiratory chain complexes III and IV in mitochondria[13, 14]. The study of the interaction between sphingomyelin species 18 (SM18) and

the transmembrane domain of the COPI machinery protein p24 revealed a conserved signature sequence (VXXTLXXIY) in a number of mammalian transmembrane proteins[15, 16]. UniProt analysis using this sphingolipid-binding motif resulted in a list containing 615 novel candidates for sphingolipid-protein interactions[16]. Two of these proteins are the endoplasmic reticulum (ER) localised transmembrane proteins glycosylphosphatidylinositol anchor (GPI) attachment 1 protein (GPAA1) and GPI inositol-deacylase (PGAP1). GPAA1, being part of the transamidase complex (PIGK/S/T/U and GPAA1), plays a crucial role in the transfers of the GPI-anchor to the C-terminus of the receiving protein. Before GPI anchored proteins (GPI-APs) are sorted into ER exit sites, the GPI anchor undergoes multiple steps of post-attachment modifications and part of this maturation process is PGAP1 (see section 3.2.1). The remodelled GPI-APs are then efficiently recognised by members of the p24 protein family, packaged into COPII-derived vesicles for ER export[17].

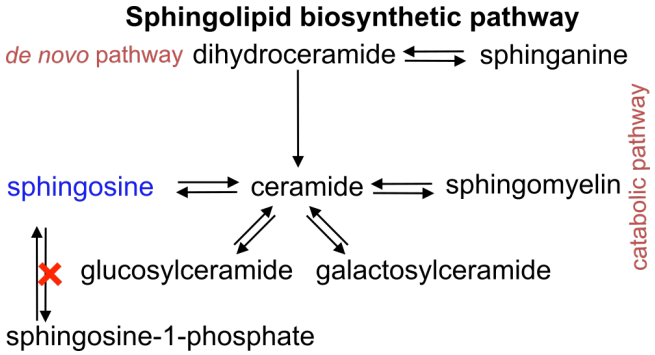

Figure 1: Simplified schematic drawing of the sphingolipid biosynthetic pathway Sphingolipids are either synthesised *de novo*, or products of the catabolic pathway, consisting out of the salvage pathway and the recycling of exogenous ceramides[6]. To study specific protein-sphingolipid interactions, a knock-out of the sphingosine-1-phosphate lyase (red cross) prevents sphingosine derivatives to be channeled into the sphingolipid-to-glycerolipid metabolic pathway[18].

3.2 The glycosylphosphatidylinositol (GPI)-anchor

Eukaryotic organisms produce many membrane proteins that are anchored to the outer cell membrane by GPI-anchor[19]. The GPI-anchor is a glycolipid consisting of PI, glucosamine (GlcN), mannose (Man), and ethanolaminephosphate (EtNP) and acts as a lipid anchor for various plasma-membrane proteins[5] (see figure 2A). GPI-anchored proteins play important roles, for example in host self-defence or intracellular signal transduction. Besides, some of them function as receptors for viruses and toxins[20, 21]. The GPI-anchor is widely distributed with over 150 different human proteins, conserved in various eukaryotes, essential for development in higher animals as well as for growth of yeasts and protozoan parasites[22, 23, 24]. Malfunctions of the GPI-anchor biosynthesis (see section 3.2.1) and consequently the missing representation of GPI-anchored proteins at the surface of the plasma membrane has major implications on human health and is known to be involved in many diseases [19, 22, 25, 26]. Especially the transamidase complex members (see section 3.2.3) of the biosynthetic pathway of the GPI anchor are linked to different cancers[27, 28].

3.2.1 Biosynthesis of the GPI-Anchor

The synthesis of the GPI-anchor until its attachment to a protein containing a GPI-attachment sequence occurs in different steps in the ER. This procedure is described in the following and schematically depicted in figure 2B. In the first step N-acetylglucosaminyl-phosphatidylinositol (GlcNAc-PI) is generated by attachment of N-Acetylglucosamine (GlcNAc) to phosphatidylinositol (PI), thus generating GlcNAc-PI. This step is catalysed by an enzyme complex consisting of at least seven components, PIGA, PIGC, PIGH, PIGP, GPI1, DPM2 and PIGY[29]. Afterwards, the N-acetyl group is removed by PIGL (de-N-acetylation[30]) to generate glucosaminyl-PI (GlcN-PI)[31]. After completion, GlcN-PI flips from the cytosolic side of the ER to the luminal side where the ER-associated multi-transmembrane acyl transferase PIGW adds an acyl chain (e.g. palmitate or myristate) to the second position of the inositol ring (GlcN-aPI)[31]. Mannose-P-dolichol (MPD) is transported into the ER by the cytosolic located enzyme complex DPM1/2/3d. Required for this process is SL15, also known as Mannose-P-dolichol utilization defect 1 protein (MPDU1), which is needed for all known classes of monosaccharide-P-dolichol-dependent glycosyltransferase reactions in mammals[32] and is predicted to be involved in vesicle formation and in protein trafficking[33]. After availability of mannose in the ER lumen, the glycosylphosphatidylinositol mannosyltransferase complex 1 (GPI-MT-1), consisting out of PIGM and its stabilising cofactor PIGX, transfers one mannose group to the fourth position of the glucosaminyl group, thus forming Manα4GlcNα6(acyl-2)myo-inositol-phospholipid (ManGlcN-aPI)[34]. PIGV (GPI-MT-2) transfers then a second mannose group to position 6 of the previous primary mannose group, resulting in the formation of Manα6Manα4GlcNα6(acyl-2)myo-inositol-phospholipid (ManManGlcN-aPI)[35]. Afterwards, an ethanolamine phosphate group (EtNP) is added to position 2 of the first mannose group by PIGN, an ethanolamine phosphate transferase (EtNPT-1)[36], thus generating Manα6(EtNP-2)Manα4GlcNα6(acyl-2)myo-inositol-phospholipid (Man(EtNP)ManGlcN-aPI). PIGB (GPI-MT-3) adds the third mannose group at position 2 of the second one, resulting in Manα2Manα6(EtNP-2)Manα4GlcNα6(acyl-2)myo-inositol-phospholipid (ManMan(EtNP)ManGlcN-aPI)[37]. PIGO, together with the catalytic subunit PIGF forms the ethanolamine phosphate transferase-2 (EtNP-T2), which binds EtNP to position 6 of the third mannose (EtNP-6Manα2Manα6(EtNP-2)Manα4GlcNα6(acyl-2)myo-inositol-phospholipid, short EtNPManMan(EtNP)ManGlcN-aPI)[38]. By switching partners, PIGF forms together with GPI7 the ethanolamine phosphate transferase-3 (EtNP-T3), which binds an EtNP on position 6 of the second mannose and therefore forms the last stage of the GPI-anchor (EtNP-6Manα2(EtNP-6)Manα6(EtNP-2)Manα4GlcNα6(acyl-2)myo-inositol-phospholipid (EtNPMan(EtNP)Man(EtNP)ManGlcN-aPI), before transferred to a protein containing the necessary GPI-attachment sequence[39]. It has been shown that certain GPI proteins contain a fourth mannose group which is linked as a side branch towards the GPI core at the third mannose and is transferred by PIGZ in humans[40].

3.2.2 GPI-anchor attachment signal

Proteins marked for GPI modification (see figure 2C) contain two signal peptides, an N-terminal one for import into the ER as well as a C-terminal one for the attachment of the GPI-anchor which consists out of the following structural domains[5]. At the GPI attachment side ω, amino acids with short side chains are present, namely glycine, alanine, serine, asparagine, aspartic acid or cysteine[41]. Similar to ω, short side chained amino acids (glycine, alanine, serine) are also found

in the positions named ω_{+1} and ω_{+2}, which describes the first and second amino acid of the cleaved signalling peptide[41]. An unstructured linker of approximately 10 amino acids precedes ω [42]. ω_{+2} is followed by a hydrophilic spacer sequence with six or more residues (ω_{+3}) and is concluded by a 15-20 amino acid long hydrophobic sequence at the C-terminal end (ω_{+4}), which is long enough to span the ER membrane[41, 42].

3.2.3 Attachment of the GPI-anchor by the mammalian transamidase complex

Responsible for the transfer of the GPI-anchor to the C-terminus of the receiving protein is the transamidase complex[41, 43] (see table 1). This complex, located in the ER membrane and facing the luminal side, consist out of the catalytic subunit PIGK (also known as GPI8), the subcomponents PIGS/T/U and GPAA1[41, 44]. Even though the players are known, there are still unsolved questions about the structure and the spatial arrangement of the transamidase complex. While the 3D structure of PIGK is determined[42] (at least in yeast), and for PIGT[45] and GPAA1[46] predicted, relatively less is known about PIGS and PIGU. A disulfide-link between PIGT (Cys182) and PIGK (Cys92) is crucial for the complex activity and it is predicted that the unspecific cleavage activity of PIGK, belonging to the C13 cysteine peptidase family, is being regulated by its covalent bound partner PIGT[44, 46, 47]. GPI transamidase complex forms a carbonyl intermediate with the GPI-attachment sequence protein, cleavage between the ω and ω_{+1} residues takes place, and nucleophilic attack by GPI on the activated carbonyl yields a GPI-anchored protein[48, 49, 50].

Table 1: Subunits of the mammalian transamidase complex

Gene name[1]	NCBI Gene ID[2]	UniProt ID[3]	Protein name
GPAA1	8733	O43292	GPI anchor attachment 1 protein
PIGK	10026	Q92643	phosphatidylinositol glycan anchor biosynthesis class K
PIGS	94005	Q96S52	phosphatidylinositol glycan anchor biosynthesis class S
PIGT	51604	Q969N2	phosphatidylinositol glycan anchor biosynthesis class T
PIGU	128869	Q9H490	phosphatidylinositol glycan anchor biosynthesis class U

[1]HUGO: human gene nomenclature committee (http://www.genenames.org); [2] https://www.ncbi.nlm.nih.gov/gene; [3] https://www.uniprot.org/

GPAA1 contains an approximately 300 amino acid long luminal side preceded by a transmembrane domain, which is closed up by the cytoplasmic located N-terminus, and followed by six transmembrane domains until the luminal located C-terminal end is reached[51, 52]. The luminal loop matches with a 290 amino acid stretch that identifies this domain as a M28 family metallopeptide and thus indicates that GPAA1 is the complex subunit that catalyses the formation of the peptide bond between the ω site and the EtNP group of the GPI anchor[44, 46]. Being a metallo proteinase it is suggested that suitable binding sites for zinc residues are located at Asp153, ASP188, Glu226 and Tyr328[46]. Other members of the M28 family of metalloproteases are known to function as aminopeptidases, carboxylpeptidases, cyclisation of N-terminal glutamine and it cannot be excluded that GPAA1 might have some exopeptidase activity[46]. Interestingly, GPAA1 does not contain any ER localisation information, whereas PIGT and PIGK do[52]. It is to be noted, that the ER quality control mechanisms that targets terminally misfolded proteins for ER-associated degradation (ERAD), is not the main degradation pathway for misfolded glycophosphatidylinositol-anchored proteins, who are disposed of mainly via the vacuole/lysosome pathway and indicate that the GPI-anchor sterically obstructs ERAD[53].

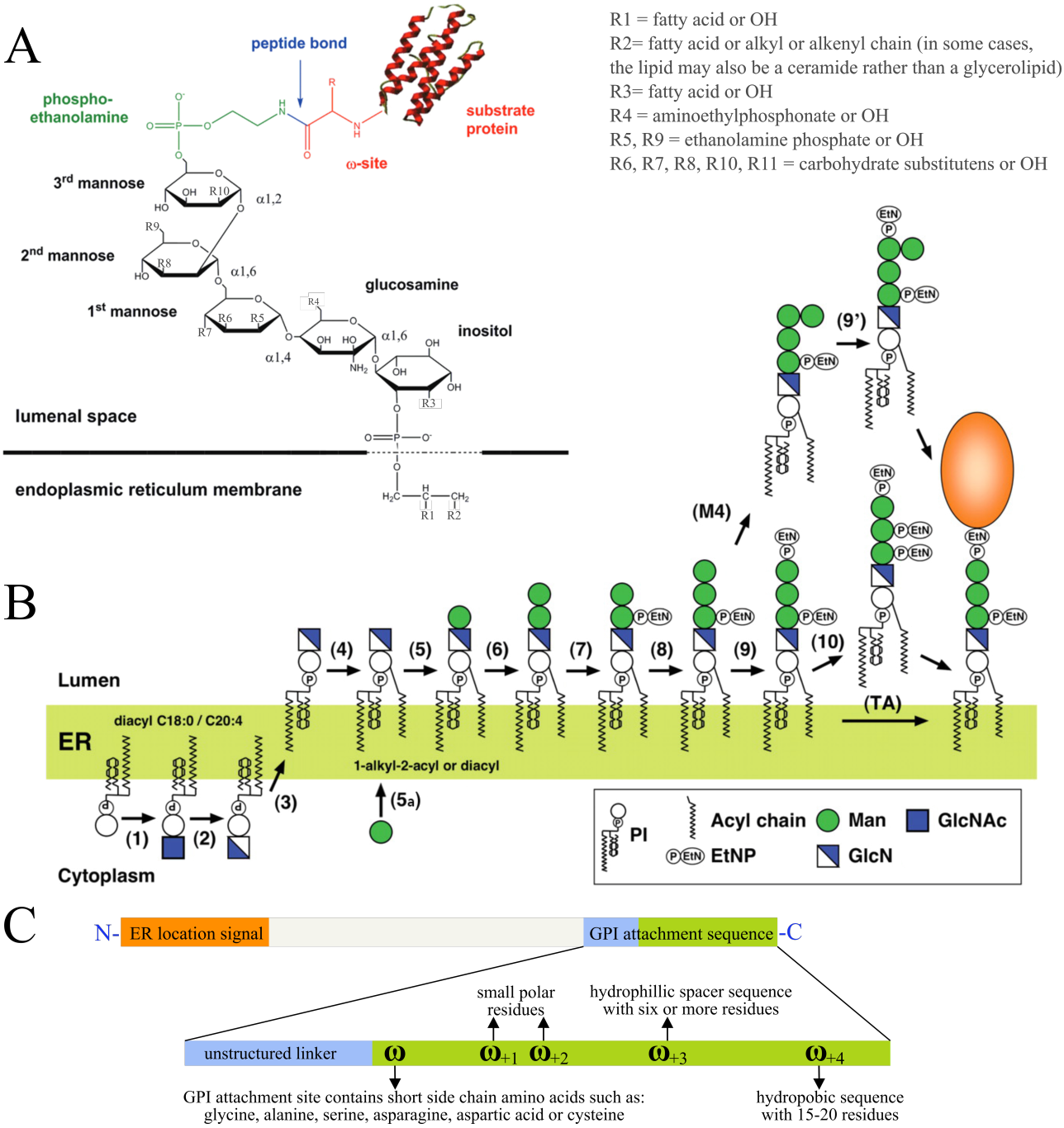

Figure 2: The mammalian GPI-anchor synthesis in the ER A) The typical chemical structure of the GPI lipid anchor and its linkage via the *ω*-site to the substrate protein for the transamidase reaction are schematically illustrated. Heterogeneity in GPI anchors is derived from various substitutions of this core structure and is represented as R groups. Adapted and modified from[5, 46]. **B)** The synthesis of the GPI starts on the cytoplasmic side of the ER by attachment of N-acetylglucosamine to phosphatidylinositol (1), followed by de-N-acetylation to generate glucosaminyl-PI (2). The intermediate gets transported to the lumenal side of the ER membrane (3), followed by attachment of an acyl chain (4), which can be palmitate or myristate. Successive additions of mannose, derived from mannose-P-dolichol from the cytoplasm (5a), and ethanolamine phosphate groups to the glucosaminyl group (5-9) prepare for the attachment of the GPI-anchor to its respective protein. The attachment is facilitated by the transamidase complex (TA). Adapted and modified from[41]. **C)** Schematic drawing of a hypothetical GPI-anchor protein with its N-terminal ER localisation signal and the C-terminal attachments sequence, with the GPI-attachment site *ω*. Adapted and modified from[5].

3.2.4 Post-attachment remodelling of the GPI-anchor and transport to the plasma membrane

The first post-attachment remodelling (figure 3) step of the GPI-anchor is performed by PGAP1, which removes the acyl chain attached by PIGW[17]. PGAP5 removes in the second step the EtNP group from the second mannose[54]. These two GPI remodeling reactions in the ER are critical for the sorting of GPI-APs to ER-exit sites (ERES), as the remodeled GPI-anchor acts as an ER exit signal and is efficiently recognised by the p24 protein family complex that concentrates GPI-APs into COPII-derived vesicles[17, 54].

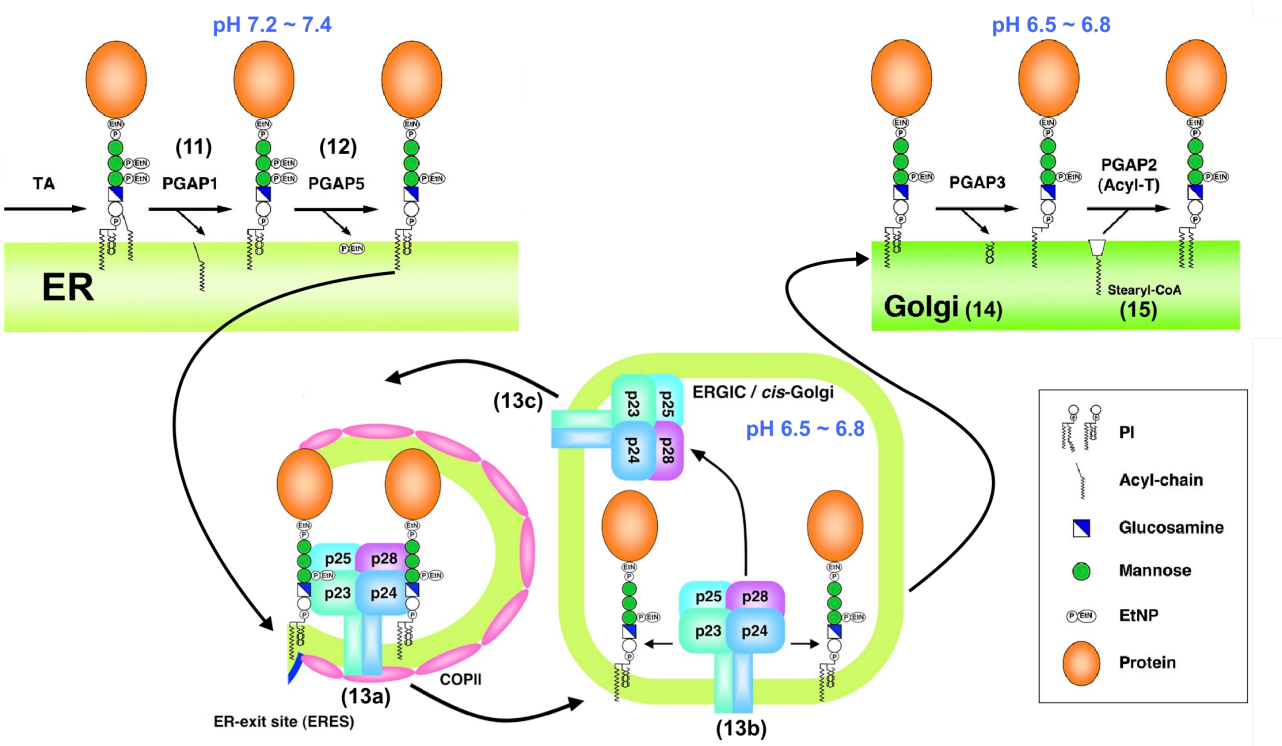

Figure 3: Post-attachment remodelling of the GPI-anchor After the transamidase complex (TA) transfers the protein with a GPI-attachment signal to a GPI-anchor, multiple post-attachment remodelling steps are performed. The acyl chain from the inositol ring (11) and the ethanolamine phosphate group from second mannose are removed (12). Followed by sorting of the GPI-anchored protein into ER exit sites by binding to the p24γ2subunit (13a), transport to the Golgi and pH dependent disassembly of the p24 complex (13b) and recycling of the transport machinery (13c). Finally, the unsaturated fatty acid is removed (14) and replaced through attachment of a saturated fatty acid (15). At last, GPI-anchor proteins are transported to their final destination via the the Golgi apparatus. Figure adapted and modified from[17].

The transport from ER to Golgi depends on the activity of the GTP-binding protein SAR1a and the transport velocity of not mature GPI-anchors is significantly reduced[54, 55, 56]. The lower pH in the Golgi, when compared to the pH in the ER, induces a dissociation of the p24 protein complex and the GPI-anchored protein[17]. The third step of the post-attachment remodelling is performed in the Golgi by PGAP3, which performs fatty acid remodelling and removes an unsaturated acid at the sn2 position in the GPI lipid[57]. The free spot at the *sn2* position is then taken by an saturated fatty acid, attached via PGAP2[57, 58]. This fatty acid remodeling of GPI-anchored proteins was suggested to be required for raft association[57]. Once these modifications are completed, the mature GPI-anchor protein is transported to the plasma membrane via the

Golgi apparatus[17]. A specific role play GPI-APs in human erythrocytes, such as CD55 (decay-accelerating factor), CD59 and acetylcholine esterase, which maintain unsaturated fatty acids at the *sn2* position and a palmitoyl chain linked to the 2-position of the inositol ring[41]. At the plasma membrane, GPI-anchored proteins have been shown to reside in cholesterol-dependent nanoscale assemblies of sphingolipids and GPI-anchored proteins[2, 59]. It has been suggested that transbilayer interactions between outer-leaflet long-acyl-chain-containing lipids and inner-leaflet phosphatidylserine are pivotal in generating actin-dependent nanoclusters of membrane lipid-anchored proteins, such as GPI-anchored proteins[60].

3.3 Methods to study protein lipid interactions

3.3.1 Methods for solubilisation of proteins with transmembrane domains

Proteins containing one or more transmembrane domains (TMD) interact with lipids in their near micro-environment. Ways to study proteins with TMDs involves some difficulties, as the TMDs consist of amino acids characterised by their mostly hydrophobic nature and tend to lose their specific tertiary structure as soon as the stabilising lipid environment is removed. Traditional ways employ solublisation of proteins via detergents micelles (figure 4A) or via amphipols (figure 4B)[61, 62]. These are so called non-bilayer systems, as they disrupt the local lipid micro-environment during the solublisation process[63]. Generally, the detergent induced solubilisation occurs in three stages (see figure 4B)[64]. The lipid bilayer usually remains intact but selective extraction of some membrane proteins might take place at molar detergent to membrane lipid ratios of 0.1-1:1[65]. Solubilisation of the membrane and generation of mixed micelles (phospholipid–detergent, detergent–protein, and lipid–detergent–protein micelle) occurs at a ratio of to 2:1[65]. At a ratio of 10:1, all native membrane lipid-protein interactions are effectively exchanged for detergent-protein interactions[65]. The solubilisation efficacy and functionality of extracted proteins might vary greatly, depending on the type of detergent (cationic, anionic, zwitterionic) and selected lysis parameter (e.g. duration, temperature, lysis buffer composition). One example are detergent resistant membranes, which contain proteins surrounded by a stiff membrane section that mostly consists of sphingolipid/cholesterol [66, 67].
So called bilayer systems approach the solublisation of proteins by preserving a stabilising lipid environment or reconstitute extracted proteins with synthetic lipids[63]. One method of this type is the bicelle, which is a discoidal structure obtained by mixing phospholipids (often short-chain phospholipids) with detergents in a defined ratio (figure 4C)[63, 68]. Recent techniques to study proteins containing TMDs are based on the extraction of proteins with their surrounding micro-environment. This can be achieved by employing the artificially engineered membrane scaffold protein (MSP, figure 4D) or the styrene-maleic acid (SMA) copolymer (figure 4E)[69, 70, 71, 72]. Especially SMA has shown profound implications on TMD protein research, due to its compatibility with cryo-electron microscopy, mass spectrometry (e.g. analysis of lipids in the micro-environment) and its ease of use [62, 73, 74, 75]. The mechanism of SMA derives from its pH-dependent change of tertiary structure, which results in formation of a scaffold around the membrane protein that is trapped with the annular membrane lipids[62, 76]. These SMA lipid particles (SMALP) can differ in size (e.g. from 10 nm up to 35 nm) and the actual size of the SMALP depends solely on the weight ratio of SMA to lipid (e.g. 1.25-4:1)[62, 72, 77, 78, 79]. SMA copolymers are available in different styrene/maleic acid ratios and chain lengths, thus possessing different charge densities, hydrophobicities, and solubilisation properties[80]. It has been shown that

nanodiscs prepared using this polymer are very dynamic structures with rapid exchange of the different components and there is a controversy about a potential preference of lipids included into SMALPs, but for now it is assumed that SMA does not differentiate[62, 81, 82].
In summary, different methods for solubilisation of proteins with TMD exist, but the best conditions for solubilisation and subsequent analytics are to be determined for each protein anew.

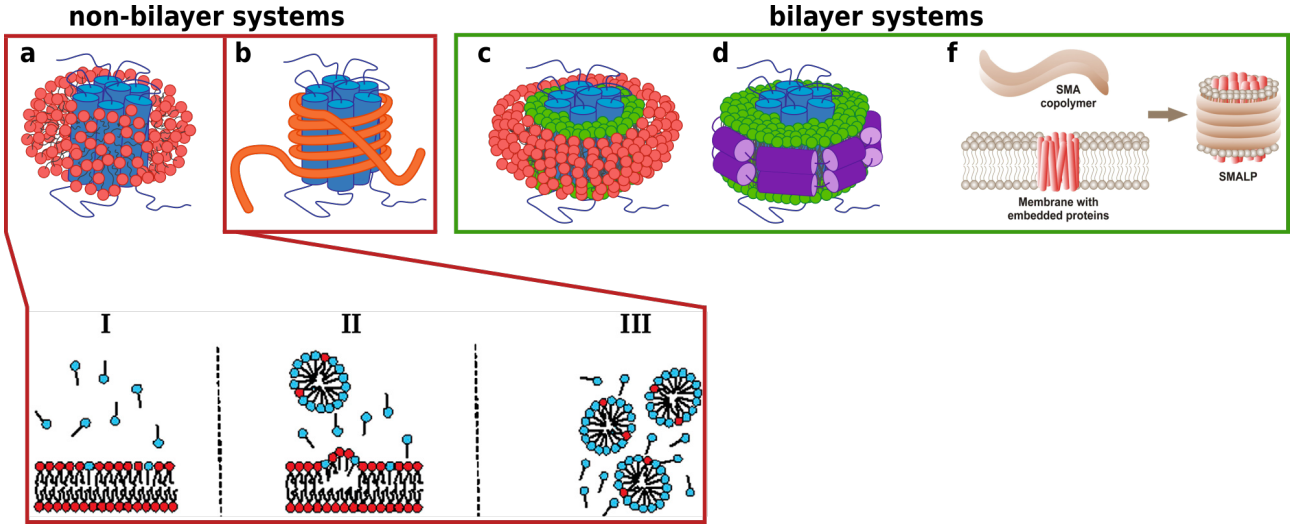

Figure 4: Membrane-mimetic systems for membrane protein stabilisation. A) A Protein in detergent (red) micelle. **AI)** At low detergent:membrane lipid molar ratios (e.g. 0.1-1:1), the detergent (light blue) integrates at low quantities into the lipid bilayer. **AII)** With increasing ratios (2:1), partial solubilisation and formation of micelles containing protein complexes starts. **AIII)** If the ratio increases further (e.g. 10:1), all native lipid-protein interactions are exchanged and detergent-protein micells are formed. **B)** Protein stabilised by amphipol (orange). **C)** Protein in bicelle (detergent in red, lipids in green). **D)** Protein in nanodisc stabilised by membrane scaffold protein (MSP in purple, lipids in green). **E)** Protein in nanodisc stabilised by SMA. The addition of the styrene-maleic acid (SMA) copolymer (brown) to native membranes (gray) that contain proteins (red) at elevated pH results in the formation of SMA lipid particles (SMALP) that form a scaffold around the membrane protein trapped with the annular phospholipids. Figure and figure legend adapted and modified from[62, 63, 64, 65].

3.3.2 Bioorthogonal tagging of protein lipidation via click chemistry

One way to study specific protein-lipid interactions is the use of photoactivatable and clickable (pac) lipid analogues[83]. After the introduction of click chemistry in 2001, different bifunctional lipid species have been synthesised[83, 84]. Of these, pacSphingosine (pacSph, figure 5A) has been used to define over 180 potentially sphingolipid-binding proteins, one of them being GPAA1 which was also identified as sphingolipid-binding protein in [85]. UV irradiation cross-links pacSph and its metabolites via their photoactivatable diazirine ring to proteins in close proximity. Cross-linked proteins are enriched (e.g. via IP) and specific protein-lipid interactions are detected via copper-catalysed azide-alkyne cycloaddition (CuAAC, figure 5B) mediating covalent linkage of a functional group (e.g. fluorphores) to the alkyne moiety of pacSph[85, 86].

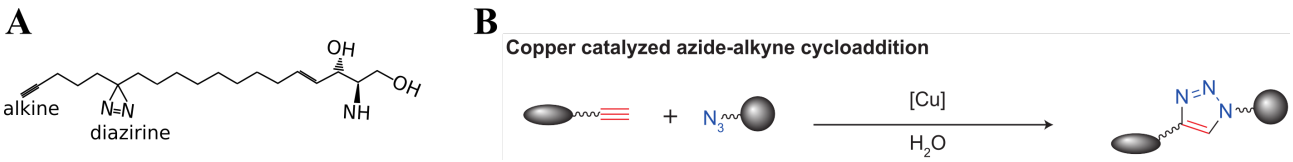

Figure 5: Structure of the bifunctional pacSph and bioorthogonal tagging of protein lipidation via click chemistry. A) A photoactivatable diazirine ring allows for UV irradiation induced cross-link to proteins, while the alkyne group is available for attachment of functional groups via copper-catalysed azide-alkyne cycloaddition (CuAAC). Adapted from[85]. **B)** Simplified schema of the CuAAC. Adapted and modified from[87].

3.3.3 Tagging of endogenous proteins via CRISPR/Cas9

A way to facilitate the analysis of endogenous proteins is genome engineering. For example, addition of N- or C-terminal tags allow to study proteins in living cell as well as to extract protein complexes with their endogenous stoichiometric subunit composition[88, 89]. One way to achieve this, is the CRISPR/Cas9 system. [88, 90, 91, 92]. CRISPR stands for Clustered Regularly Interspaced Short Palindromic Repeats and describes a bacterial host defense system which produces specific small single stranded nucleotide stretches recognised by a nuclease to defend against foreign genomic material[93, 94]. Jumping forward in time, specific alterations were made to adapt the system for genomic engineering in eukaryotic cells. Nowadays, online tools[1][2][3][4] for the design of sequences specific to certain genomic regions, in short called gRNAs, exist. When brought into cells in conjunction with a nuclease, such as the CRISPR-associated protein-9 nuclease (Cas9), they can be employed for gene inactivation or incorporation of designed sequences into the DNA (see figure 6). Gene inactivation is mediated by the introduction of a double strand break in the genomic region of the targeted gene. The DNA damage is repaired by an error prone process called non-homologous end joining (NHEJ) and, through introduction or deletion of nucleotides, shifting the reading frame and resulting in non functional proteins[95, 96]. If a template for repair is available, the process is called homology directed repair (HDR). This process is a precise way for genome modification by insertion of sequences of interest, such as tags for immunoprecipitation or fluorescent proteins[88, 89]. For example, high throughput and high resolution mapping of protein localization in mammalian brain by *in vivo* genome editing have been developed as well as endogenous C-terminal tagged GAA1, the yeast homolog of human GPAA1, that allowed for immunopurification of the whole transamidase complex and furthermore provided structural insight by small-angle X-ray scattering [97, 98]. In summary, combinations of CRISPR/Cas9 and detergent free extraction (e.g. SMA) of endogenous protein complexes are suitable tools to study proteins containing TMDs.

[1]Zhang Lab (MIT, USA): http://crispr.mit.edu/
[2]Wittbrodt lab (COS, Germany): http://crispr.cos.uni-heidelberg.de/
[3]Joung lab (Massachusetts General Hospital, USA): http://www.jounglab.org/guideseq/
[4]Boutros's lab (DKFZ, Germany)http://www.jounglab.org/guideseq/

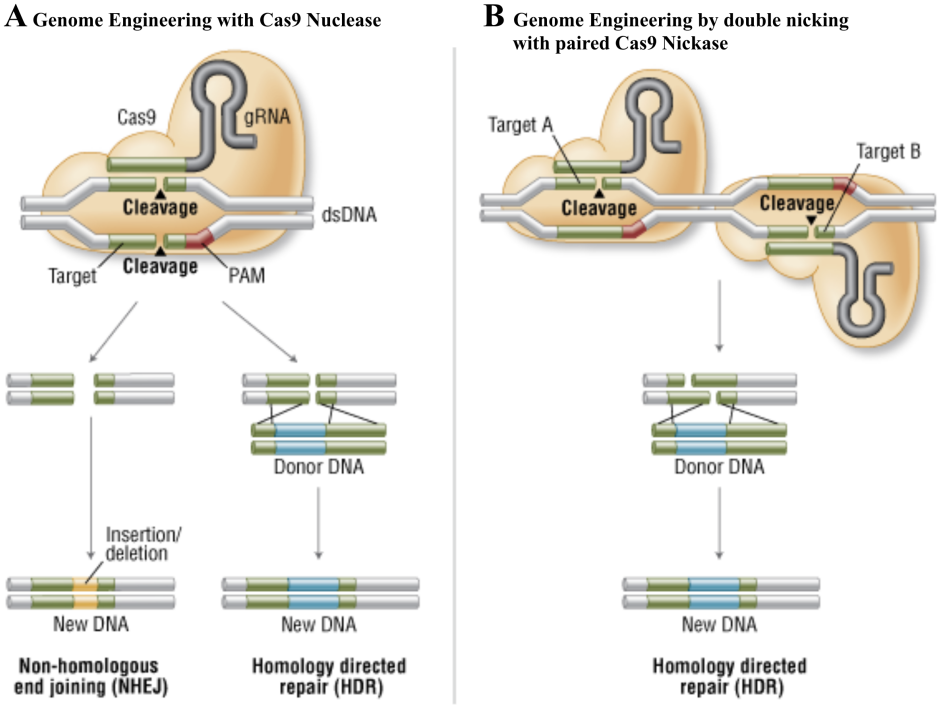

Figure 6: Genome engineering with CRISPR/Cas9 A) The nuclease Cas9 is directed, by the specific binding of a gRNA to its target sequence, to the genomic DNA and introduces a double strand break. Repair will be facilitated through either NHEJ or HDR. **B)** Using two gRNAs and a Cas9 incapable of introducing a double strand break increases precision of HDR. Figure adapted and modified from[99].

3.4 Aim of the thesis

The GPI-anchor is a lipid moiety attached to over 150 human proteins and plays a crucial role in cell surface display at the plasma membrane. The transamidase complex, located in the ER, transfers the GPI-anchor to the receiving protein. Previously, interactions between the transamidase complex subunit GPAA1 and a sphingolipid have been shown.
The aim of this thesis was to establish an experimental setup to analyse protein lipid interactions of the transamidase complex. For this, a cell model suitable to study sphingolipids was employed. Interactions were assessed via in-gel fluorescence and western blot quantification through click chemistry with bifunctional sphingolipids in conjunction with transient expression of transamidase subunits. TLC was used to verify the metabolic status of exogenous pacSph at given time points. CRISPR/Cas9 was utilised to created a cellular model to study sphingolipid interactions with the endogenous transamidase complex. The subset of specific sphingolipid species interacting with the transamidase complex were be elucidated by selective inhibition of enzymes involved in the sphingolipid metabolism.

4 Materials & Methods

All chemicals, solutions and enzymes are listed in table 2 with their name that is used throughout the thesis as well as the brand name, except they were solely used for one set of experiments. If the latter is the case, the details are enclosed in the specific section containing the description of the experimental procedures.

4.1 Tables

Table 2: Chemicals/Solutions used in this thesis in alphapetical order

Name	Product name	Provider	Article number	Purity [%]
Acrylamide	Rotiphorese® Gel 30 (37,5:1)	CarlRoth	3029.1	NA
AcOH	Acetic acid AnalaR NORMAPUR® ACS	VWR	20104.298	≥99.8
Agar	Bacto™ Agar	BD	214010	NA
Agarose	Agarose NEEO, Roti®garose low electroendosmosis	CarlRoth	2267.4	NA
APS	Ammonium peroxydisulphate	CarlRoth	9592.2	≥98
Alexa-647	Alexa Fluor® 647 Azide, Triethylammonium Salt	ThermoFisher	A10277	≥99
Biotin-azide	PEG4 carboxamide-6-azidohexanyl biotin	ThermoFisher	B10184	research grade
Benzonase	Benzonase® Nuclease HC	Merck	71206	≥99
BSA	Albumin Fraktion V	CarlRoth	8076.2	≥98
CaCl	Calcium chloride dihydrate	Sigma-Aldrich	31307	≥99
$CHCl_3$	LiChrosolv® Chloroforom	Merck	102444	≥99.8
CHAPS	CHAPS hydrate	Sigma-Aldrich	C5070	≥98
CHAPS	CHAPS for 2D gel electrophoresis	Sigma-Aldrich	GE171314-01	NA
clickSM-Standard	N-(octadec-17-yn)-Sphing-4-enin-1-phosphocholine	synthesised in the lab	NA	NA
Coumarin	3-azido-7-hydroxycoumarin	Jena Bioscience	CLK-FA047-1	≥95
$CuS0_4$	Copper(II) sulfate pentahydrate	Sigma-Aldrich	203165	≥99.999
$Cu[MeCN]_4BF_4$	Tetrakis(acetonitrile)copper(I) tetrafluoroborate	Sigma-Aldrich	677892	≥97
Digitonin	Digitonin	Sigma-Aldrich	D5628	≥50

Table 2: Chemicals/Solutions used in this thesis in alphapetical order

Name	Product name	Provider	Article number	Purity [%]
DMEM	Dulbecco's Phosphate Buffered Saline	Sigma-Aldrich	D6046	cell-culture grade
DTT	DL-Dithiothreitol	Sigma-Aldrich	D0632	$\geq$99
Ethylacetate	Ethylacetate	diverse suppliers	NA	$\geq$98
EtOH	LiChrosolv® Ethanol	Merck	111727	$\geq$99.8
FBS	Fetal bovine serum	Merck	S0615	EU-approved
FBS,delipid-ated	Charcoal Stripped Fetal Bovine Serum	ThermoFisher	12676029	research grade
Glycine	Glycine	Sigma-Aldrich	33226	$\geq$99.7
HEPES	PUFFERAN® Hepes	CarlRoth	9105.4	$\geq$99.5
Hexane	n-Hexane ACROS Organics	FisherScientific	AC197360010	$\geq$95
Hünig's base	N,N-Diisopropylethylamine	Sigma-Aldrich	496219	$\geq$99.5
LDS-sample buffer	NuPAGE® LDS Sample Buffer	ThermoFisher	NP0007	NA
L-ascrobic acid	(R)-5-[(S)-1,2-Dihydroxyethyl]-3,4-Dihydroxy-5-(H)-Furan-2-one	AppliChem	A1052,0100	$\geq$99
MeOH	Methanol	Sigma-Aldrich	32213	$\geq$99.8
β-Mercapto-ethanol	2-Mercaptoethanol	Sigma-Aldrich	M6250	$\geq$99
Milk	Powdered milk	CarlRoth	T145.2	blotting grade
MOPS	4-Morpholinepropanesulfonic acid	Sigma-Aldrich	M1254	$\geq$99
NaCl	Sodium chlorid	Sigma-Aldrich	31434-M	$\geq$99.5
$NaCHO_3$	1,1,3,3-Tetramethylbutyl isocyanide	Sigma-Aldrich	226491	technical grade
Na-deoxycholate	Deoxycholic acid sodium salt	CarlRoth	3484.3	$\geq$98
Nonident P40	Nonident P40 Substitute IGEPAL CA-630 (Octylphenoxy poly(ethyleneoxy)ethanol)	Sigma-Aldrich	11754599001 Roche	NA
Octylglucosid	n-Octyl-β-D-glucopyranoside	CalBioChem	494459	NA
PBS	Phosphate-buffered saline	Sigma-Aldrich	D8537	cell-culture grade
pacCer-Standard	N-(9-(3-pent-4-ynyl-3-H-diazirin-3-yl)-nonanoyl)-D-erythro-sphingosine	Avanti	900404P	$\geq$95

Table 2: Chemicals/Solutions used in this thesis in alphapetical order

Name	Product name	Provider	Article number	Purity [%]
pacSph-Standard	(2S,3R,E)-2-amino-13-(3-(pent-4-yn-1-yl)-3H-diazirin-3-yl)tridec-4-ene-1,3-diol	synthesised after[85]	NA	NA
pacPC-Standard	1-(9-(3-pent-4-ynyl-3-H-diazirin-3-yl)-nonanoyl)-2-oleoyl-sn-glycero-3-phosphocholine	Avanti	900408P	≥95
pacGlucCer-Standard	D-glucosyl-ß-1,1' N-(9-(3-pent-4-ynyl-3-H-diazirin-3-yl)-nonanoyl)-D-erythro-sphingosine	Avanti	900405P	≥95
Pen/Strep	Penicillin and Streptomycin	Sigma-Aldrich	P4333	cell-culture grade
PIC	cOmplete™, EDTA-free Protease Inhibitor Cocktail	Roche	11873580001	NA
RbCl	Rubidium chloride	AlfaAsar	12892	≥99
SDS	Dodecylsulfate-Na-salt	Serva	20765	≥99
SDS-PAGE standard	Precision Plus Protein™ All Blue Prestained Protein Standards	Bio-Rad	1610373	NA
TBTA	Tris[(1-benzyl-1H-1,2,3-triazol-4-yl)methyl]amine	Sigma-Aldrich	678937	≥97
TCEP	Tris(2carboxyethyl)phosphine hydrochloride	Sigma-Aldrich	C4706	≥98
TEMED	Tetramethylethylenediamine	Bio-Rad	1610800	≥99
Thiourea	Thiourea	Sigma-Aldrich	GERPN6301	NA
Triton-X-100	4-(1,1,3,3-Tetramethylbutyl)phenyl-polyethylene glycol	Merck	108643	≥98/Ph Eur
TRIS	TPUFFERAN® Tris, Tris(hydroxymethyl)-aminomethane	CarlRoth	4855.2	≥99.9
Trypan-Blue	Trypan Blue solution	Sigma-Aldrich	T8154	cell-culture grade
Tryptone	Bacto™ Tryptone	BD	211705	NA
Tween-20	Polyoxyethylene-20-sorbitan monolaurate	CarlRoth	9127.1	Ph Eur
Urea	Urea	Sigma-Aldrich	33247	≥99.5
Yeast Extract	Bacto™ Yeast Extracts	BD	212750	NA

Table 3: Antibodies used for detection via western blotting.

Target	Conjugate	Species	Provider	Article number	working dilution
α-calnexin		rabbit	Stressgene	SPA-865	1:1000
α-CD59		mouse	Santa Cruz Biotechnology	sc-133170	1:500
α-PIGU		rabbit	NovusBio	NBP1-98429	1:750
α-PIGK		rabbit	Proteintech	15151-1-AP	1:1000
α-PIGT		rabbit	Proteintech	16906-1-AP	1:1000
α-PIGS		rabbit	Proteintech	18334-1-AP	1:750
α-GPAA1		mouse	Santa Cruz Biotechnology	sc373710	1:750
α-GPAA1		rabbit	NovusBio	NBP2-16709	1:750
α-DDDDK tag		rabbit	Abcam	ab1162	1:1000
α-DDDDK tag		mouse	Sigma-Aldrich	F1804	1:1000
α-biotin	IRDye® 800CW Streptavidin		Li-cor	925-32230	1:10000
α-rabbit I_gG (H+L)	IRDye800CW	goat	Rockland	611-131-002	1:10 000
α-rabbit I_gG (H+L)	Alexa Fluor®680	goat	ThermoFisher Scientific	A-21076	1:10 000
α-mouse I_gG (H+L)	Alexa Fluor®680	goat	ThermoFisher Scientific	A-21075	1:10 000

Table 4: Vectors and their corresponding sequencing primers

Target-Vector	Name	Sequence	GATC standard primer
pCMV6+insert	Origene_FW	5-'GGCACCAAAATCAACGGGAC-3'	no
pCMV6+insert	Origene_Rev (inside of tag region)	5-'CGTCGTCATCCTTGTAATCCAG-3'	no
pCMV6+insert	CMV-F	5'-CGCAAATGGGCGGTAGGCGTG-3'	yes
pCMV6+insert	Origene_Rev2 (outside of tag region)	5'-ACTGGAGTGGCAACTTC-3'	synthesised at GATC
pCMV6-PIGT (RC201926)	PIGT_middle	5'-CAATGACACTGACCACTAC-3'	synthesised at GATC
pCMV6-PPIGS (RC209631)	PIGS_middle	5'-CAGGCCATGTCTTTGACTG-3'	synthesised at GATC
pCMV6-PPIGK (RC204728)	PIGS_middle	5'-CAGGCCATGTCTTTGACTG-3'	synthesised at GATC
pME-mCherry–CD59	CD59_FW	5'-GTGAGCAAGGGCGAGGAGGAT-3'	synthesised at GATC
pME-mCherry-FLAG-CD59	CD59_Rev	5'-CTTGTACAGCTCGTCCATGCC-3'	synthesised at GATC
px458 (pSpCas9(BB)-2A-GFP)	LKO1 (gRNA insertion site)	5'-GACTATCATATGCTTACCGT-3'	synthesised at GATC
AAVS1_Puro_PGK1_3xFLAG_Twin_Strep	pcDNA3.1-RP/1	5'-CAAACAACAGATGGCTGGC-3'	yes
AAVS1_Puro_PGK1_3xFLAG_Twin_Strep	pBR1	5'-CGAAAAGTGCCACCTGAC-3'	yes
AAVS1_Puro_PGK1_3xFLAG_Twin_Strep	RHA (inside of tag region)	5'-ATCACGACATCGACTAC-3'	yes
hCas9	CMV-F	5'-CGCAAATGGGCGGTAGGCGTG-3'	yes
MLM3636	GATC-OS280-1566504	5'-CAGGGTTATTGTCTCATGAGCGG-3'	synthesised at GATC

Table 5: 1.5mm 7.5% SDS page

Component	Volume [mL]	
	Separation	Stacking gel
H_2O	4.85	3.05
1.5M Tris pH 8.8	2.5	-
0.5M Tris pH 6.8	-	1.25
30% Acrylamide	2.5	0.65
10% SDS	0.1	0.05
10% APS	0.1	0.05
TEMED	0.01	0.005

Table 6: Equipment and Materials used for SDS-PAGE and western blot

Modell/Article name	Company	Article number
Mini-PROTEAN® Tetra Vertical Electrophoresis Cell	BioRad	1658004
Mini Trans-Blot® Cell	BioRad	1703930
Odyssey® CLx	Li-cor	9140
polyvinylidene fluoride (PVDF) membrane immobilon	Merck	IPVH00010
PowerPac Basic	BioRad	1645050
Tube Roller	StarLab	N2400-701
Whatman® gel blotting paper	Sigma-Aldrich	WHA10426892

Table 7: gRNA sequences

# gRNA	location on genomic strand	Sequence
GPAA1_gRNA#1_A	+	5-'ACACCTGAGATTGCCTGTCCGGGCG-3'
GPAA1_gRNA#1_B	-	5-'AAAACGCCCGGACAGGCAGATCTCAG-3
GPAA1_gRNA#2_A	+	5-'ACACCGAGATCTGCCTGTCCGGGCTG-3'
GPAA1_gRNA#2_B	-	5-'AAAACAGCCCGGACAGGCAGATCTCG-3'
GPAA1_gRNA#3_A	-	5-'ACACCATTCCAGAAAAGCAGCCAGCG-3'
GPAA1_gRNA#3_B	+	5-'AAAACGCTGGCTGCTTTTCTGGAATG-3'

Table 8: Primer for amplification of genomic GPAA1

name	sequence
genomic_GPAA1_FW2	5-'GTGGGATGGTGGTGGTCTTT-3'
genomic_GPAA1_REV2	5-'CAGCTCCAGCCTCAGTCCTA-3
genomic_GPAA1_FW3	5-'AAAAAAAAGAATTCGTGGGATGGTGGTGGTCTTT-3'
genomic_GPAA1_REV3	5-'AAAAAAAACTCGAGCAGCTCCAGCCTCAGTCCTA -3

4.2 Cell Culture

All cell lines were maintained at 37°C in a humidified atmosphere with 5% CO_2. Research group (RG) Thil provided human Fibroblasts (growth medium: DMEM + 10% FBS, Pen/Strep, 4500mg/L glucose). RG Wieland provided two cell lines, the mouse embryonic fibroblasts H806 (growth medium: DMEM + 10% FBS, Pen/Strep, L-glutamine) and the mus musculus brain neuroblastoma N2A (growth medium: DMEM + 10% FBS, Pen/Strep, L-glutamine). The adenocarcinomic human alveolar basal epithelial cell line A549 (growth medium: DMEM + 10% FBS, Pen/Strep) was kindly provided by RG Kräusslich. The hepatocarcinoma cell line Huh-7 (growth medium: DMEM high glucose (41965, ThermoFisher), L-glutamine, without pyruvate) was kindly provided by RG Ruggieri. The cervix carcinoma cell line HeLa and the human embryonic kidney cell line HEK293 (growth medium: DMEM + 10% FBS, Pen/Strep, L-glutamine) as well as the lymphoblast-like cell line Raji (growth medium: RPMI1640 + 10% FBS, Pen/Strep) were already in our possession. All research groups mentioned are associated with either Heidelberg University or the Heidelberg University medical centre.

4.3 Creation of chemically competent cells

To create chemically competent cells, a pre-culture of the bacterial strain and 10 mL antibiotic free LB-medium (see section 4.4) was grown overnight at 37°C and 180 rpm. The next day, 400 mL antibiotic free LB-medium were inoculated with 4 mL of pre-culture and grown until OD_{600}=0.4. All the following aseptic steps were done on ice with pre-cooled reagents and materials. The main culture was centrifuged (15min/4000rpm/4°C) and the pellet resuspended in 50 mL of sterile filtered TFB1 buffer (50 mM MnCl, 100 mM RbCl, 10 mM CaCl, 30 mM potassium acetate, 15% glycerol, pH 5.8 with acetic acid). The cells were pelleted (10min/3000rpm/4°C), resuspended in 10 mL sterile filtered TFB2 buffer (10 mM MOPS pH 7.0, 75 mM CaCl2, 10 mM RbCl, 15% glycerol), distributed into 250 µL aliquots and stored at -80°C. TFB1 and TFB2 were stored at 4°C.
To determine transformation efficiency, chemically competent cells were transformed (see section 4.4) with 1000/100/10pg of bacterial plasmid. Colony forming units (CFU) were counted the next day and efficiency (CFU/µg of transfected DNA) was calculated according to the following formula: transformation efficency $= \frac{\text{CFU on plate}}{\text{µg of DNA transfected}} \times 1000 \times \frac{\text{ng}}{\text{µg}}$

4.4 Transformation of bacteria

Before addition of 10 ng plasmid, aliquots of chemically competent *E. coli* DH-5α (DSMZ 6897, Deutsche Sammlung von Mikroorganism und Zellkulturen GmBH), *E. coli* Stbl3 (C737303, Thermo Scientific), and *E. coli* BW23473 (kindly provided by RG Wieland, BZH, Heidelberg) were thawed up on ice for 30 minutes. To facilitate plasmid DNA uptake, bacterial suspensions were subjected to a 45-90 seconds long heat-shock at 42°C. Recovery of bacteria was achieved by short incubation on ice and followed by addition of 1 mL Luria-Bertani (LB) medium (1% (w/v) tryptone, 0.5% (w/v) NaCl, 1% (w/v) yeast extract in H_2O). After a growth phase (30min/180rpm/37°C), bacteria were pelleted (1min/8000g/RT), resuspended and streaked out with a drigalski spatula on LB agar plates with respective antibiotics. Bacteria were grown overnight at 37°C or for 3 days at room temperature. Positive clones were identified by colony PCR/restriction digest or sequencing.

4.5 Colony polymerase chain reaction

To analyse successful uptake of plasmid DNA after transformation of *E. coli* strains (see chapter 4.4), polymerase chain reaction was employed to screen bacterial transformants. In short, 2 µL of 10x reaction buffer B, 0.8 µL of 50 mM $MgCl_2$, 10 mM dNTPs (732-3182,VWR Peqlab), 0.4 µL of 10 pmol forward and reverse primer, 14.7 µL H_2O, and 0.2 µL of taq DNA polymerase (22466, Axon Labortechnik) were mixed and inoculated with a freshly picked colony. PCR was performed according to the following program: 5 min/95°C, 30x (denaturing:30 sec/95°C, annealing: 52°C/30 sec, extension: 72°C/3 min 40 sec), 72°C/5min and stored at 4°C. Forward and reverse primers for origene vectors with the pCMV6 backbone are listed in table 4.

4.6 Sequencing of plasmids

All plasmids used for transient expression were either named in their specific experiment, were ordered from Origene, USA (RC200271 encoding for GPAA1, RC204728 encoding for PIGK, RC209631 encoding for PIGS, RC201926 encoding for PIGT, and RC207146 encoding for PIGU), or were already available in our lab, such as the vectors encoding for p24 and calnexin. Twenty µL of plasmid containing solutions with a concentration of $50\frac{ng}{\mu L}$ were sent to for sequencing to GATC Biotech AG. Primers used are listed in table 4. Primers sent to GATC for sequencing were prepared at $10\frac{pmol}{\mu L}$.

4.7 Thin layer chromatography (TLC) and coumarin click reaction

To analyse *in vivo* metabolic conversion of pacSph after distinct labeling durations, cells were washed four times with ice-cold PBS, scraped into 1.5 mL eppendorf tubes, centrifuged (5min/4°C/3000g) and pellets resuspended in 300 µL PBS. Lipid extracts were prepared as described in[85]. Briefly: 600 µL MeOH and 150 µL $CHCl_3$ were added, mixed and centrifuged (5min/14000g/RT). The supernatant was transferred into 2 mL eppendorf tubes, mixed with 300 µL $CHCl_3$ and 600 µL 0.1% acetic acid in H_2O and centrifuged (5min/14000g/RT). The lower phase was transfered into a clean 1.5 mL eppendorf tube end evaporated under vacuum in a speedvac (20min/30°C). Lipids were then either used directly for a copper derived click reaction with 3-azido-7-hydroxycoumarin or overlaid with N_2 and stored at -20°C.
A 10 mM $[MeCN]_4BF_4Cu$ containing solution was prepared by resuspension of the lyophilized powder in acetonitril according to the following formula: $\frac{[MeCN]_4BF_4Cu[\text{in mg}]\times 10^{-3}\times 10^6}{314.56\ \text{g/mol}\times 10^{-3}\times 10\ \text{mM}} = \mu L$. Final click mix consisted out of 250 µL 10 mM $[MeCN]_4BF_4Cu$, 1 µL of 44 mM 3-azido-7-hydroxycoumarin (in DMSO) and 1 mL EtOH. The standard mix consisted out of each 0.5 µL of 1 mM pacCer-/pacGlucCer-/pacPC-/pacSph- and clickSM-standard. Lipids were redissolved in 7 µL $CHCL_3$ and 30 µL of the click mix was added before evaporation in the speedvac (20min/45°C). Lipids were resuspended in 20 µL and the standard in 100 µL of mobile phase I ($CHCl_3$/MeOH/H_2O/AcOH 65:25:4:1). 20µL of lipids and standard were applied on a 10x10cm HPTLC Silica 60 glas plate (1.05641.001, Merck) with a CAMAG Linomat 5 and the TLC was developed with the CAMAG AUTOMATIC DEVELOPING CHAMBER 2 (ADC 2) or manually. TLC plates were developed using mobile phase I until 6 cm, followed by 8 cm with mobile phase II (hexane/EtOAc 1:1). Lipids were fluorescently labeled with 4% (v/v) 'Hünig's base' in hexane. Lipids were visualised using an Amersham Imager 600 and analysed with ImageJ (https://imagej.nih.gov/ij/).

4.8 Sodium Dodecyl Sulfate Polyacrylamide Gel Electrophoresis (SDS-PAGE)

Separation of proteins by size was achieved by employment of Laemlli's one-dimensional discontinuous SDS-PAGE[100]. Table 5 shows exemplarily the composition of a 1.5mm 7.5% SDS-PAGE. Samples mixed with SDS gel-loading buffer (for the respective loading buffers, see in the specific method sections) were added into the wells of the SDS-PAGE gel and run together with the SDS-PAGE pre-stained protein standard (1610373, Bio-Rad Laboratories GmbH) in SDS electrophoresis buffer (25 mM Tris, 192 mM Glycine, 0.1% SDS) for 15 min at 100V and then for the rest of the run at 200V. Detection of proteins was done by either a successive transfer to a PVDF membrane (see section 4.9) or by colloidal coomassie (B2025, Sigma-Aldrich) staining of the gel according to manufacturer's instructions.

4.9 Western blot

SDS-PAGE separated proteins were transferred onto a 45 µm polyvinylidene fluoride (PVDF) membrane via a wet blot protocol according to the Biorad Mini Trans-Blot® electrophoretic transfer cell manual. The PVDF membrane was activated by MeOH incubation, followed by equilibration in blotting buffer (25 mM Tris, 192 mM Glycine, 20% methanol). The transfer was conducted at room temperature at either 100V for 70 min (0.75mm gels), 180 min (1.5mm gels) or in the cold room at 30V for 16 hours (1.5mm gels). Afterwards, the membrane was blocked for one hour at room temperature or overnight at 4°C in 5% skim milk in PBS-T (0.05 % Tween-20). To remove unbound milk components, the membrane was washed four times with PBS-T before being incubated with primary antibodies for one hour at room temperature or overnight at 4°C. Incubation with secondary antibodies took place for one hour at room temperature or overnight at 4°C after the membrane was washed four times. All antibodies used are listed in table 3 and were diluted in PBS-T with 3-5% BSA. Before analysis with Li-cor Odyssey® CLx, membranes were washed 4x with PBS-T and taken up in PBS. Afterwards, membranes were taken up in MeOH and air-dried, before being stored at room temperature. Quantification of blots was done with Image Studio™ Lite from Li-cor. Equipment used for SDS-page and western blot are listed in table 6.

4.10 Analysis of transient expression of transamidase subunits

4.10.1 Optimisation of transient transfection parameters

HeLa cells were seeded ($1x10^5$ cells per 12-well) and 24 hours later transiently transfected with different concentrations of plasmid DNA (0.25/0.5/1/1.5 µg) encoding for the different subunits (PIGK/S/T/U and GPAA1) and the corresponding amounts of Fugene HD (E2311, Promega) according to manufacturer's instructions. Cells were harvested 24 hours later by washing with ice-cold PBS, incubated on ice (500 µL PBS/10min), scraped off in pre-cooled 1.5 mL tubes and pelleted (6min/13000 g/4°C). Pellets were resuspended in 50 µL HEPES lysis buffer (100 mM HEPES-NaOH pH 7.4, 100 mM NaCl, 5 mM EDTA, 1% (v/v) Triton-X-100, 0.5% (v/v) Na-deoxycholate, 1x PIC), incubated on ice (40 min/agitated every 10 min) and centrifuged (8min/16000g/4°C). Supernatant was transferred into a new 1.5 mL tube, while the pellet was resuspended with 50 µL of lysis buffer. Samples were stored overnight at -20°C. 11.25 µL of samples and 3.75 µL of 4x sample buffer were heated up (10min/95°C), loaded on a 13% SDS-PAGE (see section 4.8), transferred to

a PVDF-membrane (see section 4.9) and developed with mouse α-DDDKK antibody (see table 3). The amount of protein found in the supernatant was set into relation to the protein signal in the pellet to define the solubilisation efficency as $\frac{\text{A680}_{\text{Supernatant}}}{\text{A680}_{\text{Pellet}}} \times 100$. As a positive control, EGFP was used. GPAA1 expression was analysed for 24 and 48 hours.

4.10.2 Optimisation of solubilisation parameters for transient transfected GPAA1

Different detergents were tested to optimise solubilisation efficiency of transient GPAA1 transfections in HeLa cells ($1x10^5$ cells per 12-well, 0.25/0.5/1 µg plasmid DNA, 24 and 48 hours transfection time). The basic buffer (100 mM HEPES-NaOH pH 7.4, 100 mM NaCl, 1x PIC) was completed by addition of different detergents to form lysis buffer 1 (1% (v/v) Triton-X-100, 0.5% (v/v) Na-deoxycholate), buffer 2 (1% (v/v) octylglucoside), buffer 3 (1% (v/v) Nonident P40), and buffer 4 (1% (v/v) CHAPS). Experiment was executed as described in section 4.10.1. Calnexin, an ER resident protein, served as solubilisation control.

4.11 Immunprecipitation of transiently expressed or endogenous transamidase subunits

4.11.1 FLAG-beads: Immunoprecipitation (IP) of transiently transfectecd transamidase complex subunits with FLAG-beads

HeLa cells were seeded ($3x10^5$ cells per 6-well) and 24 hours later transiently transfected with 1 µg of plasmid DNA encoding for the different subunits (PIGK/S/T/U and GPAA1) and the corresponding amounts of Fugene HD (E2311, Promega) according to manufacturer's instructions. Cells were harvested 24 hours later by washing with ice-cold PBS, incubation on ice (750 µL PBS/10min), scraped off in pre-cooled 1.5 mL tubes, pelleted (6min/13000 g/4°C). Pellets were resuspended in 50 µL HEPES lysis buffer (100 mM HEPES-NaOH pH 7.4, 100 mM NaCl, 1% (v/v) Nonident P40, 1x PIC), lysis was performed on a test-tube rotator (1 1/2h/4°C) in the cold room and centrifuged (8min/16000g/4°C). Supernatant was transferred into a new 1.5 mL tube and 13.5 µL were used as input sample for the immunnoprecipitation (IP input). The rest of the supernatant was mixed with 50 µL three times pre-washed (500 µL PBS/30sec/8200g) FLAG-beads (F2426, Sigma-Aldrich) and incubated overnight on a test-tube rotator in the cold room. Samples were centrifuged (1min/8200g/4°C) and the supernatant transferred into a new 1.5 mL tube to be used as the flow-through (FT) sample containing proteins that did not bind to the FLAG-beads. Beads were washed as before and SDS sample loading buffer (250 mM Tris, pH 6.8, 20% (w/v) SDS, 40% (v/v) glycerol, 20% (v/v) β-mercaptoethanol, and 0.02% (w/v) bromophenol blue) was added to the different tubes (IP input:6.25 µL, FT:6.25 µL, beads: 25 µL), heated up (5min/95°C), loaded on a 13% SDS-PAGE (see section 4.8), transferred to a PVDF-membrane (see section 4.9) and developed with mouse α-DDDKK antibody (see table 3).

4.11.2 FLAG-beads: Co-IP of transiently transfectecd transamidase complex subunits

To analyse if transiently expressed GPAA1 can co-immunoprecipitate (co-IP) transamidase subunits the following experiment was performed:

HeLa cells were seeded ($2x10^6$ cells per 10 cm dish, 11 dishes overall) and 24 hours later transiently transfected with 4.3 µg of plasmid DNA encoding for (10 dishes GPAA1, 1 dish EGFP) and the corresponding amounts of Fugene HD (E2311, Promega) according to manufacturer's instructions. Cells were harvested 24 hours later by washing with ice-cold PBS (10 mL/dish), scraped off in ice-cold PBS and transferred into a pre-cooled 15 mL tube, pelleted (1min/500g/4°C), resuspended pellet in 8 mL lysis buffer (25 mM HEPES-NaOH pH 7.6, 200 mM NaCl, 0.5% (v/v) Nonident P40, 1x PIC), distributed equally into 1.5 mL ultracentrifuge tubes, and pelleted (90min/100.000g/4°C). Supernatants were pooled, input sample was taken (0.25% IP input: 20 µL + 4µl SDS sample loading buffer, 15min/95°C), mixed with 120µL three times pre-washed (1 mL PBS/30sec/8200g) FLAG-beads (F2426, Sigma-Aldrich) and incubated for 4 hours on a test-tube rotator in the cold room. One of the pellets of the centrifugation step was mixed with 50 µL of SDS sample loading buffer (250 mM Tris, pH 6.8, 20% (w/v) SDS, 40% (v/v) glycerol, 20% (v/v) β-mercaptoethanol, and 0.02% (w/v) bromophenol blue) and heated up (15min/95°C). 0.75 µL were taken out and mixed with 23.25 µL of SDS sample loading buffer to create a 0.25% sample (P) for SDS-PAGE. Took flow-through (FT) sample (0.25% FT: 20 µL + 4µl SDS sample loading buffer, 15min/95°C), transferred beads into 1.5 mL tubes, washed 3 times with wash buffer (lysis buffer + 10 mM DTT, 1min/8000g), added 200 µL of SDS sample loading buffer and eluted bound protein by heating up (15min/90°C). Samples were loaded on a 13% SDS-PAGE (see section 4.8), transferred to a PVDF-membrane (see section 4.9) and developed with antibodies against PIGS/K (rabbit) and α-DDDKK (mouse) antibody (see table 3).
To analyse if transiently expressed PIGT can co-IP transamidase subunits the following experiment was performed: HeLa cells were seeded ($2x10^6$ cells per 15 cm dish, 3 dishes overall) and 24 hours later transiently transfected with overall 12 µg of plasmid DNA encoding for PIGT and the corresponding amounts of Fugene HD (E2311, Promega) according to manufacturer's instructions. Cells were harvested 24 hours later by washing with ice-cold PBS (15 mL/dish), scraped off in ice-cold PBS and transferred into a pre-cooled 15 mL tube, pelleted (1min/500g/4°C), resuspended pellet in 8 mL lysis buffer (100 mM HEPES-NaOH pH 7.4, 100 mM NaCl, 1% (v/v) Triton-X-100, 0.5% (v/v) Na-deoxycholate, 1x PIC), incubated for 1 hour on a tube rotator in the cold room, transferred into 2 mL tubes, centrifuged (20min/10000g/4°C), transferred into 1.5 mL ultra centrifuge tubes and centrifuged (1h/100000g/4°C). Supernatant was pooled, mixed with 100 µL of four times pre-washed (1 mL lysis buffer/30sec/8200g) FLAG-beads and incubated overnight. As before samples before IP and not bound protein after IP were collected and used for SDS-PAGE. On the next day, samples were washed as before and proteins were eluted three times for 30 minutes in the cold room on the test tube rotator with 200 µL of 1 mg/mL FLAG-peptide (F3290,Sigma-Aldrich). Afterwards, to analyse the elution efficiency, beads were heated up (10min/70°C) with 100 µL of sample buffer (100 mM Tris, pH 8.3, 4 M Urea, 8% (w/v) SDS, 10% (v/v) glycerol, 50 mM DTT, and 0.01% (w/v) bromophenol blue). Samples were loaded on a 13% SDS-PAGE (see section 4.8), transferred to a PVDF-membrane (see section 4.9) and developed with antibodies against PIGK/T/S (rabbit, see table 3).

4.11.3 CNBr-beads: Co-IP of endogenous transamidase complex subunits

4.11.3.1 Coupling of α-GPAA1 antibody to CNBr-beads CNBr-beads (GE17043001, Sigma-Aldrich) were coupled with an α-GPAA1 antibody (sc-373710, SantaCruz) to immunoprecipitated endogenous GPAA1 according to manufacturer's instructions. Briefly, beads were washed with 10 mL of activation buffer (1 mM HCl). Antibodies were transferred into coupling buffer (100 mM $NaCHO_3$ pH 8.3, 500 mM NaCl) by using MicroSpin™ G-25 Columns (45001397, ThermoScientific)

and mixed with activated CNBr-beads. Beads were washed three times with 1 mL coupling buffer (1min/50g/4°C) and were blocked by addition of 1 mL of blocking buffer (100 mM TRIS-HCl pH 8) for 2 hours in the cold room. Afterwards, beads were washed (90sec/50g/4°C) four times, alternating with wash buffer A (100 mM AcOH, 500 mM NaCl) and B (100 mM TRIS-HCl pH 8, 500 mM NaCl). Finally, the beads were stored in 1 mL PBS (long term sotrage with 0.02% (w/v) sodium azide).

4.11.3.2 Validation of α-GPAA1 coupled CNBr-beads capability to IP endogenous GPAA1 from HeLa cell line To validate the functionality of the α-GPAA1 coupled CNBr-beads, HeLa cells were seeded ($2x10^6$ cells per 15 cm dish, 10 dishes overall) and grown for three days until approximately 90% confluency (around $1x10^8$). Cells were harvested 24 hours later by washing all plates with ice-cold PBS, scraped off in total 7 mL lysis buffer (20 mM HEPES-NaOH pH 7.6, 200 mM NaCl, 0.5% (v/v) Nonident P40, 1x PIC), washed plates with additional 7 mL lysis buffer and pooled samples. The overall 15 mL of lysate were incubated for 1 hour on a test tube rotator in the cold room. Samples were equally distributed in ultracentrifuge tubes, centrifuged (1h/100000g/4°C), pooled in a 15 mL falcon tube, mixed with CNBr-beads and rotated overnight in the cold room. One pellet of the centrifugation step was mixed with 50 µL of SDS sample buffer (250 mM Tris, pH 6.8, 12.5 mM EDTA, 500 mM DTT, 10% (w/v) SDS, 25% (v/v) glycerol, 0.1% (w/v) bromophenol blue), heated up (5min/95°C) and 5.2 µL of the solution was taken out and mixed with 16 µL SDS sample buffer and 59.2 µL H_2O to create a 0.13% pellet fraction for the SDS-PAGE. Beads were pelleted (3min/100g/4°C) and 80 µL of the supernatant was mixed with 16 µL of SDS sample buffer and heated up as before. Proteins were eluted from the beads by the following procedure. First, beads were washed twice (90sec/50g/4°C) with 1 mL PBS to reduce the detergent concentration. Beads were taken dry, placed on ice, mixed with 100 µL of elution buffer (100 mM glycine, pH adjusted to 2.4 with HCl), centrifuged (1min/50g/4°C), supernatant transferred into a new tube and mixed with neutralisation buffer (500 mM TRIS, 1500 mM NaCl) until the pH was between 6-7. The volume required was determined by mixing elution and neutralisation buffer in a 1.5 mL tube and periodically checking the pH value with pH paper. Beads were washed (1min/50g/4°C) with 1 mL elution buffer followed by 1 mL neutralisation buffer, repeated and stored in PBS at 4°C. Of the samples, 20 µL were loaded (pellet: 0.13%, flow-through:0.16%, eluate:7.81%) on four 13% SDS-PAGEs (see section 4.8), transferred to a PVDF-membrane (see section 4.9) and developed with α-PIGK/S/T/U (rabbit) and α-GPAA1 (mouse/rabbit) antibodies (see table 3).

4.11.3.3 Detection of endogenous transamidase complex with CNBr-beads from Raji cell line Raji cells (growth medium: RPMI1640 + 10% FBS, Pen/Strep) were grown in T75-flasks and $1x10^8$ cells were harvested by centrifugation (5min/200g/4°C), resuspended once in ice-cold PBS, pooled in a 15 ml falcon tube, centrifuged (2min/200g/4°C), resuspended in 10 mL lysis buffer (20 mM HEPES-NaOH pH 7.6, 200 mM NaCl, 0.5% (v/v) Nonident P40, 1x PIC) and incubated on a test tube rotator for 30 minutes in the cold room. Samples were transferred into 2 mL test tubes and two times centrifuged (20min/10000g/4°C, 1h/100000g/4°C). CNBr-beads from 4.11.3.2 were used and proceeded as described in that section. Only difference was that this time an input sample was taken and only input (0.135%), flow-through (0.135%) and the eluate (7.81%) were loaded. Experiment was repeated once more, this time with $1x10^9$ cells and 12.7% of the eluate loaded.

4.11.3.4 Efficency of GPAA1 IP between CNBr-beads and FLAG-beads To verify that CNBr-beads enrich a significant portion of GPAA1 available in a cell lysate, two 15 cm dishes of HeLa

cells were seeded ($2x10^6$) and 24 hours later transiently transfected with GPAA1 encoding plasmid (8 µg/dish) and the corresponding amounts of Fugene HD (E2311, Promega) according to manufacturer's instructions. Cells were harvested 24 hours later by washing with ice-cold PBS (10 mL/dish), scraped off in ice-cold PBS and transferred into a pre-cooled 15 mL tube, pelleted (1min/500g/4°C), resuspended pellet in 1.8 mL lysis buffer (20 mM HEPES-NaOH pH 7.6, 200 mM NaCl, 0.5% (v/v) Nonident P40, 1x PIC). Lysate was pre-cleared with two centrifugation steps (20min/10000g/4°C, 1h/100000g/4°C). 1.6% input sample was taken before the lysate was mixed with the CNBr-beads and incubated overnight on a test tube rotator in the cold room. Proteins were eluted as described in 4.11.3.2. 20% of eluate and 1.6% of flow-through (FT) were mixed with according volumes of SDS sample buffer (250 mM Tris, pH 6.8, 12.5 mM EDTA, 500 mM DTT, 10% (w/v) SDS, 25% (v/v) glycerol, 0.1% (w/v) bromophenol blue) and heated up (5min/95°C). The rest of the eluate was mixed with 30 µL three times pre-washed (1 mL lysis buffer/30sec/8200g) FLAG-beads (F2426, Sigma-Aldrich) and incubated overnight in the cold room. Beads were washed as before and bound protein was eluted by heating up (15min/90°C) after addition of 30 µL of SDS sample loading buffer. 1.6% flow-through (FT2) was taken and processed as before. Samples were loaded on a 13% SDS-PAGE (see section 4.8), transferred to a PVDF-membrane (see section 4.9) and developed with mouse α-DDDKK antibody (see table 3).

4.11.4 NHS-activated column: Co-IP of endogenous transamidase complex subunits

4.11.4.1 Coupling of α-GPAA1 antibody to NHS-activated column HiTrap® NHS (N-hydroxysuccinimide)-activated High Performance column (GE17071601, Sigma-Aldrich) was coupled with an α-GPAA1 antibody (sc-373710, SantaCruz) to immunoprecipitate endogenous GPAA1 according to manufacturer's instructions. To verify that the coupling reaction was successful before addition of the antibody, a test experiment was performed using BSA. Afterwards, the experiment was repeated with the antibody.
Briefly, coupling buffer (200 mM $NaHCO_3$, 500 mM Nacl, adjusted to pH 8.3), wash buffer A (500 mM ethanolamine, 500 mM NaCl, adjusted to pH 8.3), wash buffer B (100 mM sodium acetate, 500 mM NaCl, adjusted to pH 4), and activation buffer (1 mM HCl) were filtered through a 0.45 µM filter before use. Antibody was transferred into coupling buffer by using PD-10 columns (GE17085101, Sigma-Aldrich) and impurities were removed by an amicon Ultra-15 centrifugal filter unit (UFC901008, Merck). The NHS-column was connected to an GE Healthcare ÄKTA pure, washed with activation buffer and incubated with the antibody solution (30min/4°C) followed by three times recirculation of the anitbody solution over the column. Coupling efficiency was measured according to manufactures instructions. Column was stored at 4°C in storage buffer (50 mM Na_2HPO_4 pH 7, 0.1% sodium acetate).

4.11.4.2 Validation of α-GPAA1 coupled NHS-column capability to IP endogenous GPAA1 from HeLa cell line Five dishes of HeLa cells were seeded ($5x10^6$/15cm dish) and 24 hours later transiently transfected with GPAA1 encoding plasmid (8 µg/dish) and the corresponding amounts of Fugene HD (E2311, Promega) according to manufacturer's instructions. Cells were harvested 24 hours later by washing with ice-cold PBS (15 mL/dish), scraped off in ice-cold PBS and transferred into pre-cooled 15 mL tube, pelleted (5min/300g/4°C), resuspended pellet in 13 mL lysis buffer (20 mM HEPES-NaOH pH 7.6, 200 mM NaCl, 0.5% (v/v) Nonident P40, 1x PIC), incubated on a test tube rotator for 30 minutes in the cold room, and centrifuged (3min/300g/4°C). Supernatant was pre-cleared (20min/10000g/4°C, 1h/100000g/4°C) and NHS-column (see section 4.11.4.1) was equilibrated with lysis buffer. Pellets from both centrifugation steps were mixed with SDS sample

buffer (250 mM Tris, pH 6.8, 12.5 mM EDTA, 500 mM DTT, 10% (w/v) SDS, 25% (v/v) glycerol, 0.1% (w/v) bromophenol blue) and heated up (5min/95°C). The sample was injected via super loop (19785001, GE LifeSciences), column was washed with lysis buffer, proteins were eluted with elution buffer (100 mM glycine pH 3), and 250 µL fractions were taken. Eluted fractions were mixed 1:10 with neutralisation buffer (1 M glycine pH 9). 20 µL of the fractions were mixed with 5 µL SDS sample buffer and heated up (5min/95°C). After sample application, the flow-through was mixed with 40 µL three times pre-washed (1 mL lysis buffer/30sec/8200g) FLAG-beads (F2426, Sigma-Aldrich) and incubated overnight in the cold room. Beads were washed as before, taken dry, mixed with 30 µL of SDS sample loading buffer and bound protein was eluted by heating up (15min/90°C). An input sample was taken before mixing sample with beads and a flow-through sample was taken after the overnight incubation. Both were mixed with SDS sample buffer and heated up as before. Samples were loaded on a 13% SDS-PAGE (see section 4.8), transferred to a PVDF-membrane (see section 4.9) and developed with mouse α-DDDKK antibody (see table 3).

4.11.5 FLAG-beads: Separation of transiently expressed transamidase subunits via 2D-gel electrophoresis

A 2D-gel electrophoresis experiment was conducted to simultaneously analyse protein-lipid interactions of different transamidase subunits (PIGK/T/S and GPAA1). For this experiment, an Ettan IPGphor 3 IEF System, kindly provided by professor Krauth-Siegel from the BZH Heidelberg, was used together with 7 cm long Immobiline® DryStrip pH 3-11 NL(GE17600373, Sigma). Strips were rehydrated overnight with 150 µL of rehydration solution (7 M urea, 2 M thiourea, 2% (w/v) CHAPS, 0.5% (v/v) IPG buffer (RPN6301, GE Healthcare), 0.002% bromophenol blue) in an immobiline drystrip reswelling tray and covered with cover fluid (GE171335-01, GE Healthcare). Samples used for the experiment were prepared according to the following procedure. HeLa cells were seeded ($2x10^6$ cells per 10 cm dish) and 24 hours later transiently transfected with 4.3 µg of plasmid DNA (PIGK/T/S or GPAA1) and the corresponding amounts of Fugene HD (E2311, Promega) according to manufacturer's instructions. Cells were harvested 24 hours later by washing with ice-cold PBS (10 mL/dish), scraped off in 1 mL of ice-cold PBS, centrifuged (5min/300g/4°C), resuspended in 800 µL lysis buffer (20 mM HEPES-NaOH pH 7.6, 200 mM NaCl, 0.5% (v/v) Nonident P40, 1x PIC) and incubated for 30 minutes on a test-tube rotator in the cold room. Not solubilised proteins were removed by two centrifugation steps (10min/10000g/4°C, 1h/100000g/4°C) and 80 µL of the supernatant was mixed with 16 µL of sample loading buffer (250 mM Tris, pH 6.8, 20% (w/v) SDS, 40% (v/v) glycerol, 20% (v/v) β-mercaptoethanol, and 0.02% (w/v) bromophenol blue). Pellets of the centrifugation steps were mixed with 50 µL of sample loading buffer and all samples were heated up (10min/95°C). 20 µL of the supernatant sample (2%) and an equal amount of the pellets (1 µL with 19 µL of sample loading buffer) were loaded on a 13% SDS-PAGE (see section 4.8), transferred to a PVDF-membrane (see section 4.9) and developed with mouse α-DDDKK antibody (see table 3). Supernatants were pooled, mixed with 30 µL three times pre-washed (1 mL PBS/30sec/8200g) FLAG-beads (F2426, Sigma-Aldrich) and incubated overnight. Beads were washed 3 times with lysis buffer, eluted for 5 minutes with 100 µL of elution buffer (100 mM glycine-HCL pH 3.5), centrifuged (5sec/8200g), supernatant transferred into new tube, pH adjusted by addition of 10 µL of buffer B (500 mM TRIS-HCL pH 7.4, 1500 mM NaCl), snap frozen in liquid N_2 and stored at -20°C.
After verification of successful expression of the different subunits via western blot, the input samples as well as the eluted IP fractions were used for 2D-gel electrophoresis. Protein concentrations were measured via BCA-Assay (23225, ThermoFisher) and 20 µg of each sample set (input

IP, eluted IP fraction) were desalted according to Wessel Flügge[101]. Proteins were resuspended in 30 µL sample preparation solution (7M urea, 2M thiourea, 4% (w/v) CHAPS, 2% (v/v) IPG buffer, 40mM DTT, 0.002% bromophenol blue), pooled together and applied to the IPG strip via cup loading. Isoelectric focussing was performed overnight with a two-step program (Grad at 700V for 12-16 hours and Step at 3000 V for 2-4 hours). After isoelectric focussing, the IPG strip was equilibrated for SDS-PAGE. First, the strip was rinsed with H_2 before placed in SDS equilibration buffer (75 mM Tris-HCl pH 8.8, 6 M Urea, 29.3% (v/v) glycerol, 2% (w/v) SDS, 0.002% bromophenol blue) for 10 minutes each. The strip was then, together with a whatman cellulose filter paper soaked with 3 µL of SDS-PAGE standard, placed on top of a 12% SDS-PAGE separation gel and overlaid with agarose (20 mL Läemmli[100] buffer (60 mM Tris-Cl pH 6.8, 2% (w/v) SDS, 10% (v/v) glycerol, 5% (v/v) β-mercaptoethanol, 0.01% bromophenol blue), 100 mg agarose, 0.002% bromophenol blue). After solidification, SDS-PAGE and the following western blot were performed as before. For detection, mouse and rabbit α-DDDKK antibodies were used and the gel was stained with colloidal coomassie.
To determine hydrophobic properties of different transamidase subunits and their susceptibility for 2D-gel electrophoresis, the grand average of hydropathy (GRAVY) score was calculated with the bioinformatics tool http://www.gravy-calculator.de/. Sequences used as input for this tool are listed in the appendix (see section 8.5).

4.12 CRISPR/Cas9 guided cell line generation and validation containing C-terminal tagged GPAA1 to study protein-lipid interactions of the transamidase complex

The general principal of the endogenous tagging of GPAA1 is the introduction of a double strand break in the genomic sequence of GPAA1. To achieve this, specific guide RNAs (gRNA) target the CRISPR associated protein 9 (Cas9) into close proximity of the 3'-terminal region of the genomic GPAA1 sequence. Once in place, Cas9 will introduce a double strand break in the DNA and, by providing a homologous DNA template containing the 3xFLAG-Twin-Streptag, the cellular homology directed repair (HDR) mechanism is hijacked. Positive single cell clones are selected via PCR and insertion is verified by sequencing of the PCR products (see chapter 4.6).
The plasmids necessary to facilitate the addition of a 3xFLAG-Twin-Streptag to the c-terminal part of endogenous GPAA1 were purchased from Addgene (Cambridge, USA). The vector MLM3636 for expression of GPAA1 specific gRNAs was a gift from Keith Joung (Addgene plasmid # 43860). The plasmid hCas9[102] encodes for a human codon optimised caspase 9 and was a gift from George Church (Addgene plasmid # 41815). The vector containing the tag, AAVS1-Puro-PGK1-3xFLAG-Twin-Strep[88] was a gift from Yannick Doyon (Addgene plasmid # 68375).

4.12.1 Selection of cell line for endogenous tagging

Different cell lines (human fibroblasts, mouse embryonic fibroblasts H806, mus musculus brain neuroblastoma N2A, adenocarcinomic human alveolar basal epithelial cell line A549, hepatocarcinoma cell line Huh-7, cervix carcinoma cell line HeLa, human embryonic kidney cell line HEK293, lymphoblast-like cell line Raji) were tested for endogenous GPAA1 expression levels to select a cell line suitable for C-terminal tagging of GPAA1.
Cells were washed once with ice-cold PBS, resuspended (PBS with 2xPIC), centrifuged (1h/100000g/4°C), resuspended with lysis buffer (PBS, 1% (v/v) Triton-X-100, 0.1% (v/v), 1x PIC)

and rotated for one hour on a spinning wheel in the cold room. Protein concentrations were measured via BCA-Assay (23225, ThermoFisher) and 50 µg of cell lysate were precipitated according to Wessel Flügge [101]. Proteins were resuspended in 20 µL SDS sample buffer (250 mM Tris, pH 6.8, 12.5 mM EDTA, 500 mM DTT, 10% (w/v) SDS, 25% (v/v) glycerol, 0.1% (w/v) bromophenol blue), heated up (10min/95°C), loaded on a 13% SDS-PAGE (see section 4.8), transferred to a PVDF-membrane (see section 4.9) and developed with a mouse α-GPAA1 antibody (see table 3). GPAA1 intensities were quantified and compared against the signal of the HeLa cell line.

4.12.2 Design of gRNAs for genomic GPAA1 loci

To design guide RNAs (gRNA), the genomic context of the GPAA1 loci on chromosome 8 was retrieved from Ensembl (release 84, 25.02.2016, ftp://ftp.ensembl.org/pub/release-84/fasta/homo_sapiens/dna/, for full sequence see section 8.1) and a search query containing partially GPAA1 exon 12, the stop codon and a short sequence of the 3'untranslated region (UTR) (CCCTGCTGGCTGCTTTTCTGGAATGTGCTCTTCTGGAAGTGAGATCTGCCTGTC) was designed and used as input for the gRNA prediction tool CRISPR Design (http://crispr.mit.edu/) from the Zhang lab (MIT, USA) to retrieve possible gRNA candidates. The top 3 candidates were ordered as 5'-phosphorylated single stranded nucleotides (biomers.net GmbH) containing 5'-ACACC and 3'-G on the plus strand as well as a 5-'AAAAC and 3'-G on the minus strand (see table 7 for the full sequences). Plus and minus strands oligonucleotides for each gRNAs were mixed in a 1:1 ratio and heated up until 95°C before stepwise lowering the temperature to 4°C to create gRNA dimers ready for insertion into the gRNA vector MLM3636.

4.12.3 Cloning of gRNAs into MLM3636

10 µg of MLM3636 were digested (30min/50°C) with 25 units BsmBI (R0580S, New England Biolabs), heat-inactivated (20min/80°C) and ethanol precipitated. In short: One tenth volume of sodium acetate pH 5.0 and two and a half volume of 100% EtOH were added to digested plasmids. DNA was precipitated (20min/-20°C), centrifuged (15min/17900g), pellet washed with 1 mL 70% EtOH (5min/17900g), and air dried. Pellet was resuspended in 20.25 µL H_2O and dephosporylated (30min/37°C) with 25 units calf intestinal alkaline phosphatase (M0290L, New England Biolabs). Finally, DNA was separated by agarose gel electrophoresis and fragments of interest were purified with the QIAquick Gel Extraction Kit (28706, Qiagen). To insert the gRNA into MLM3636, the amount of insert and vector DNA needed for the ligation reaction were calculated according to the following formula.

$$\text{insert [ng]} = \frac{\text{insert size [bp]}}{\text{vector size [bp]}} \times \text{ng of vector} \times 5 \text{ (for blunt end) or } 3 \text{ (for sticky end) ligation}$$

T4 DNA Ligase (M0202S, New England Biolabs) catalysed ligation reaction took place at 16°C overnight in a total volume of 10 µL and bacteria were transformed as described before (see section 4.4).

4.12.4 Determination of gRNA capabilities to induce double strand breaks in genomic GPAA1

To determine the capability of selected gRNAs to introduce double strand breaks in the genomic region of GPAA1, HelaΔS1PL cells were seeded at a concentration of $1x10^5$cells/6-well and co-transfected 24 hours later with 0.6 µg of MLM3636-gRNA# 1-3 and hCas9, respectively. After 24 and 72 hours transfection, cells were washed twice with ice-cold PBS, scraped off in 500 µL PBS and pelleted (5min/3000g/4°C). After resuspension in 200 µL PBS, genomic DNA was extracted according to manufactures instructions with the DNeasy Blood & Tissue Kit (69504, Qiagen) and used for amplification of a 1350bp long fragment covering the area around the STOP codon of the genomic GPAA1 loci. For this, the primer pair genomic_GPAA1_FW2 and genomic_GPAA1_REV2 was used (see table 8). PCR fragments from wild-type and gRNA transfected cells were mixed in a 1:1 ratio, heated up (10min/95°C) to create single stranded DNA fragments which then were allowed to form DNA-heteroduplexes by stepwise temperature reduction to 4°C. Employing the fact that specific nuclease exist that cut mismatched double stranded DNA, such as the result of an error in the double strand break repair mechanism, the surveyor mutation detection kit for standard gel electrophoresis (71269249, Integrated DNA Technologies, Belgium) was used according to manufactures instruction to determine which gRNA was able to introduce a double strand break.

4.12.5 Design and cloning of homology arms for creation of 3xFLAG and 2xStrep-tag donor plasmid

To generate the donor plasmid carrying the homology directed repair template, a 747bp long section upstream and a 776bp long section downstream of the genomic GPAA1 stop codon sequence were selected and complemented with restriction enzyme target sequences (5'-NdeI/3'-NgoMIV for the upstream section, 5'-BstBI/3'-EcoRI for the downstream section) as well as a short 5'- and 3'-poly(A)-section to facilitate restriction enzyme binding. All mentioned enzymes (R0111S/R0564S/R0519S/R3101S) were obtained from New England Biolabs. The upstream section represents the left homology arm (LHA), while the downstream section represents the right homology arm (RHA). LHA and RHA were synthesized as g-Block fragments (Integrated DNA Technologies, Belgium). For exact sequences used, see section 8.4. 100 ng of LHA were digested with 20 units of NdeI and NgoMIV (30min/37°C) and the ready-to-insertion fragments were gel purified as described in section 4.12.3. 33ng of the LHA were used in an overnight ligation reaction with 50 ng of NdeI/NgoMIV digested pAAVS1_Puro_PGK1_3xFLAG_Twin_Strep. Following heat-inactivation (20min/65°C), the ligation reaction was used for transformation (see section 4.4) of *E. coli* DH-5α. After verification of successful integration of the LHA, 10 µg of plasmid were sequentially digested with 30 units of EcoRI (1h/37°C, 20min/65°C heat-inactivation) and 30 units BstBI (1h/65°C). 50 ng Methanol precipitated plasmid (see section 4.12.3) was then used for ligation reaction with 39 ng identically digested RHA g-BLock fragment. Finally, clones were tested by sequencing for correct insertion of LHA and RHA and used for the CRISPR experiment.

4.12.6 Endogenous tagging of GPAA1 and selection of positive clones

HelaΔS1PL cells were seeded at a concentration of $1x10^6$cells on a 10 cm dish and 24 hours later triple transfected with 2 µg MLM3636-gRNA#1-3, 2 µg hCas9 and 4 µg of the donor plas-

mid as described in [88]. After 72 hours of transfection, single cell clones, derived by serial dilutions, were seeded in 96 well plates and propagated until 6-well format was reached. At this point cells were harvested and genomic DNA was extracted as before (see section 4.12.4) and success of tag integration was determined for each single cell clone via PCR with the primer pair genomic_GPAA1_FW2/genomic_GPAA1_REV2 (see table 8). Clones containing one band at 1527bp were expected to be a successful homozygous tag integration, while one band at 1350bp defined a wild-type clone. Having two bands at the respective heights were termed a heterozygous integration, containing wild-type and tagged allele of GPAA1. Verification of clones was achieved by gel-purification of the PCR product and amplification with the primer pair genomic_GPAA1_FW3/REV3 (see table 8). The 1356bp product was digested with EcoRI/XhoI (40min/37°C, heat-inactivated for 20min/65°C), ethanol precipitated (see section 4.12.3), ligated into EcoRI/XhoI digested pCMV6 (4816bp), and transformed into bacteria as before (see section 4.4). Finally, positive clones were verified by sequencing as described in 4.6 with the primers genomic_GPAA1_FW2 and genomic_GPAA1_REV2 from table 8.

4.12.7 Affinity enrichment of endogenous C-terminal tagged GPAA1

The following experiments were conducted to determine if the endogenous addition of C-terminal 3xFLAG and 2xStrep-tag allows for affinity enrichment of GPAA1. For experiments regarding the ability to enrich transamidase complex subunits over the FLAG-tag, see section 4.12.8.

4.12.7.1 Streptactin affinity enrichment of endogenous GPAA1 from whole cell lysate To determine conditions for successful enrichment of endogenous GPAA1 with streptactin-beads (2120125, Iba), the following experiment was conducted. Three dishes of HeLaΔS1PL GPAA1#76 cells were seeded (3x10^6 cells/ 10 cm dish) per condition. 24 hours later, cells were washed once with ice-cold PBS, scraped off in 1 mL ice-cold PBS, centrifuged (5min/3000g/4°C), resuspended in 1 mL lysis buffer (100 mM Hepes-NaOH ph 7.4, 100 mM NaCl, 1% (v/v) Triton-X-100, 0.1% (v/v) Na-deoxycholate, 2x PIC) and rotated for 1 hour on a test tube rotator in the cold room. Supernatant was cleared up by two centrifugation steps (20min/10000g/4°C and 1h/100000g/4°C) and all three tubes of one condition were pooled. 150 µL were taken out as an input sample and MeOH/$CHCl_3$ preciptated as described in 4.12.7.2 with the following volumes used for first step: 600 µL MeOH, 300 µL $CHCl_3$, 450 µL H_2O. Samples were resuspended (10 µL 4% SDS in lysis buffer, 10min/1400rpm/37°C), mixed with 10 µL SDS sample buffer (250 mM Tris, pH 6.8, 12.5 mM EDTA, 500 mM DTT, 10% (w/v) SDS, 25% (v/v) glycerol, 0.1% (w/v) bromophenol blue), heated up (10min/95°C) and stored at -20°C. The supernatant was diluted with lysis buffer to a final volume of 9 mL and 10% SDS containing lysis buffer was added to a final concentration of 0.1% SDS. The sample was mixed with 60/400 µL of three times pre-washed (800 µL lysis buffer, 1min/100g/4°C) streptactin-beads slurry (2120125, Iba) and rotated overnight on a test tube rotator in the cold room. Beads were washed as before and flow-through was taken and precipitated as the input sample. Beads were taken dry, mixed with 400 µL of elution buffer (SDS sample buffer with 30 mM biotin), incubated (15min/RT), heated up (15min/95°C), distributed into 2 mL tubes and MeOH/$CHCl_3$ preciptated (800 µL MeOH, 400 µL $CHCl_3$, 600 µL H_2) and resuspended (20 µL 4% SDS in PBS, 10min/1400rpm/37°C) and transferred into a new tube. Samples were loaded on a 7.5% SDS-PAGE (see section 4.8), transferred to a PVDF-membrane (see section 4.9) and developed with a mouse α-DDDKK antibody (see table 3).

4.12.7.2 Streptactin affinity enrichment of Alexa-647-N_3 clicked whole cell lysate and MeOH/$CHCl_3$ precipitation steps HeLaΔS1PL GPAA1#76 cells were seeded ($4x10^6$ cells/ 10 cm dish). 24 hours later, cells were washed once with 10 mL PBS and labeled with 5 mL of labeling media (DMEM containing Pen/Strep, DL-FBS (delipidated FBS) and 5 µM pacSph). After 4 hours of labeling time, cells were washed 3x with 10 mL ice-cold PBS, then overlayed with 5 mL and subjected to UV-light irradiation under a high intensity lamp for 5 min. PBS was aspirated and cells were scraped off in 1 mL ice-cold PBS and centrifuged (5min/4°C/3000g). The pellet was taken up in 1 mL lysis buffer (PBS, 1% (v/v) Triton-X-100, 0.1% (v/v) SDS, 0.125 U/mL benzonase, 2x PIC), resuspended by sonication (5x10 seconds, on ice between) and lysis was performed for 2 hours on a test-tube rotator in the cold room. Supernatant was centrifuged twice (20min/10000g/4°C, 1h/100000g/4°C), distributed equally on four tubes (250 µL/tube) and snap frozen in liquid N_2 and stored overnight at -20°C.
Proteins were two times MeOH/$CHCl_3$ precipitated. First, samples were sequentially mixed with 600 µL MeOH/200 µL $CHCl_3$/850 µL H_2O, centrifuged (5min/14000g/RT), upper phase removed, 400 µL MeOH added, centrifuged (30min/14000g/RT, swing out rotor) and supernatant decanted. Pellet was air-dried, resuspended (vortex/sonicate/37°C at 1400rpm) in 50 µL buffer A (4% SDS in PBS, 2x PIC) and diluted to 1% SDS by addition of 150 µL buffer B (PBS, 2x PIC). For the second precipitation round, 480 µL MeOH, 160 µL $CHCl_3$, and 680 µL H_2O were used. Protein concentrations were measured via BCA-assay (23225, ThermoFisher) and adjusted to 100 µg per tube. 3.25 µL of the click mix (1.36 µL 40 mM $CuSO_4$ in H_2O, 1.08 µL 50 mM TCEP H_2O, 0.54 µL 10 mM TBTA, and 0.54 µL 10 mM Alexa-647-N_3) was added to 200 µL supernatant and incubated in the dark (4h/1000rpm/37°C). Afterwards, the click reaction was two times MeOH/$CHCl_3$ precipitated as before, only that samples were pooled between the first and the second precipitation, snap frozen in N_2 and stored overnight at -20°C. After the second precipitation, 10% input sample was taken, mixed with SDS sample buffer (250 mM Tris, pH 6.8, 1.8% (w/v) SDS, 45% (v/v) glycerol, 22.5% (v/v) β-mercaptoethanol and 0.003% (w/v) bromophenol blue) and heated up (10min/95°C). The rest of the sample was diluted to 0.1% SDS concentration by addition of lysis buffer, mixed with 50 µL three times pre-washed (800 µL lysis buffer, 1min/100g/4°C) streptactin-beads (2120125, Iba) and rotated for 2 hours on a test tube rotator in the cold room. Beads were washed three times with lysis buffer, proteins were eluted by addition of 15 µL elution buffer (100 mM Tris/HCl pH 6.8, 4% SDS (w/v), 4% (v/v) β-mercaptoethanol), heated up (15min/95°C) and transferred into a new 1.5 mL tube. Beads were subjected to a second elution step (20 µL SDS sample buffer, 15min/95°C), supernatant taken off an pooled with first elution step. 0.3% flow-through (FT) sample was taken and treated as the input sample before. Samples were loaded on a 7.5% SDS-PAGE (see section 4.8), in-gel fluorescence was measured, transferred to a PVDF-membrane (see section 4.9) and developed with a mouse α-GPAA1 antibody (see table 3)

4.12.7.3 Streptactin affinity enrichment of Alexa-647-N_3 clicked whole cell lysate and MeOH precipitation steps This experiment was, except the listed changes in this paragraph, conducted as before (see 4.12.7.2) to investigate the possibility to exchange the MeOH/$CHCl_3$ precipitation steps with MeOH precipitation steps. Cell lysate was distributed in 4 tubes with each 200 µL and directly snap frozen in N_2. After samples were thawed up, a BCA-Assay (23225, ThermoFisher) was conducted and 3.25 µL of click mix were added to each aliquot. Click reactions were stopped by addition of 1.8 mL of ice-cold MeOH and stored overnight at -80°C. Samples were centrifuged (20min/17000g/4°C in a swing out rotor), pellets resuspended (vortex/sonication) in 1 mL of MeOH, and centrifuged as before. This step was redone 1-3 times and finally the pellets were

air dried and resuspended with 20 µL of 4% (w/v) SDS in PBS. Aliquots were pooled and protein concentrations were determined by BCA-Assay. Samples were diluted to 0.1% SDS concentration by addition of lysis buffer, mixed with streptactin beads, and incubated on a test tube rotator (1h/RT in the dark). Beads were washed three times, 20 µL 3 mM biotin (29129, ThermoFisher) was added to the beads, incubated for 15 minutes, heated up (15min/95°C), and supernatant was transferred to a new tube. For each sample, 400 µL flow-through (3.5%) was taken, split into two 2 mL test tubes, precipitated according to Wessel Flügge [101], resuspended in 20 µL of 4% (v/v) SDS in lysis buffer, pooled, mixed with 10 µL SDS sample buffer (250 mM Tris, pH 6.8, 12.5 mM EDTA, 500 mM DTT, 10% (w/v) SDS, 25% (v/v) glycerol, 0.1% (w/v) bromophenol blue) and heated up (10min/95°C). SDS-PAGE and the rest of the experiment was conducted as before (see section 4.12.7.2).
In a variation of this experiment, the click reaction was diluted to 0.1% SDS concentration and directly applied to the streptactin beads, without previous precipitation steps, and incubated overnight.

4.12.7.4 Neutravidin affinity enrichment of Alexa-647-N_3 clicked whole cell lysate To verify that the strep tag did not interact in any way with neutravidin-beads (29202, ThermoFisher) used for the biotin click protocol, an Alexa-647-N_3 experiment as described in 4.12.7.2 was conducted. The only difference was that, instead of Streptactin-beads for affinity enrichment, neutravidin-beads were used.

4.12.8 Separation of endogenous transamidase subunits via SDS-PAGE

To analyse if it is possible to separate the endogenous subunits with comparable molecular weight (PIGS/T and GPAA1) via SDS-PAGE, different commercially available kits as well as a hand made gel electrophoresis chamber were compared. The commercial kits NuPAGE™ 4-12% Bis-Tris protein gel, NuPAGE™ 7% Tris-Acetate protein gel and the Bolt™ 8% Bis-Tris plus gel (NP0321BOX, EA0355BOX, NW04120BOX, ThermoFisher) were used according to manufactures instructions. Additionally, 7% and 10% tris-glycine gels (as described in 4.8) were compared and run until only the 37 kDa protein marker band was left on the gel. Furthermore, a hand made 7% tris-glycine gel with dimensions 18x16cm was cast to see if the elongated separation gel allows for spearation of the subunits. This gel was then transferred to a Trans-Blot® Cell(1703946,Bio-Rad), kindly provided by RG Wieland from the BZH Heidelberg, blotted for 16 hours, the PVDF-membrane cut into four equal size sections, and developed as described before (4.9). To measure the effective separation range, the width of the marker sizes and the distance between the 37, 50 and 75 kDA bands were measured with a ruler.
Samples were prepared as follows: fully confluent 15 cm dishes with HeLaΔS1PL GPAA1#76 cells were washed once with ice-cold PBS, scraped off, centrifuged (5min/3000g/4°C), resuspended in 1 mL lysis buffer (100 mM HEPES-NaOH pH 7.5, 100 mM NaCl, 1% (v/v) Triton-X-100, 0.1% Na-Deoxycholate, 1xPIC), rotated for 1 hour on a spinning wheel in the cold room, centrifuged twice (20min/10000g/4°C, 1h/100000g/4°C) and used for IP as described in 4.11.1.

4.12.9 Purification of endogenous transamidase complex using styrene maleic anhydride (SMA) co-polymer

4.12.9.1 FLAG-IP of endogenous transamidase complex after solubilisation with SMA A fully confluent 15 cm dish of HeLaΔS1PL GPAA1#76 was used for the experiment. Cells were washed with 13 mL ice-cold PBS, scraped off in 1 mL ice-cold PBS in a 1.5 mL ultracentrifuge tube, centrifuged (5min/3000g/4°C), and supernatant was aspirated and pellet's wet weight was determined. The pellet was resuspended with 500 µL homogenisation buffer (100 mM Hepes pH 7.2, 500 mM NaCl, 2x PIC, 1 µL benzonase/2 mL buffer) per 25 mg wet weight by pipetting and sonication until solution was homogeneous. 1 µL of cell solution was mixed with 4 µL homogenisation buffer and 5 µL trypan blue and applied to a Neubauer counting chamber to verify successful disruption of the cell wall. Membrane fractions were created by centrifugation (1h/100.000g/4°C/) and the wet weight of the pellet was determined. To aid formation of styrene maleic anhydride co-polymer (XIRAN SL30010 S30, Polyscope) micro domains, protein solutions were adjusted to 42.5 mg/mL. Volume of SMA lysis buffer needed for solubilisation was calculated according to the following formula. $\frac{\text{wet weight pellet}}{42.5\frac{mg}{mL}} \times 1000 = \text{Volume of 2.5\% SMA solution}$. A 10% SMA stock was created (100 mM Hepes, pH 6.5, 500 mM NaCl, 2x PIC, 10% SMA) and the protein was resuspended as before in 75% of the calculated volume with SMA devoid buffer (100mM Hepes pH 6.5, 500 mM NaCl, 2.66x PIC). To create a 2.5% SMA concentration in the lysate, the solution was adjusted to the calculated volume by addition of the 10% SMA stock. Lysis was performed for 2 hours on test tube rotator in the cold room. Samples were centrifuged (1h/100000g/4°C), 10% of the supernatant was taken as input sample, buffer was added until a final volume of 100 µL, and stored overnight at -20°C. The rest of the supernatant was mixed with 50 µL three times pre-washed (1 mL buffer, 1min/500g/4°C) FLAG-beads (F2426, Sigma-Aldrich) and incubated overnight on a test-tube rotator in the cold room. Beads were washed as before and 10% flow-through was taken and adjusted to 100 µL. Input and sample were precipitated according to Wessel Flügge [101]. Pellets were resuspended in 40 µL sample buffer (250 mM Tris, pH 6.8, 20% (w/v) SDS, 40% (v/v) glycerol, 20% (v/v) β-mercaptoethanol, and 0.02% (w/v) bromophenol blue) and heated up (10 min/95°C). Proteins were eluted from the beads by addition of 40 µL sample buffer under the same conditions. All samples were loaded on a 13% SDS-PAGE (see section 4.8), transferred to a PVDF-membrane (see section 4.9) and sequentially developed with rabbit α-PIGU/K/T and mouse α-DDDKK antibody (see table 3).
The same experiment was repeated, this time with the order of sequentially administered antibodies being rabbit α-PIGK/S and mouse α-DDDKK antibody.

4.12.9.2 FLAG-IP of endogenous transamidase complex after solubilisation with SMA and mass spectrometric analysis Experiment was performed as described in section 4.12.9.1 with the following differences: 8x15 cm dishes of HeLaΔS1PL GPAA1#76 were seeded. On day two, beads were washed, transferred to a glass tube, volume was brought to 500 µL with wash buffer and handed to Iris Leibrecht for lipid extraction. Mass spectrometric analysis was performed jointly with Christian Lüchtenborg (both RG Brügger).

4.12.10 Validation of transamidase function by monitoring GPI-anchor protein CD59 surface arrival via surface biotinylation

HeLaΔS1PL GPAA1#76 and HeLaΔS1PL cells were seeded (3x10^5 cells/ 6-well) and 24 hours later transfected with 1 µg pME-mCherry-FLAG-CD59-GPI, which was a gift from Reika Watanabe (Addgene plasmid # 50378). After 48 hours, cells were washed once with PBS Ca/Mg (1 mM $MgCl_2$, 0.1 mM $CaCl_2$), incubated under shaking conditions (30min/4°C) with incubation buffer (824 mM

Sulfo-NHS-SS-Biotin, 10 mM Triethanolamine pH 9.0, 150 mM NaCl, 2 mM $CaCl_2$), washed with quenching buffer (PBS Ca/Mg, 100 mM Glycine), and incubated 20 minutes under previous conditions. Cells were washed with ice-cold PBS, scraped off, centrifuged (5min/3000g/4°C), and the pellet was resuspended in 300 µL lysis buffer (PBS, 1% (v/v) Triton-X-100, 0.1% (w/v) SDS in PBS, 2x PIC) by pipetting and sonication until solution was quite homogeneous. After lysis (15min/1200rpm/24°C) and centrifugation (10min/16000g/4°C), supernatant was transferred into a new tube, 30 µL were taken out as 10% input sample and stored at -20°C. The rest of the supernatant was mixed with 50 µL three times pre-washed (500 µL lysis buffer, 1min/3000g/4°C) high capacity BCA-assay beads (29202, ThermoFisher) and incubated overnight on a test-tube rotator in the cold room. Beads were washed as before and 10% flow-through (FT) sample was taken. Input and FT were mixed 1:1 with SDS sample buffer (250 mM Tris, pH 6.8, 12.5 mM EDTA, 500 mM DTT, 10% (w/v) SDS, 25% (v/v) glycerol, 0.1% (w/v) bromophenol blue). 50 µL of SDS sample buffer were added to elute proteins from beads. All samples were incubated (30min/1000rpm/50°C) before being loaded on a 13%SDS-PAGE (see section 4.8), transferred to a PVDF-membrane (see section 4.9) and sequentially developed with rabbit α-DDDKK and α-CD59 antibody (see table 3) Input and eluate signal intensities were quantified and derived ratios ($\frac{eluate}{input}$) used to test for difference between both cell lines via two-sided T-Test.

4.13 Analysis of protein-lipid interactions of transiently transfected GPAA1

4.13.1 Optimisation of pacSph labeling of transiently transfected GPAA1 in HeLaΔS1PL cells

4.13.1.1 CuAAC of Alexa-647-N_3 on FLAG-beads with Nonident P40 HeLaΔS1PL cells were seeded ($1.5x10^5$ cells per 6-well) and 24 hours later transiently transfected with 0.75 µg of plasmid DNA encoding for GPAA1 and the corresponding amounts of Fugene HD (E2311, Promega) according to manufacturer's instructions. The next day, cells were washed once with PBS before 1 mL labeling media (DMEM containing Pen/Strep, delipidated FBS, 3 µM pacSph) was added and incubated for 30 minutes (37°C/5% CO_2). Cells were washed with ice cold PBS (3x 1 mL), overlaid with 1 mL ice-cold PBS, subjected to UV-light irradiation under a high intensity lamp for 5 min, scraped off in 1 mL of ice-cold PBS, centrifuged (5min/3000g/4°C) and the pellet resuspended in 100 µL of lysis buffer (20 mM HEPES-NaOH pH 7.5, 200 mM NaCl, 1% (v/v) Nonident P40, 1x PIC). Lysis was performed on a test-tube rotator (1h/4°C) in the cold room, centrifuged (8min/16000g/4°C), supernatant transferred into a new 1.5 mL tube and diluted to a concentration of 0.1% Nonident P40 by addition of 900 µL of lysis buffer without Nonident P40. 30 µL supernatant were used as IP input sample, mixed with 7.5 µL of SDS sample buffer (250 mM Tris, pH 6.8, 12.5 mM EDTA, 500 mM DTT, 10% (w/v) SDS, 25% (v/v) glycerol, 0.1% (w/v) bromophenol blue) and the rest of the supernatant was mixed with 50 µL three times pre-washed (1 mL lysis buffer with 0.1% Nonident P40, 30sec/8200g/4°C) FLAG-beads (F2426, Sigma-Aldrich) and incubated overnight on a test-tube rotator in the cold room. Pellets were mixed with 50 µl SDS sample buffer and stored at -20°C overnight. Beads were washed four times as before and 30 µL of flow-through sample were taken and mixed with 7 µL of SDS sample buffer. Protein on the beads were subjected to CuAAC. In short, 0.68 µL 40 mM $CuSO_4$ in H_2O, 0.54 µL 50 mM TCEP H_2O, 1.08 µL 10 mM TBTA, and 0.27 µL 10 mM Alexa-647-N_3 were mixed, added to the beads, incubated in the dark (3h/800rpm/37°C) and finally heated up together with the other samples (10min/70°C) after addition of 25 µL SDS sample buffer. Samples were loaded on a 13% SDS-PAGE (see section 4.8), in-gel fluorescence was

measured before proteins were transferred to a PVDV-membrane (see section 4.9) and developed with antibody against DDDDK-tag (rabbit, see table 3).
To analyse if the addition of the fluorophor plays a role in the weak GPAA1 signal after the click reaction on the beads, HeLaΔS1PL cells were processed as before, labeled for 15 minutes with 1.5 mL of 3µM pacSph labeling media, and split before the IP. One sample was afterwards subjected to click reaction, while the other one was not. The samples that did undergo the click reaction where eluted in two steps. First, 25 µL SDS sample buffer were added, the sample heated up (10min/70°C), centrifuged (30sec/8000g/RT) and supernatant transferred into a new 1.5 mL tube. Second step, 25 µL of SDS sample buffer were added, the sample heated up (10min/95°C), centrifuged and all off the sample were subjected to SDS-PAGE as before.

4.13.1.2 CuAAC of Alexa-647-N_3 in whole cell lysate with Nonident P40 HeLaΔS1PL cells were seeded ($1.5x10^5$ cells per 6-well) and 24 hours later transiently transfected with 0.75 µg of plasmid DNA encoding for GPAA1 and the corresponding amounts of Fugene HD (E2311, Promega) according to manufacturer's instructions. The next day, cells were washed once with PBS before addition of 1 mL labelling media (DMEM containing Pen/Strep, delipidated FBS, 4.5 µM pacSph) and incubated for 30 minutes (37°C/5% CO_2). Cells were washed with ice cold PBS (3x 1 mL), overlaid with 1 mL ice-cold PBS, subjected to UV-light irradiation under a high intensity lamp for 5 min, scraped off in 1 mL of ice-cold PBS, centrifuged (5min/16000g/4°C) and the pellet resuspended in 230 µL of lysis buffer (20 mM HEPES-NaOH pH 7.5, 200 mM NaCl, 1% (v/v) Nonident P40, 1x PIC). Lysis was performed on a test-tube rotator (1h/4°C) in the cold room, centrifuged (8min/16000g/4°C), supernatant transferred into a new 1.5 mL tube and 3.25 µL of the click mix (1.36 µL 40 mM $CuSO_4$ in H_2O, 1.08 µL 50 mM TCEP H_2O, 0.54 µL 10 mM TBTA, and 0.54 µL 10 mM Alexa-647-N_3) was added to 200 µL supernatant and incubated in the dark (4h/1000rpm/37°C). The other 30 µL were used as input sample before click and mixed with 12 µL of SDS sample buffer (250 mM Tris, pH 6.8, 12.5 mM EDTA, 500 mM DTT, 10% (w/v) SDS, 25% (v/v) glycerol, 0.1% (w/v) bromophenol blue). The cell pellet was mixed with 50 µL of SDS sample buffer and both samples were heated up (10min/95°C) before being stored overnight at -20°C. The click reaction was stopped by addition of 1.8 mL of ice-cold methanol and stored at -80°C until the next day. Methanol precipitated proteins were pelleted (20min/17000g/4°C), supernatant decanted, resuspended in 1 mL ice-cold methanol (vortex, sonication) and again pelleted. This step was done twice, pellets were resuspended, air dried for 10 minutes, and resuspended (vortex, sonication) in 20 µL 4% SDS. Sample was diluted to 1:10 by addition of 180 µL of 0.1% Nonident P40 lysisbuffer before 10 µL of input IP sample (+ 5 µL of SDS sample buffer) were taken and the sample ultimately being diluted to 0.1% SDS concentration. The sample was then incubated overnight on 50 µL three times pre-washed (1 mL lysis buffer with 0.1% Nonident P40/1min/8000g/4°C) FLAG-beads (F2426, Sigma-Aldrich). Beads were washed 3 times as before, taken dry and eluted (30 µL SDS sample buffer) by heating up (10min/95°C) and flow-through sample was taken (100 µL + 25 µL SDS sample buffer). SDS-PAGE and western blot were done as described in section 4.13.1.1.

4.13.1.3 Efficiency of Nonident P40 and Triton-X-100 on CuAAC in whole cell lysate Experiment was performed as described in 4.13.1.2, except the following changes. 300 µL of two different lysis buffer (A: 20 mM HEPES-NaOH pH 7.5, 200 mM NaCl, 1% (v/v) Nonident P40, 2x PIC, B:100 mM HEPES-NaOH pH 7.5, 100 mM NaCl, 1% (v/v) Triton-X-100, 0.1% (w/v) Na-deoxycholate, 2x PIC) were compared. After lysis cells were pelleted (10min/3000g/4°C) and everything was transferred to 2 mL tubes. After resuspension in 4% SDS, samples were diluted to 0.1% SDS with a Tritin-X-100 (1% (v/v) Triton-X-100 in PBS, 2xPIC) based buffer. The same buffer was used to

wash the beads. Proteins were eluted two times with 25 µL SDS sample buffer (100 mM Tris, pH 8.3, 4 M Urea, 8% (w/v) SDS, 10% (v/v) glycerol, 50 mM DTT, and 0.01% (w/v) bromophenol blue) from beads by heating up (10min/75°C).

4.13.2 Analysis of sphingolipid binding kinetics of transiently expressed GPAA1 by continuously labeling with pacSph and detection with Alexa-647-N_3

HeLaΔS1PL cells were seeded ($1.5x10^5$ cells per 6-well) and 24 hours later transiently transfected with 1 µg of plasmid DNA encoding for GPAA1 or P24 and the corresponding amounts of Fugene HD (E2311, Promega) according to manufacturer's instructions. The next day, cells were washed once with PBS before addition of 2 mL labeling media (DMEM containing Pen/Strep, delipidated FBS, 2 µM pacSph) and incubated for 15/60/120/180/360 minutes (37°C/5% CO_2). Cells were washed with ice-cold PBS (4x 1 mL), overlaid with 1 mL ice-cold PBS, subjected to UV-light irradiation under a high intensity lamp for 5 min, scraped off in 500 µL of ice-cold PBS, centrifuged (5min/3000g/4°C), pellet resuspended in 300 lysis buffer (100 mM HEPES-NaOH pH 7.5, 100 mM NaCl, 1% (v/v) Triton-X-100, 0.1% (w/v) Na-deoxycholate, 2x PIC). Lysis was performed on a test-tube rotator (1h/4°C) in the cold room, centrifuged (8min/16000g/4°C), supernatant transferred into a new 1.5 mL tube, 15 µL input sample were mixed with 15 µL of SDS sample buffer (100 mM Tris, pH 8.3, 4 M Urea, 8% (w/v) SDS, 10% (v/v) glycerol, 50 mM DTT, and 0.01% (w/v) bromophenol blue), and pellets were mixed with 50 µL of sample buffer. Supernatant was subjected to click reactions with Alexa-647-N_3 as described in 4.13.1.2.

4.13.3 Analysis of sphingolipid binding kinetics of transiently expressed GPAA1 by pulse-chase labeling with pacSph and detection with Alexa-647-N_3

Experiment was done as described in section 4.13.2. Variations of this procedure were the following. First, cells were pulse-chase labeled with 2 µM pacSph as described in 4.13.5. Second, cells were clicked on FLAG-beads as described in 4.13.1.1. Third, lysis buffer used in this experiment was (100 mM HEPES-NaOH pH 7.5, 100 mM NaCl, 1% (v/v) Triton-X-100, 0.1% (w/v) Na-deoxycholate, 2x PIC).

4.13.4 Comparing pulse-chase and continuously labeling of transiently expressed GPAA1 with pacSph and detection with Alexa-647-N_3

Experiment was done as described in section 4.13.3. The single variation was, that only the concentrations 2 and 6 µM were tested for 6 hours.

4.13.5 Analysis of sphingolipid binding kinetics of transiently expressed GPAA1 by pulse-chase labeling with pacSph and detection with biotin-azide

For each indicated condition, one 10 cm dish ($2x10^6$ cells per dish) and one 6-well of HelaΔS1PL cells ($3x10^5$ cells per well) in DMEM (10% FBS, Pen/Strep) were seeded 24 hours before transfection. Cells were transfected the next day with plasmid DNA containing either GPAA1 or the known sphingomyelin binding protein p24 [15] (transfection mix: 5.8 µg DNA, added up OptiMEM until 282.6 µL, 17.4 µL Fugene HD). The next day, cells were washed once with ice-cold

PBS before addition of 5 mL (10cm dish) or 2 mL (6-well) of 2 µM pacSph containing labeling media (DMEM containing Pen/Strep, DL-FBS (delipidated FBS)). After 10 min of labeling, cells were washed four times with PBS and then overlaid with normal DMEM growth medium. For the 10 cm dishes, the media was aspirated at indicated time points (0/15/60/120/240min), cells were overlaid with 5 mL of ice-cold PBS, subjected to UV-light irradiation under a high intensity lamp for 5 min, scraped off in 1 mL ice-cold PBS, centrifuged (5min/4°C/3000g), resuspended in lysis buffer (1xPBS, 2xPIC, 0.125 U/µL benzonase (71206, Merck)) by 5x5 seconds of sonification, and incubated for 1 hour on ice before addition of 23 µL lysis reagent (10% SDS in PBS, 2xPIC). Samples were heated up (10min/70°C), centrifuged (5min/4°C/3000g) and the supernatant transferred into 2 mL eppendorf tubes. To remove not cross-linked pacSph, proteins were two times MeOH/$CHCl_3$ precipitated. First, 607 µL MeOH, 202 µL $CHCl_3$, and 800 µL H_2O were mixed, centrifuged (5min/14000g/RT), the upper phase removed, 300 µL MeOH added and once more centrifuged (30min/14000g/RT, swing out rotor). Pellet was air-dried, resuspended (vortex/sonicate/37°C at 1400rpm) in 50 µL buffer A (4%SDS in PBS, 2x PIC) and diluted to 1% SDS by addition of 150 µL buffer B (PBS, 2xPIC). For the second precipitation round, 480 µL MeOH, 160 µL $CHCl_3$, and 680 µL H_2O were used. Half of the sample was frozen in N_2 and stored at -80°C, while the other half was subjected to click reactions. 25 µL click mix consisted out of 5 µL 25 mM $CuS0_4$, 5 µL 25 mM L-ascorbic acid (both in H_20), 5µL 2.5 mM biotin-azide and 5 µL 2.5 mM TBTA (both in DMSO). $CuS0_4$, L-ascorbic acid and TBTA were prepared freshly, while 25 mM biotin-azide aliquots were stored at -20°C. $CuS0_4$, L-ascorbic acid and biotin-azide were brought together, vortexd for 10 seconds, spun down and incubated for 2 min at RT before TBTA was added. After 3h/37°C/800rpm in the dark, 75 µL PBS were added and the samples were once more MeOH/$CHCl_3$ precipitated, resuspended in 50 µL buffer A, frozen in liquid N_2 and stored at -20°C overnight. The 6-well samples were washed once with ice-cold PBS, then scraped off in 500 µL MeOH and stored at -80°C until time of lipid extraction for TLC.

The next day, samples were thawed up (10min/37°C/1400rpm), 150 µL of PBS were added, MeOH/$CHCl_3$ precipitated, resuspended in 50 µL of 4% SDS in PBS and diluted to 1% SDS in PBS by addition of 150 µL PBS. 10 µL were taken as input sample, mixed with 10 µL of 3x sample buffer (250 mM Tris, pH 6.8, 1.8% (w/v) SDS, 45% (v/v) glycerol, 22.5% (v/v) β-mercaptoethanol and 0.003% (w/v) bromophenol blue) and heated up (5min/95°C). The samples were diluted further to to 0.2% SDS in PBS by addition of 760 µL PBS+2x PIC. For pull-down of biotinylated protein-lipid complexes, 50 µL slurry of neutravidin-beads (29202, ThermoFisher) was pre-cleared (washed 3 x with 1 mL 0.2% SDS in PBS, 1min/500g/4°C) before it was given to the samples and incubated for one hour at RT on the test-tube rotator. To analyse non-lipid cross-linked protein populations, 20 µL of flow-through was combined with 20 µL 3x sample buffer, denaturated (15min/95°C) and kept at RT. Beads were washed 10x with 1% SDS in PBS, before samples were eluted in two steps. Supernatant of the first step (20 µL of elution buffer (4% SDS (w/v), 4% β-mercaptoethanol (v/v), 100 mM Tris/HCl pH 6.8)) was combined with the supernatant of the second step (15 µL of 3x sample buffer, 15min/95°C, 1min/RT/FS). Samples were analysed by 1.5mm 13% SDS-PAGE and via western blot (see section 4.9). To analyse the pacSph metabolites at the indicated time points, 6-well samples were taken out of -80°C, 300 µL of PBS, 100 µL of MeOH and 150 µL of $CHCl_3$ were added, lipids were extracted and TLC was performed as described in section 4.7.

4.14 Analysis of protein-lipid interactions of endogenous transamidase complex subunits

4.14.1 Sphingolipid binding of endogenous transamidase complex subunits in whole cell lysate

Eighteen hours before labeling, two 10 cm dishes per condition of HelaΔS1PL GPAA1 #76 ($4-5x10^6$ cells per dish) in DMEM (10% FBS, Pen/Strep) were seeded. Cells were washed once with 10 mL PBS, before being labeled with 6 µM pacSph (DMEM containing Pen/Strep, 10% DL-FBS (delipidated FBS) and pacSph). After 4 hours of labeling time, cells were washed 3x with 10 mL ice-cold PBS, then overlayed with 5 mL and subjected to UV-light irradiation under a high intensity lamp for 5 min. PBS was aspirated and cells were scraped off in 1 mL ice-cold PBS and centrifuged for 5min/4°C/3000g. The pellet was taken up in 200 µL lysis buffer (PBS, 1% Triton-X-100, 0.1% SDS, 0.125 U/mL benzonase, and 2x Protease inhibitor cocktail (11836170001, Roche) in PBS, resuspended by sonication (5x10 seconds, on ice between) and the lysis was performed for 2 hours on a test-tube rotator in the cold room. Post-nuclear supernatant (8min/4°C/16000g) was snap frozen in N_2 and stored overnight at -20°C.
On the next day, samples were thawed up on ice and not cross-linked pacSph was removed by MeOH/$CHCl_3$ precipitation after Wessel Flügge[101]. In short, 800 µL MeOH, 400 µL $CHCl_3$, and 600 µL H_20 were sequentially added and rigorously mixed by vortexing for 10 seconds. After phase separation (2min/RT/20000g), the upper phase was carefully removed without disturbing the intermediate phase. 600 µL MeOH were added, mixed and centrifugated (5min/RT/16000g in swing out rotor) before the liquid phase was decanted and the pellet air-dried for 10 minutes. After resuspension of the pellets by addition of 50 µL 4% SDS in PBS (vortex/sonicate/37°C at 1400rpm), the lysates of each condition were combined in one tube, diluted to 1% SDS concentration by addition of 330 µL of PBS and 2x1 µL were used for protein concentration determination via BCA-assay. Lysate aliquots of 187 µL (200-400 µg/tube) were subjected to click reactions by addition of 13 µL click mix, which consisted out of 5 µL 40 mM $CuS0_4$, 4 µL 50 mM TCEP (both in H_20), 2 µL 10 mM biotin-azide and 2 µL 10 mM TBTA (both in DMSO). $CuS0_4$, TCEP and TBTA were prepared freshly, while biotin-azide aliquots were stored at -20°C. $CuS0_4$, TCEP and biotin-azide were brought together, vortexd for 10 seconds, spun down and incubated for 2 min at RT before addition of TBTA. After 4h/37°C/800rpm in the dark, the click reaction was stopped by addition of 1800 µL of ice-cold MeOH and stored at -80°C overnight.
To remove click reagents, proteins were pelleted (20min/4°C/16000g in swing out rotor), MeOH decanted, pellet resuspended in 1 mL ice-cold MeOH by alternations of vortexing and sonication until solution cleared up and precipitated a second time for 1h at -80°C. After centrifugation as before, pellet was air-dried for 10 minutes and resuspended (vortex/sonicate/37°C at 1400rpm) with a maximum of 70 µL 4% SDS in PBS per condition. Insoluble material was removed by centrifugation (5min/RT/3000g) and supernatant was transferred into a new tube. PBS+2x PIC was added for a total volume of 400 µL and 40 µL were taken aside for 10% input sample (+13.40 µL LDS sample buffer, 15 min 95°C, stored at room temperature). The remaining sample was diluted to 0.2% SDS by addition of 760 µL of PBS+2x PIC. For pull-down of biotinylated protein-lipid complexes, 50 µL FLAG-beads (F2426, Sigma-Aldrich) slurry was pre-cleared (washed 3 x with 1 mL 0.2% SDS in PBS, 1min/500g/4°C) before it was added to the samples and incubated (3h/RT) on the test-tube rotator. 40 µL of flow-through were combined with 15 µL LDS sample buffer, denaturated (15min/95°C) and kept at RT. Beads were washed 15x with 1% SDS in PBS, before samples were eluted in two steps. Supernatant of first elution (20 µL of LDS sample buffer, 15 min at 95°C, 1min/RT/FS) was combined with supernatant of second elution (20 µL of LDS sample buffer, 15

min at 95°C, 1min/RT/full speed). Samples were analysed by 1.5mm 7.5% SDS-PAGE and western blot (see section 4.9).

4.14.2 Sphingolipid/cholesterol binding of endogenous transamidase complex subunits in membrane fractions

Procedure was the same as described in section 4.14.1. The only difference was that instead of whole cell lysate a membrane fraction was prepared before lysis. In short, after subjection of the cells with 5 mL of labeling media/10 cm dish (4 hours with 6µM pacSph, 30 minutes with 10 µM pacChol), cells were washed 3x with 10 mL ice-cold PBS, overlayed with 5 mL and subjected to UV-light irradiation under a high intensity lamp for 5 min. PBS was aspirated and cells were scraped off in 1 mL ice-cold PBS, transferred into 1.5 mL ultracentrifuge tubes (357448, Beckman Coulter), centrifuged for 5min/4°C/3000g and the dry weight of the pellet was determined with an analytical balance (ABJ-120-4N, KERN & SOHN GmbH). Pellets were resuspended in $\frac{500\ \mu L}{25\ mg\ dry\ weight}$ homogenisation buffer (PBS, 2x PIC) by pipetting and sonication (5x10 seconds). One µL of the cell suspension was mixed with four µL homogenisation buffer and five µL 0.4% trypan blue (T8154, Sigma-Aldrich) and used for verification of successful cellular disintegration via Neubauer counting chamber. 50 µL pf the homogenate were transferred to Iris Leibrecht and Christian Lüchtenborg, who performed a lipid extraction and follow up lipidomics for sphingolipids as desribed in[103]. After centrifugation (1h/100.000g/4°C), the cytosolic fraction was discarded and the membrane pellet was resuspended in 200 µL lysis buffer. The rest of the experiment was performed as described before.

4.14.3 *In silico* analysis of cholesterol and sphingolipid binding sites in the transamidase complex

UniProt protein sequences (see appendix 8.5) of all transamidase subunits (PIGK/T/S/U and GPAA1) were screened *in silico* with the ScanProsite tool (http://prosite.expasy.org/scanprosite/) to define possible cholesterol interacting motifs. CRAC sequence search term: [LV]-X(1,5)-Y-X(1,5)-[KR], CARC sequence search term [KR]-X(1,5)-[YF]-X(1,5)-[LV]. The sphingolipid binding sequence was [VITL]-X(2)-[VITL][VITL]-X(2)-[VITL][FWY]. Hits taken into account required at least one amino acid of the motif to be located in a transmembrane domain.

4.14.4 Inhibition of sphingolipid binding of endogenous GPAA1 with PPMP

In a first experiment, the concentrations of PPMP required for successful inhibition of metabolic conversion of pacSph to pacGlucCer were determined. 1 mg of DL-threo-PPMP hydrochloride (17236, Cayman Chemical) was resuspended in 130 µL EtOH to create a 15 mM stock solution. HelaΔS1PL GPAA1 #76 ($3x10^5$ cells/6-well) were seeded and 24 hours later pre-incubated with 2 mL of labeling media (DMEM containing Pen/Strep and delipidated FBS) containing 8/20/41 µM PPMP. After one hour, cells were washed with PBS and media was exchanged with labeling media containing 4 µM pacSph and 8/20/41 µM PPMP. Four hours later, cells were harvested and a TLC was conducted as described in section 4.7.
The labeling experiment was performed as described in section 4.14.2. Cells were pre-incubated for one hour with 5 mL medium. After 4 hours, media was exchanged with 5 mL of 25 µM PPMP

and 4 µM pacSph containing media. 50 µL of samples labeled with either pacSph with or without PPMP were taken aside before the 100000g centrifugation step for lipid extraction and mass spectrometric analysis. Blots were developed with mouse α-DDDKK antibody (see table 3). Group differences were calculated by a two sided Student's t-test. Group differences between spingolipid metabolites, as measured via mass spectrometry, were analysed via one-way ANOVA and Tukey's honestly significant difference post hoc test.

4.14.5 Inhibition of sphingolipid binding of endogenous GPAA1 with FB1

In a first experiment, the concentrations of Fumonisin B_1 (62580, Cayman Chemical) required for successful inhibition of metabolic conversion of pacSph to pacCer were determined. 0.5 mg of FB_1 was resuspended in 46 µL PBS (pH 7.2) to create a 15 mM stock solution. HelaΔS1PL GPAA1 #76 ($3x10^5$ cells/6-well) were seeded and 24 hours later pre-incubated for 15 hours with 2 mL of labeling media (DMEM containing Pen/Strep and delipidated FBS) containing 25/50/150 µM FB_1. The labeling was then performed for 4 hours with 4 µM pacSph containing labeling media and freshly prepared FB_1. Cells were harvested and a TLC was conducted as described in section 4.7.Furthermore, the following conditions were tested. 15 hours pre-incubation with 25/50/100 µM FB_1 and one/four hours of labeling with 1 µM pacSph.
The labeling experiment was performed as described in section 4.14.2. Cells were pre-incubated for 16 hours with 5 mL medium containing 100 µM FB_1. 5 mL fresh media containing 100 µm FB_1 and 1 µM pacSph were added for one hour. 50 µL of samples labeled with either pacSph with or without FB_1 were taken aside before the 100000g centrifugation step for lipid extraction and mass spectrometric analysis. Blots were developed with mouse α-DDDKK antibody (see table 3). Group differences were calculated by a two sided Student's t-test. Group differences between spingolipid metabolites, as measured via mass spectrometry, were analysed via one-way ANOVA and Tukey's honestly significant difference post hoc test.

4.14.6 Inhibition of sphingolipid binding of endogenous GPAA1 with D609

Experiments to determine the concentrations of D609 (13307, Cayman Chemical) required for successful inhibition of metabolic conversion of pacSph to pacCer were performed. 0.5 mg of D609 was resuspended in 125 µL PBS (pH 7.2) to create a 15 mM stock solution. HelaΔS1PL GPAA1 #76 ($3x10^5$ cells/6-well) were seeded and 24 hours later pre-incubated for 1 hour with 2 mL of labeling media (DMEM containing Pen/Strep and delipidated FBS) containing 37.5/75/150/300 µM D609. The labeling was then performed for 4 hours with 4 µM pacSph containing labeling media and freshly prepared D609. Cells were harvested and a TLC was conducted as described in section 4.7.
Furthermore, the following conditions were tested and the labeling media always contained the respective D609 concentration. 1.: 1 and 4 hours pre-incubation with 187.5/375 µM D609 and labeling with 0.5/4 µM pacSph. 2.: 4 hours pre-incubation with 375 µM D609 and 4 hours labeling with 0.5/2 µM pacSph. 3.: 15 hours pre-incubation with and without 250 µM D609 and 4 hours labeling with 4 µM pacSph. 4.: No pre-incubation and labeled with 1 µM pacSph and 250/375 µM D609 for 1 hour.

5 Results

5.1 Transient expression of transamidase subunits in HeLa cells

HeLa cells were transiently transfected with DDK-tagged transamidase subunits (PIGK/T/S and GPAA1) to establish a transient expression system for the study of protein-lipid interactions in the transamidase complex.
In a first step, HeLa cells were transiently transfected for 24 hours with varying concentrations of plasmids (0.25/0.5/1/1.5 µg). Cells were then harvested, solubilised, separated by SDS-PAGE, via western blot transferred to a PVDF-membrane and the subunits were visualised by an antibody against the DDK-tag (see figure 7A). EGFP-DDK served as a solubilisation and transfection control while unspecific reactions of the antibody were monitored by a non-transfection control. Increasing amounts of plasmid DNA resulted in increased quantified signal in both, the solubilised (S) and the non-solubilised fraction (P) (see figure 7A). Furthermore, signal retention in the loading well was observed for PIGK/T and GPAA1, but not for PIGS. Calculation of the solubilisation efficiency by dividing the signal intensities $\frac{S}{P} \times 100$ revealed a reduction for PIGS/T and GPAA1 with increasing DNA concentrations (see figure 7B). PIGK solubilisation efficiency was not affected by varying plasmid DNA concentrations.

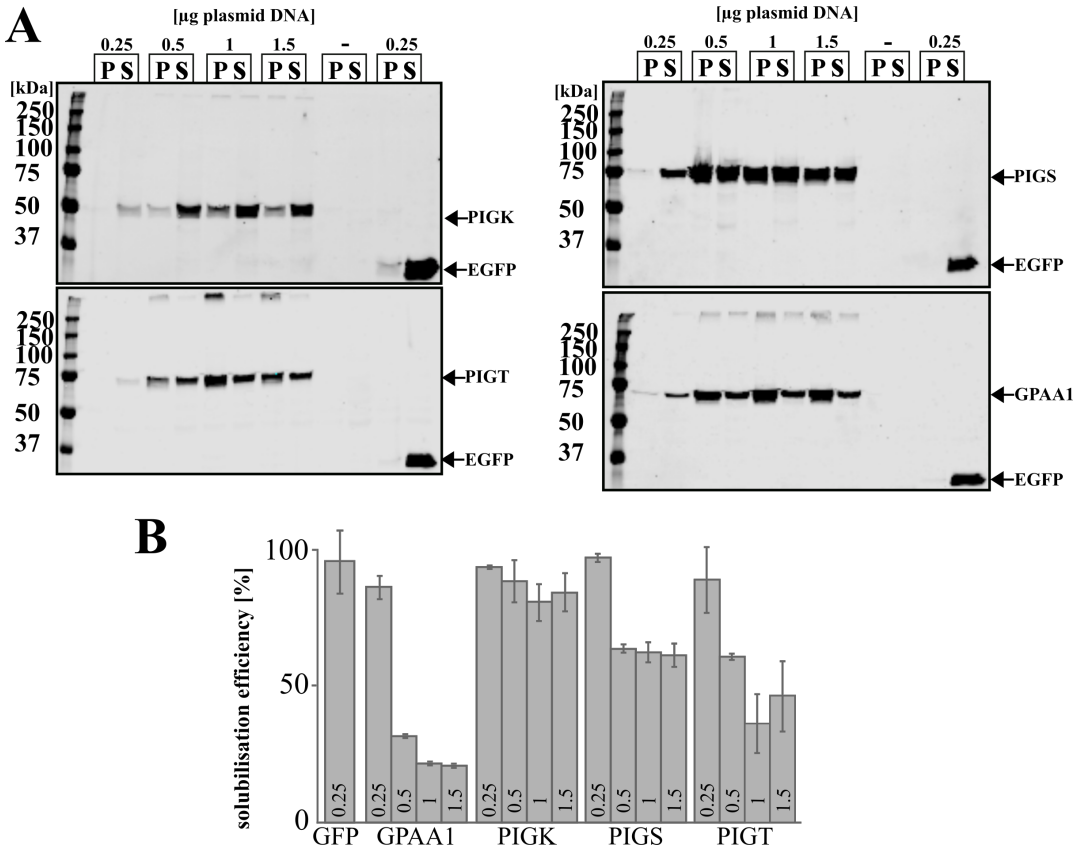

Figure 7: Optimisation of transient transamidase subunit expression and solubilisation in HeLa cells A) Cultivation of HeLa cells and transfected with varying concentrations of plasmids (0.25/0.5/1/1.5) encoding different transamidase subunits, a non-transfection and a transfection control (EGFP). Shown are representative western blots from at least two independent experiments. P, non-solubilised fraction after lysis; S, Supernatant after lysis **B)** Quantification of regions of interest indicated by arrows in A) and calculation of solubilisation efficiency ($\frac{S}{P} \times 100$). Mean, SD, n=6 for EGFP, n=2 for PIGK/S/T, GPAA1.

In a second step, lysis buffers containing different detergents (Nonident P40, Triton-X-100, Octylglucosid, CHAPS) were tested to optimise solubilisation of transiently transfected (24 and 48 hours) GPAA1-DDK in HeLa cells (see figure 8A). As a control for solubilisation the endogenous ER residing protein calnexin was used. Results for Triton-X-100 and Nonident P40 were comparable (see table 10), while CHAPS and Octylglucosid provided very weak signal intensities for GPAA1 and thus rendering the quantification values unreliable. Furthermore, 24 hours transfection of GPAA1 and cell lysis at 4°C seemed to yield the highest signal intensities (data not shown). Solubilisation of the one TMD containing ER protein calnexin seemed to be detergent independent and more robust than GPAA1 (7 TMDs) solubilisation.
In a third step, only Triton-X-100 and Nonident P40 were used to analyse the solubilisation efficiency of HeLa cells transiently transfected with 0.25 and 0.5 µg of plasmid DNA encoding for GPAA1-DDK (see figure 8B). The best efficiencies were achieved for 0.25 µg and 24 hours (see table 9), but the overall signal intensities were to low for a reliable quantification. As Nonident showed lower protein aggregation in the SDS-PAGE pockets than Triton-X-100 in both experiments (data not shown), the decision was made to continue with the following experimental conditions: Nonident P40 as the detergent of choice, 24 hours transfection with 1 µg of GPAA1 encoding plasmid, and cell lysis at 4°C.
The last transamidase subunit PIGU could not be tested, as the commercially available plasmid contained a stop codon which prevented expression after transient transfection (not shown). After fixing the sequence aberration, it was not possible to amplify the plasmid in a bacterial host and therefore no material was available for transfection experiments with the correct cDNA sequence.

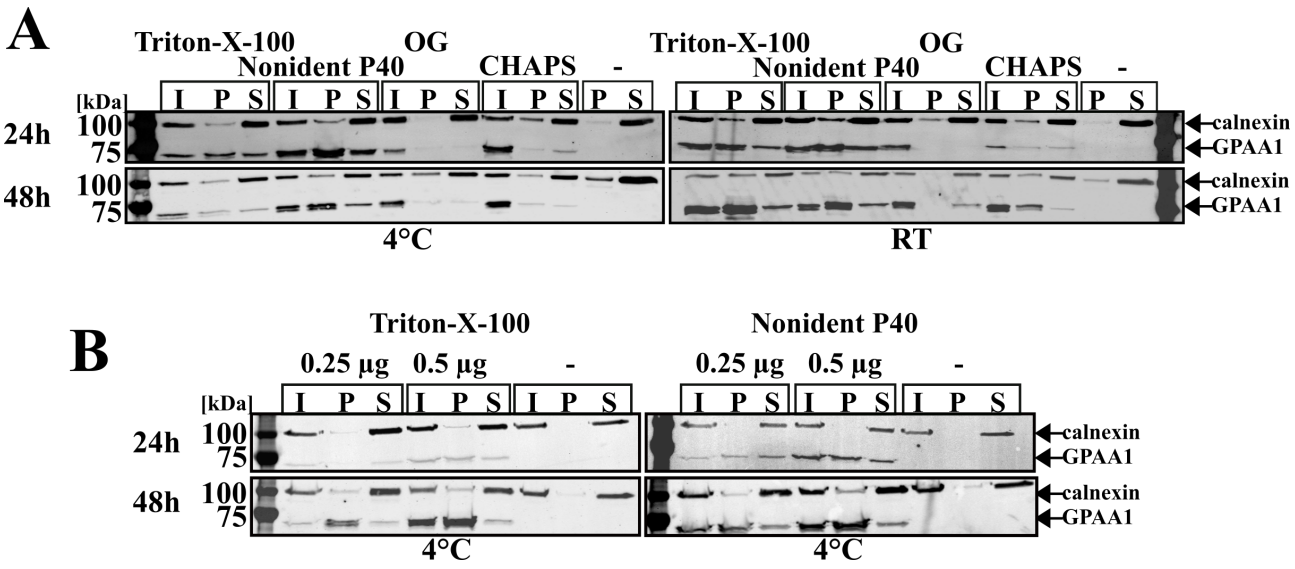

Figure 8: Solubilisation of transiently expressed GPAA1 in HeLa cells A) Effect of different detergents on solubilisation of HeLa cells transiently transfected with 1 µg of a plasmid encoding GPAA1-DDK. As a solubilisation control, the endogenous ER residing protein calnexin was used in cells expressing GPAA1-DDK as well as in not transfected cells. Shown are representative western blots from at least two independent experiments. Quantification data is shown in table 10. I, input sample before lysis; P, non-solubilised fraction after lysis; S, solubilised proteins after lysis **B)** HeLa cells transiently transfected with either 0.25 µg or 0.5 µg of GPAA1-DDK encoding plasmid to test solubilisation efficiency of the detergents Triton-X-100 and Nonident P40. Shown are representative western blots from at least one experiment. Quantification data are shown in table 9.

Table 9: Solubilisation efficiency[1] of transiently expressed GPAA1 and endogenous calnexin at 4°C. Values are derived from the analysis shown in figure 8

		Nonident P40		Triton-X-100	
time[2]	DNA[3]	GPAA1	Calnexin	GPAA1	Calnexin
24h	0.25	0.611 ± 0.003[4]	0.873[5]	0.624 ± 0.171[4]	0.946[5]
	0.50	$0.349 \pm 0.0.029$[4]	0.880[5]	0.410 ± 0.194[4]	0.906[5]
	–	–	–	–	0.980[5]
48h	0.25	0.294 ± 0.046[4]	$0.851 \pm 0.0.062$[4]	0.160 ± 0.005[4]	0.864 ± 0.055[4]
	0.50	0.224 ± 0.067[4]	$0.808 \pm 0.0.015$[4]	$0.142 \pm 0.0.099$[4]	0.785 ± 0.056[4]
	–	–	0.920[5]	–	0.960[5]

[1] division of signal intensities of solubilised and non-solubilised fraction $\frac{S}{P}$, [2]duration of transient expression,[3] µg oftransfected plasmid encoding for GPAA1-DDK, [4] mean+SD of two biological replicates,[5]single experiment quantification, [5]single experiment quantification

Table 10: Analysis of parameters effecting transiently expressed GPAA1[1] and endogenous calnexin solubilisation efficiency[2]

		GPAA1				Calnexin			
time[3]	degree[4]	Nonident P40	Triton-X-100	Octylglucosid[9]	CHAPS[9]	Nonident P40	Triton-X-100	Octylglucosid[9]	CHAPS[9]
24h	4°C	0.521 ± 0.176[5]	0.638 ± 0.071[7]	0.709 ± 0.229[6]	0.379 ± 0.258[5]	0.655 ± 0.008[7]	0.688[8]	0.685 ± 0.034[7]	0.362 ± 0.044[7]
	RT	0.540 ± 0.140[5]	0.526 ± 0.214[7]	0.492 ± 0.354[6]	0.602 ± 0.249[5]	0.652 ± 0.027[7]	0.678[8]	0.667 ± 0.022[7]	0.802 ± 0.014[5]
48h	4°C	0.314 ± 0.012[7]	0.564 ± 0.140[7]	0.952 ± 0.047[7]	0.638 ± 0.258[7]	0.868 ± 0.0127[7]	0.888 ± 0.085[7]	0.851 ± 0.151[7]	0.810 ± 0.101[7]
	RT	0.316 ± 0.0730[7]	0.295 ± 0.133[7]	0.738 ± 0.236[7]	0.292 ± 0.283[7]	0.784 ± 0.019[7]	0.736 ± 0.123[7]	0.875 ± 0.136[7]	0.802 ± 0.101[7]

[1] 1 µg of transfected plasmid encoding for GPAA1-DDK, [2] division of signal intensities of solubilised and non-solubilised fraction $\frac{S}{P}$, [3]duration of transient expression, [4] lysis conditions, [5−7] mean+SD of four, three, or two biological replicates, [8]single experiment quantification, [9] quantification values not reliable due to low signal intensities (see figure 8A)

In a fourth step, the ability to enrich transiently transfected transamidase subunits (PIGK/T/S, GPAA1) via their C-terminal tag was analysed. As seen in figure 9A, all subunits as well as the positive control EGFP were successfully IP, while the negative control showed no signal. To assess if the transiently transfected subunits GPAA1 and PIGT integrated successfully into the transamidase complex, Co-IP experiments were performed. GPAA1 (see figure 9B) and PIGT (not shown) showed both the capability to pull down endogenous PIGS and PIGK. PIGU could not be detected.

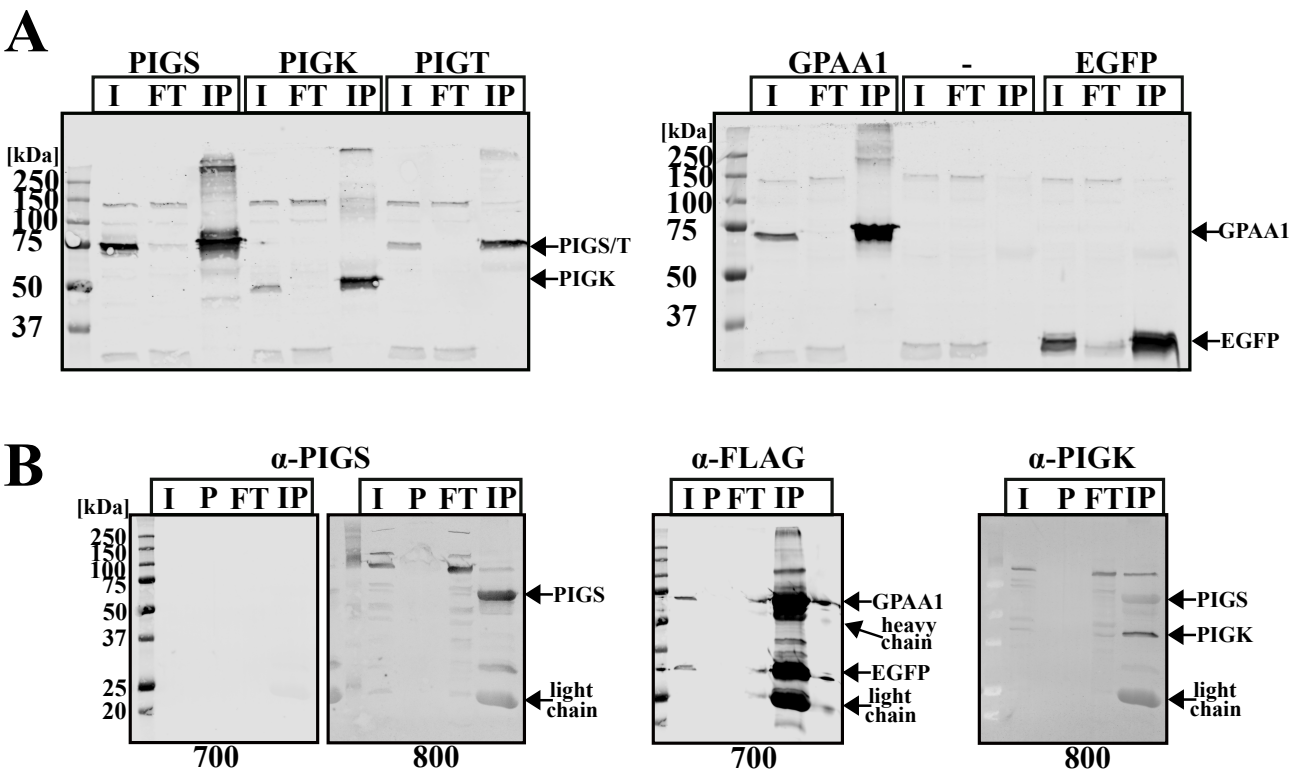

Figure 9: IP of transiently transfected transamidase subunits in HeLa cells A) HeLa cells were transfected with 1 µg of plasmid encoding for different DDK-tagged transamidase subunits (PIGK/T/S and GPAA1) and afterwards IP via FLAG-beads. EGFP-DDK served as a positive control. Not transfected cells (-) served as controls for western blot and FLAG-bead specificity. Blots shown are representatives of two independent experiments. **B)** Co-IP of HeLa cells transfected with GPAA1 to analyse pull down of transamidase subunits. EGFP used as internal IP control. Detection of subunits by subsequently administration of antibodies (α-PIGS, α-FLAG, and α-PIGK with fluorescently tagged (700/800 channel dyes) secondary antibodies). I, input sample before IP; P, non-solubilised fraction after lysis; FT, proteins not bound to beads; IP, proteins enriched via FLAG beads.

5.2 Optimisation of pacSph labelling in HeLaΔS1PL cells transiently transfected with GPAA1

HeLaΔS1PL cells were transiently transfected with a GPAA1 encoding plasmid and fed with 3 µM pacSph for 30 minutes, followed by UV irradiation to cross-link pacSph and its metabolites via their photoactivatable diazirine ring to proteins in close proximity. Proteins were allowed to bind to α-FLAG beads before attachment of Alexa-647-N_3 via CuAAC to the alkyne group (click

reaction) of the pacSph metabolites. Proteins were eluted with SDS sample buffer and subjected to SDS-PAGE. The fluorophor was detected by in-gel fluorescence before the proteins were transferred to a PVDF-membrane and detected via antibody against the FLAG-tag. To evaluate the influence of pacSph and Alexa-647-N_3 on the IP, not transfected cells were subjected to click reaction with or without previous UV irradiation. As seen in figure 10A, no bands appeared in the region where the GPAA1 signal was to be expected. Only a signal for Alexa-647 at the expected position for the heavy chain of the FLAG-beads antibody was visible. The α-FLAG signal for GPAA1 was detectable in the pellet, input and faint in the IP section with a slight overlap with the Alexa-647 signal. Additionally, a strong Alexa-647 signal is visible slightly above the expected GPAA1 band.

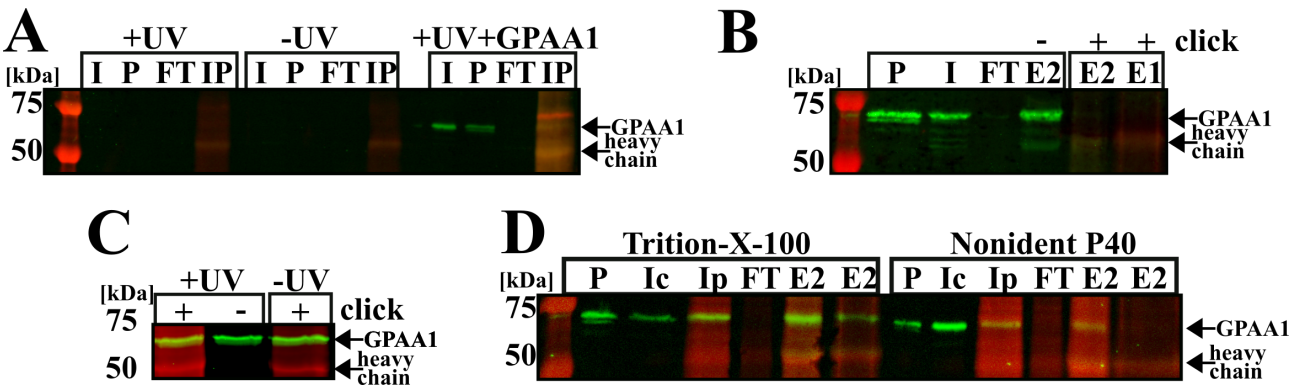

Figure 10: Optimisation of CuAAC for transient transfections of GPAA1 in HeLaΔS1PL cells A) HeLaΔS1PL cells were transfected a GPAA1 encoding plasmid and labelled for 30 minutes with 3 µM of pacSph. Controls for pacSph specificity are not transfected cells with or without UV irradiation. CuAAC was performed on proteins bound to FLAG-beads. I, input sample before IP; P, non-solubilised fraction after lysis; FT, proteins not bound to beads; IP, proteins enriched via FLAG beads after click reaction **B)** HeLaΔS1PL cells were transfected a GPAA1 encoding plasmid and labelled (15 minutes with 3 µM of pacSph). Sample was split before IP and one half was subjected to click reaction (+). This sample was eluted with SDS sample buffer twice, once for 10 minutes at 70°C (E2) and once for 10 minutes at 95°C (E1). **C)** HeLaΔS1PL cells transfected with GPAA1 and labelled with 4.5 µM pacSph for 15 minutes. Click in lysate. Shown are the IP fractions of samples with and without previous UV irradiation. **D)** Comparison between lysis buffer with either 1% Triton-X-100 or 1% Nonident P40 for click reaction in lysate. P, non-solubilised fraction after lysis, Ic, input sample before click reaction in lysate; Ip, input sample before IP; FT, proteins not bound to beads; red, Alexa-647-signal; green, α-GPAA1 signal; orange, red/green signal overlap.

An experiment was performed to determine if this loss of signal is a result of the click reaction. For this, the sample was split before IP and one half was subjected to click reaction, while the other half was not. Furthermore, the sample that underwent click reaction was eluted in two steps, to verify if the temperature (70°C and 95°C) had any impact on the elution of the GPAA1-pacSph-fluorophor product. As seen in figure 10B, the GPAA1 signal in the minus click sample is strong as expected, but after the click reaction, the signal is lost, independent of the temperature used for elution. This did not have any influence of the click reaction for p24, a positive control for pacSph interactions (not shown.)

A different click reaction protocol was used to analyse if this is a specific effect of bead bound GPAA1. This time the click reaction was performed in the cell lysate before IP and followed by multiple methanol precipitation steps to remove remaining unreacted click reagents. As a result, a strong signal for GPAA1 under all conditions (+UV±click, −UV+click) could be observed (see

figure 10C), but the Alexa-647-signal (+UV+click) was not very prominent.
To increase the click reaction efficiency in the cell lysate, two different detergents (Triton-X-100, Nonident P40) were compared against each other (see figure 10D). Samples were two times eluted (10min/70°C) to see if protein was left on the beads during the first elution step. For Triton-X-100, a strong signal for GPAA1 was observed throughout the whole experiment while Nonident P40 signal seemed to diminish after the click reaction and nothing could be observed in the second elution step. Furthermore, the second elution step for Triton-X-100 showed a signal, indicating still bound protein on the beads after the first elution round. Additionally, the overall background signal of the click reaction was more prominent in samples containing Nonident P40 than Triton-X-100. For next stage experiments, lysates were generated with Triton-X-100 as the detergent of choice and Alexa-647-N_3 click reactions were performed in whole cell lysate.

5.3 Analysis of sphingolipid binding kinetics in HeLaΔS1PL cells transiently transfected with GPAA1

To test whether GPAA1 interacts with a specific sphingolipid, HeLaΔS1PL cells were transfected with a plasmid encoding for GPAA1 and labelled for different periods of time (15/60/120/180/360 minutes) with 2 µM pacSph. Cells transfected with p24, a known interacting protein with the sphingosine metabolite sphingomyelin[15], and labelled for 360 minutes served as positive control (see figure 11A). For all time points, Alexa-647-signals were observed at the position of FLAG-signal that represents GPAA1. While for GPAA1 both signal overlap, a shift between the Alexa-647-signal and the FLAG-signal of p24 is observed. Afterwards, the IP signals for Alexa-647 (GPAA1 click) and FLAG (GPAA1) were quantified, the ratios calculated $\frac{GPAA1_{click}}{GPAA1}$, and plotted to visualise the GPAA1 sphingolipid binding kinetics (see figure 11C). An increase of labelling intensities is visible up to 180 minutes and then flattens out. When compared to the overall intensity of the Alexa-647-signal during the time course, (see figure 11B), a steadily increase was observed. To correlate the binding kinetics with available pacSph metabolites at time of UV-irradiation, a TLC with lipids extracted at the same time points as in the previous experiment was conducted (see figure 11D). At the first time points (15/60/120 minutes) sphingosine (48%, 45%, 33%) and ceramide (40%, 45%, 43%) are the dominant species, while sphingomyelin takes over at the 360 minutes time point (40%). Hexosylceramides are the lowest abundant species at all time points, but steadily increase and reach their maximum (slightly below 10%) at 360 minutes.

To exclude that continuous labelling conditions of the experiment influenced available amounts and species of pacSph metabolites at the time of UV-irradiation, a pulse-chase experiment was conducted. The only change to the protocol was that after 10 minutes of labelling, cells were washed three times with PBS and then overlaid with pacSph devoid growth media. Cells were UV-irradiated at the same time points as before.
Before the experiment was conducted, the protocol was ironed out by analysis of different technical parameters. In a first experiment, varying pacSph concentrations (2/3/4/5/6 µM) were tested to determine the minimal amount of pacSph needed for detection via TLC in a pulse-chase experiment (see figure 12A). The concentration of 2 µM pacSph, as used in the continuous labelling experiment (see figure 11), proved to be sufficient. However it was observed that the signal of 3-azido-7-hydroxycoumarin (lane C in figure 12A) overlapped with the signal of the pacSph metabolite pacGlucCer (lane 2-6 in figure 12A). To separate the two signals, the development distance of the mobile phase II in the TLC protocol was increased from 7.5 cm to 8 cm (see figure 12B). In the same experiment, 3-azido-7-hydroxycoumarin was titrated (9/35/70 µM) to determ-

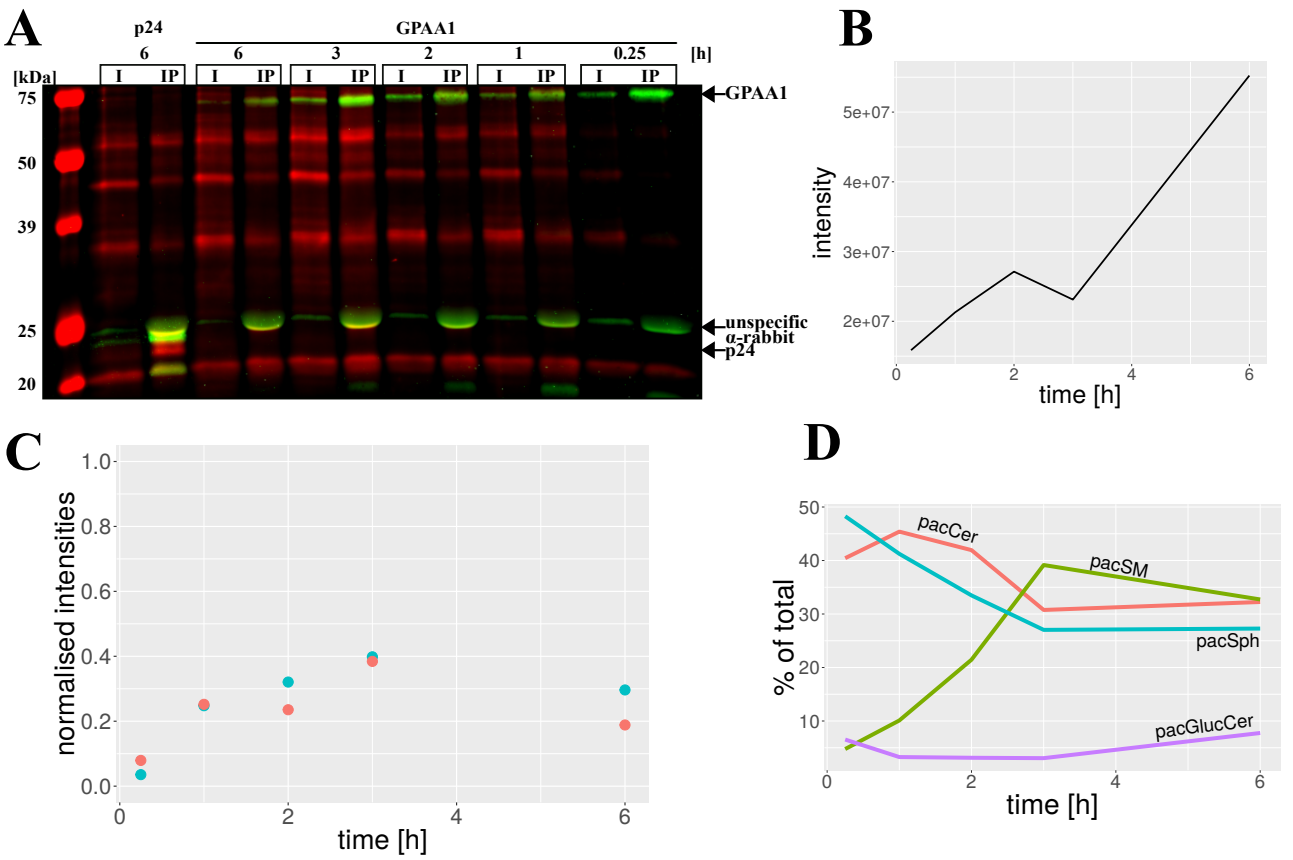

Figure 11: Analysis of sphingolipid binding kinetics of GPAA1 in transiently transfected HeLaΔS1PL cells via Alexa-647-N_3 A) HeLaΔS1PL cells were transfected with a GPAA1 encoding plasmid and labelled for certain periods of time with 2 µM of pacSph and detected via Alexa-647-N_3. Cells transfected with the known sphingosine metabolite sphingomyelin interacting protein p24 served as positive control. Shown is one of two biological replicates. I, input sample before IP; P, non-solubilised fraction after lysis; red, Alexa-647-signal; green, α-GPAA1 signal; orange, red/green signal overlap **B)** GPAA1-Alexa-647-signal intensity, n=2, SD. **C)** Analysis of GPAA1 sphingolipid binding kinetics. Quantification data of Alexa-647-signal in the 700 channel (GPAA1 click) and FLAG signal in the 800 channel (GPAA1) were used to calculate the $\frac{GPAA1click}{GPAA1}$ ratio for an experiment containing two biological experiments **D)** Quantification of pacSph *in vivo* metabolism in HeLaΔS1PL cells in one pilot study via TLC.

ine the concentration with the best trade-off between overall signal intensity in the sample and the background signal of 3-azido-7-hydroxycoumarin, as it might be the case that it is not possible to successfully separate pacGlucCer and the 3-azido-7-hydroxycoumarin signal. For the final pulse-chase experiment, 2 µM of pacSph were used for labelling and 35 µM of pacSph were used for the click reaction. One representative TLC is shown in figure 12C and the overall results of the quantification of three biological replicates are displayed in figure 12D. Compared with the continuous labelling experiment, depicted in figure 11D, a strong decline in pacSph concentration is visible at all time points, while the other metabolites (pacCer, pacSM, pac-GlucCer) show similar behaviour. This is furthermore independent of the transfected proteins present in the cell, namely GPAA1 or p24. To determine if the reduction in pacSph levels during the pulse-chase experiment had an influence on the outcome of the GPAA1-pacSph metabolite labelling kinetics, an Alexa-647-N_3 pulse chase experiment was conducted. HeLaΔS1PL cells were pulsed with the previously established minimal dose (see figure 12A) of 2 µM pacSph for 10 minutes, before being chased with delipidated DMEM for varying amounts of time (0.25/1/2/4/6h).

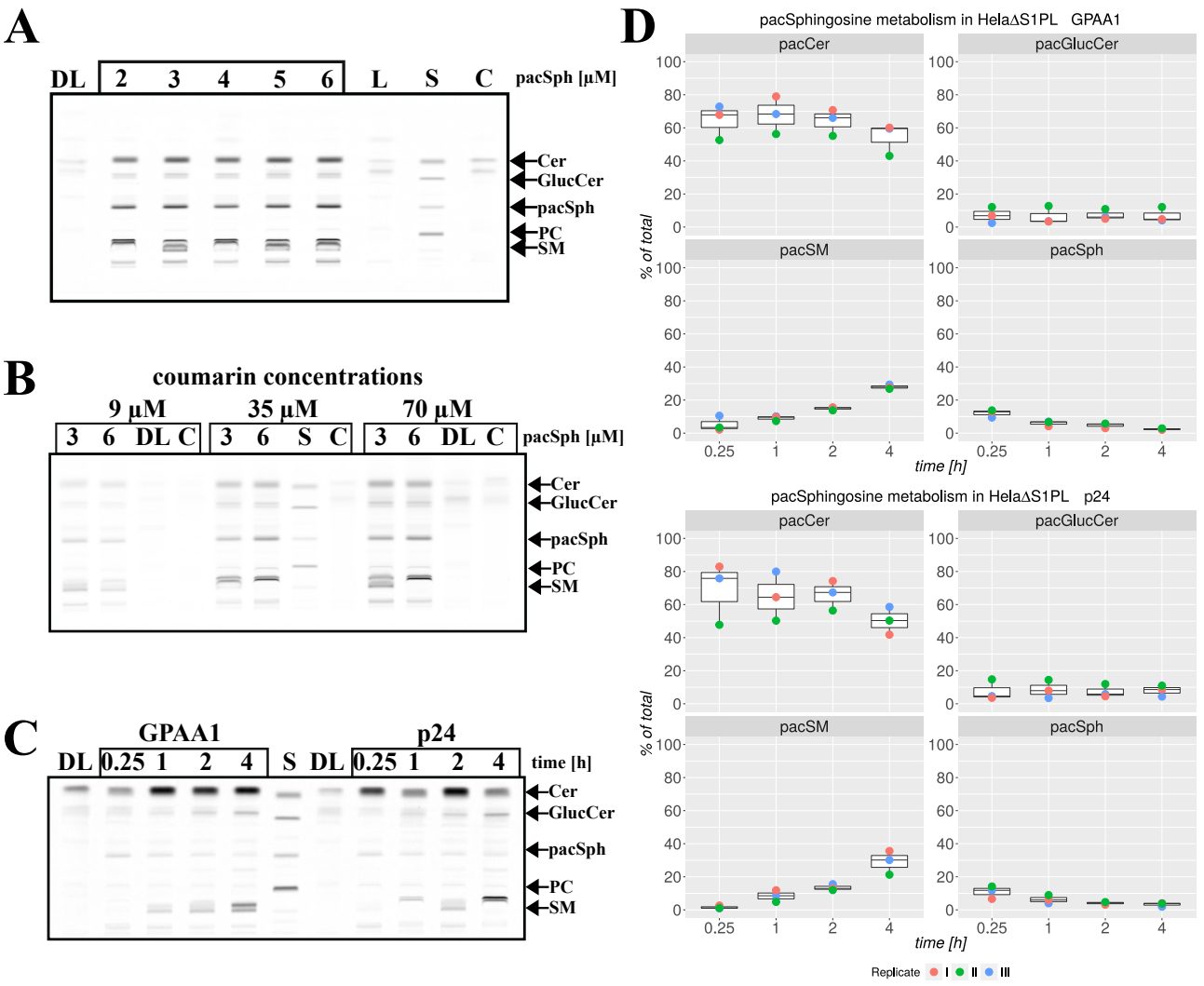

Figure 12: Analysis of sphingolipid metabolite binding kinetics in HeLaΔS1PL cells via TLC in a pulse-chase experiment A) HeLaΔS1PL cells were labelled with varying concentrations of pacSph (2/3/4/5/6 µM) and detected via 3-azido-7-hydroxycoumarin. **B)** HeLaΔS1PL cells were labelled with two concentrations of pacSph (3/6 µM) and detected with different amounts of 3-azido-7-hydroxycoumarin in the click reaction master mix (9/35/70 µM). Additionally, the TLC development protocol was changed from 7.5 cm mobile ph II to 8 cm. **C)** HeLaΔS1PL cells were transfected with a GPAA1 or p24 encoding plasmid (pGPAA1, pP24) and 24 hours later pulse-chase labelled for 0.25/1/2/4 hours with 2 µM of pacSph and detected on a TLC with 3-azido-7-hydroxycoumarin (35 µM). Shown is one of three biological replicates. **D)** Quantification of three biological replicates from C) by TLC. DL, delipidated DMEM; L, DMEM; S, standard containing pacCer, pacGlucCer, pacPC, pacSph, and clickSM; C, 3-azido-7-hydroxycoumarin.

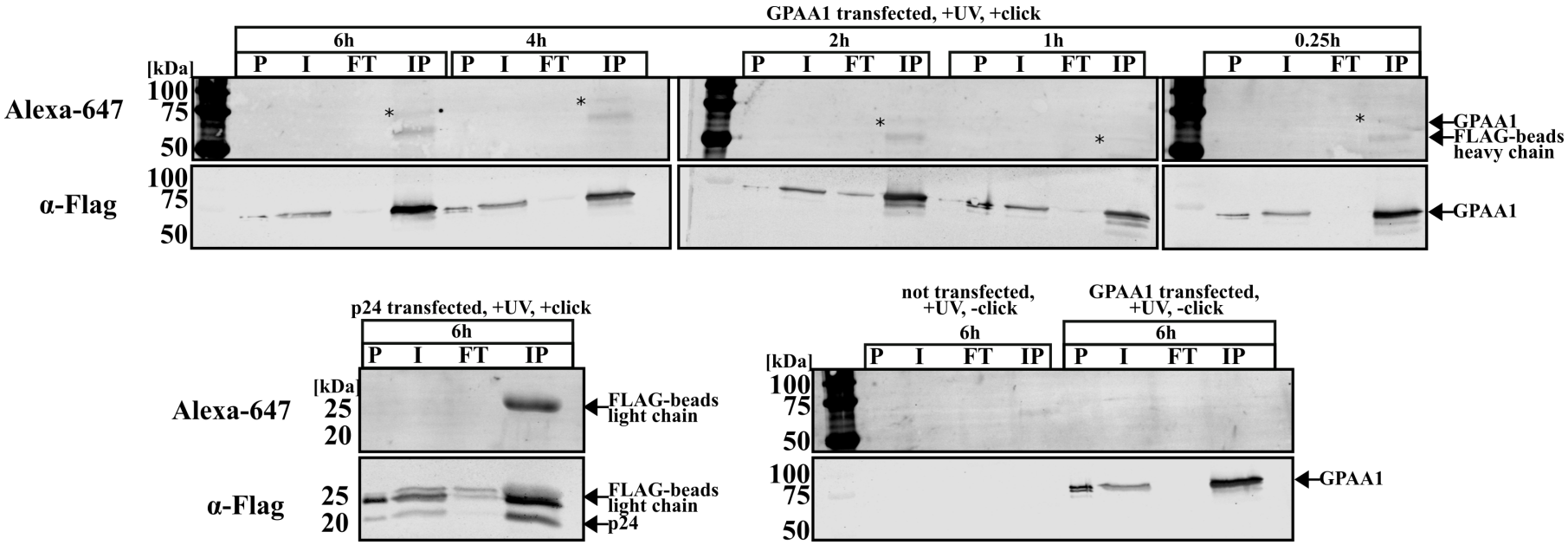

Figure 13: Pulse-chase experiment of sphingolipid binding kinetics of GPAA1 in transiently transfected HeLaΔS1PL cells via Alexa-647-N_3
HeLaΔS1PL cells were pulse-labelled with 2 µM pacSph for ten minutes, before being chased in delipidated DMEM for varying amounts of time (0.25/1/2/4/6h). Blots shown are the results of one single experiment. P, not solubilised proteins after lysis; I, input sample before IP; FT, not bound protein after IP; IP, non-solubilised fraction after lysis; IP, immunoprecipitated fraction; * depicts a weak signal for the GPAA1-pacSph-Alexa-647-complex.

As seen in figure 13, very weak (0.25/2/4/6h) or no (1h) signals for the GPAA1-pacSph-Alexa-647-complex could be detected. The same was true for the positive control p24. On the other hand, clear signal intensities for the non-clicked proteins were detected. To analyse if this was the result of overall low intracellular pacSph levels due to the short labelling time of 10 minutes, an experiment to compare directly both, pulse-chase and continuously labelling was performed (not shown). The result verified the experimental data from the pulse-chase experiment shown in figure 13 and the continuously labelling experiment shown in figure 11 by demonstrating that the conditions of a pulse-chase experiment are sufficient for detection of pacSph metabolites on TLC level (see figure 12), but not sufficient for detection of GPAA1-pacSph-Alexa-647-complexes on western blot level (see figure 13).

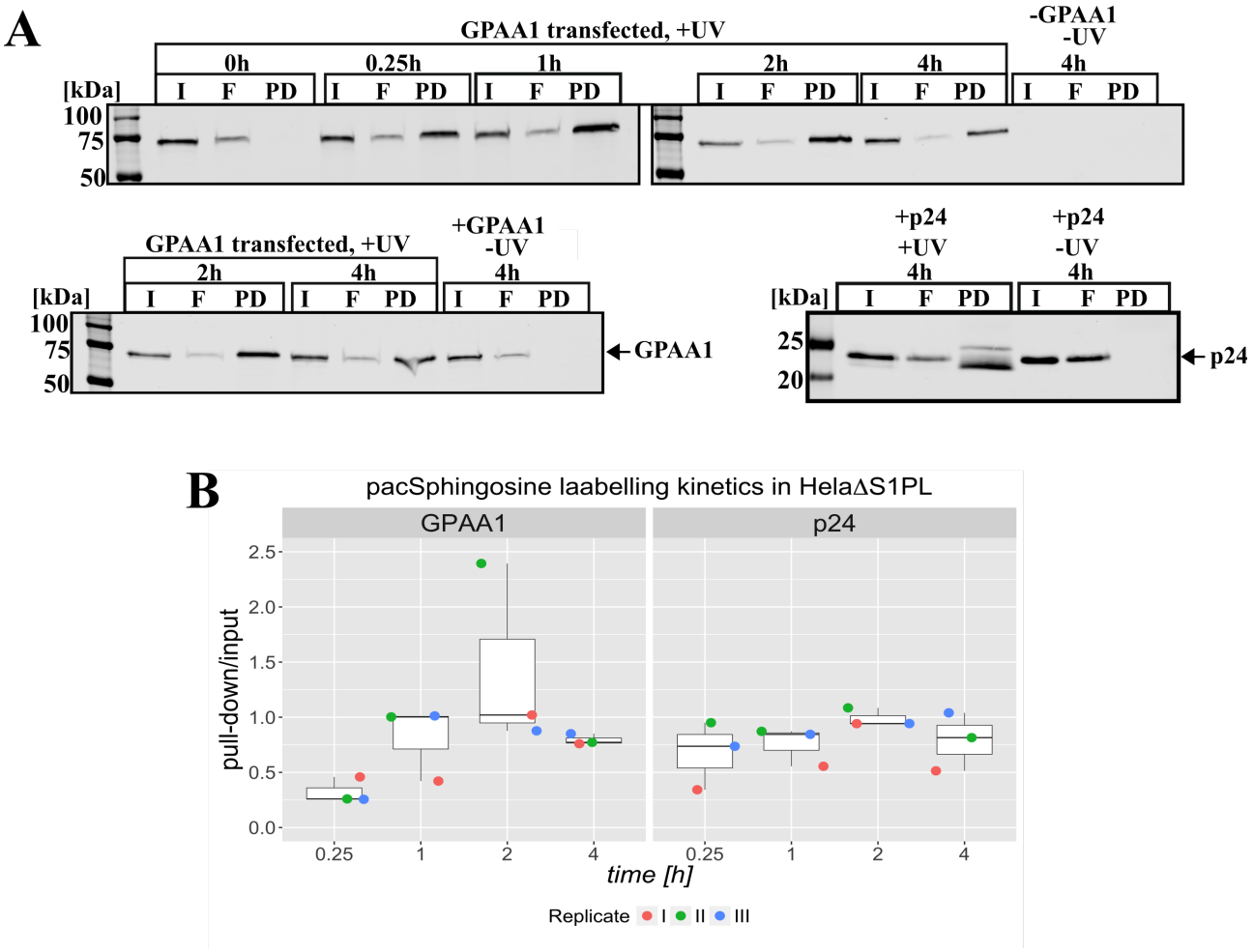

Figure 14: Analysis of sphingolipid binding kinetics of GPAA1 in transiently transfected HeLaΔS1PL cells via biotin-N_3 A) HeLaΔS1PL cells were transfected with GPAA1 for 24 hours and continuously labelled with 2 µM pacSph (0.25/1/2/4h). Interactions between GPAA1 and pacSph metabolites were detected, after UV-irradiation and attachment of biotion-N_3, via neutravidin-mediated enrichment of protein-lipid complexes. Cells transfected with the known sphingosine metabolite sphingomyelin interacting protein p24 served as positive control. Shown are selected blots out of three biological replicates. I, input before incubation with neutravidin-beads; F, flow-through of proteins not bound to neutravidin-beads; PD, pull-down fraction containing all proteins that were enriched via neutravidin-beads. **B)** depicts the ratio between quantified signal intensities $\frac{PD_X}{I_X}$ at time point X of three biological replicates from A.

To verify the previous results with a different method, biotin-N_3 was chosen as an alternative to Alexa-647-N_3 to enrich GPAA1-pacSph-complexes. In the experimental setting, HeLaΔS1PL cells

were transfected with GPAA1 and continuously labelled with 2 µM pacSph for different times (0.25/1/2/4h). Controls used were labelling without addition of pacSph, with/without GPAA1 transfection, without UV-irradiation as well as p24 transfected cells with/without UV-irradiation. The results are shown in figure 14A. Clear and distinct signals are visible in all lanes and negative controls show no signal at all. To determine pacSph labelling kinetics, the signal intensity of the biotin-enriched fraction (PD) was divided by signal intensity for the biotin-pull-down input (I). The result of three biological replicates are shown in figure 14B and the trend is comparable to the data from the Alexa-647 experiment (see figure 11C).

5.4 CRISPR/Cas9 guided cell line generation and validation containing C-terminal tagged GPAA1 to study protein-lipid interactions of the transamidase complex

5.4.1 Enrichment of endogenous transamidase complexes

As transiently expressed GPAA1 and PIGT did not allow for IP of stoichiometric correctly composed transamidase complexes (see figure 9), the decision was made to work directly with the endogenous transamidase complex. An α-GPAA1 antibody (sc-373710) was coupled to CNBr-activated beads and used in multiple experiments for IP of the endogenous transamidase complex. In a first experiment with $1x10^8$ HeLa cells, it was possible to IP endogenous GPAA1 and PIGS, while for the other subunits no signal (not shown) was detected (see figure 15A). To analyse if the low signal intensities corresponds with the amount of intracellular GPAA1, cells used for this experiment were increased by one order of magnitude. To handle this amount of cells, the suspension culture cell line Raji (lymphoblast-like cells) was used. $1x10^9$ Raji cells were used, but only a weak signal for GPAA1 and no signal at all for the other subunits (not shown) was observed (see figure 15B). But as in both experiments a signal for the heavy and light chain of the coupled antibody was detected and the relation between the GPAA1 signal and the signal of the heavy chain went from a strong GPAA1 signal (15A) to a weak GPAA1 signal(15B), an experiment was designed to analyse the GPAA1 binding capacity of the CNBr-beads (see figure 15C).
For this, $4x10^6$ HeLa cells were transiently transfected with GPAA1 and subjected to an IP with CNBr-beads. Unbound material was taken as input for an IP with FLAG-beads. The amount of GPAA1 in the flow-through was higher than what was enriched via the CNBr-beads (see figure 15C). As a conclusion, the approach with the CNBr-beads was not further followed, instead NHS-columns were coated with the antibody sc-373710 and used for high performance liquid chromatography (HPLC) with an ÄKTA^{TM} Pure system. Here, GPAA1 was transiently expressed in $1x10^7$ HeLa cells and applied to the column according to manufacturer's instructions. Small aliquots of the eluted fractions (elution buffer: 100 mM glycine pH 3) were used for SDS-PAGE, but no GPAA1 signal was detected at all (not shown). Therefore, the flow-through was subjected to enrichment via FLAG-beads and resulted in a strong GPAA-1 signal (see figure 15D).

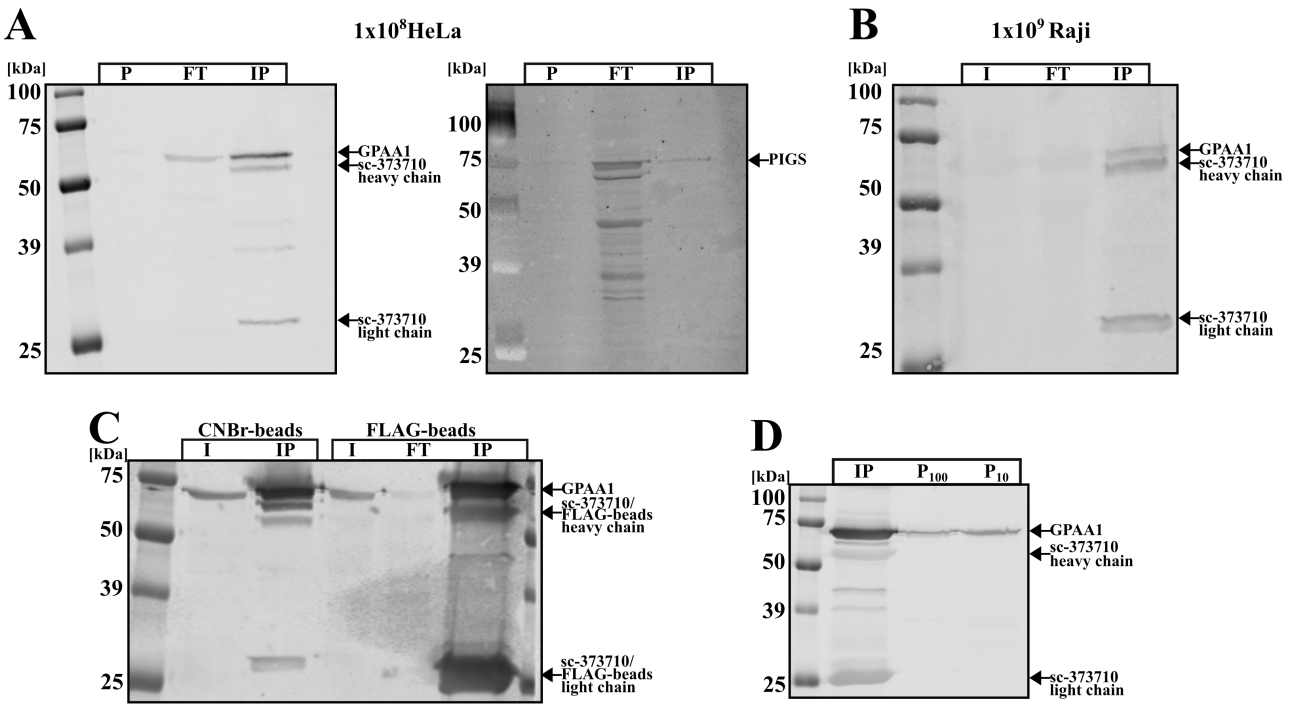

Figure 15: IP of endogenous transamidase subunits from HeLa cells A) $1x10^8$ HeLa cells were harvested and used for IP with an α-GPAA1 (sc-373710) antibody coupled to CNBr-beads. Sequentially antibodies against GPAA1, PIGT/S/K were used for detection of endogenous transamidase subunits. Only for GPAA1 and PIGS a signal was observed. P, non-solubilised fraction after lysis; FT, proteins not bound to beads, IP, proteins enriched via CNBR-beads. **B)** $1x10^9$ Raji cells were used as in A). Only for GPAA1, a signal was observed. I, input sample before IP. **C)** $4x10^6$ HeLa cells were transiently transfected with GPAA1, harvested and subjected to CNBr-beads IP. The flow-through of the CNBr-beads was used as input sample for a follow up FLAG-IP to analyse the GPAA1-binding capacity of the CNBr-beads. **D)** NHS-columns were coated with sc-373710 and used for a high performance liquid chromatography (HPLC) with an ÄKTA^{TM} Pure system. GPAA1 was transiently expressed in $1x10^7$ HeLa cells, harvested, lysed and used with the HPLC according to manufactures instructions. Before loading the samples onto the HPLC, two lysate clearing steps were (P_{10}=10.000g for 20 min; P_{100}=100.000g for 60 min) performed. The wash step was subjected to an IP with FLAG-beads. The elution fractions were loaded on different SDS-PAGEs, but as there was no signal at all, only the result of the FLAG-IP is shown. Data in A/B/D was jointly produced with Rainer Beck.

5.4.2 Selection of CRISPR/Cas9 generated cell lines containing C-terminal tagged GPAA1

The most important parameter for the CRISPR/Cas9 guided cell line generation containing C-terminal tagged GPAA1 was the intracellular available amount of GPAA1. A screening experiment of different cell lines (human fibroblasts hFib, mouse embryonic fibroblasts H806, mus musculus brain neuroblastoma N2A, adenocarcinomic human alveolar basal epithelial cell line A549, hepatocarcinoma cell line Huh-7, cervix carcinoma cell line HeLa, human embryonic kidney cell line HEK293, and lymphoblast-like cell line Raji) was performed and 50 µg of whole cell lysate were subjected to SDS-PAGE, transferred to a PVDF-membrane and analysed with an α-GPAA1 antibody. It was possible to detect weak signals for HeLa, HEK293, Raji, N2A, Huh-7 and hFib (see figure 16A). Signal intensities were, except for the HeLa cell line, poor and barely visible. Nevertheless, signals at the expected kDa height for GPAA1 were quantified, normalised against the GPAA1 signal in HeLa cell line and listed in table 11. To control for the solubilisation efficiency

of endogenous ER resident proteins, calnexin was used and did not show any exceptional strong deviation between the different cell lines. To verify the assumption that HeLa cell lines are the most suitable ones for the generation of the endogenous tagged cell line, a second experiment was performed. In this, membrane fractions of HeLa, HEK293, hFib and Raji cell lines were generated to improve the signal intensities of the whole cell lysate experiment. Loading of 50 µg of membrane fractions did show generally clearer signals (see figure 16B), but the unsatisfying signal to background ratio did not allow for a reliable quantification. HeLa cells were, as they provided the most consistent results over all experiments, selected as the prime candidate for the CRISPR/Cas9 experiment.

Table 11: Endogenous GPAA1 levels of different cell lines normalised to HeLa from figure 16A

[n]	HeLa	HEK293	Raji	N2A	Huh-7	hFib
1[1]	100%	8.5%	68.3%	35.4%	28.5%	5.2%

[1] Signal intensities divided by HeLa signal intensities*100

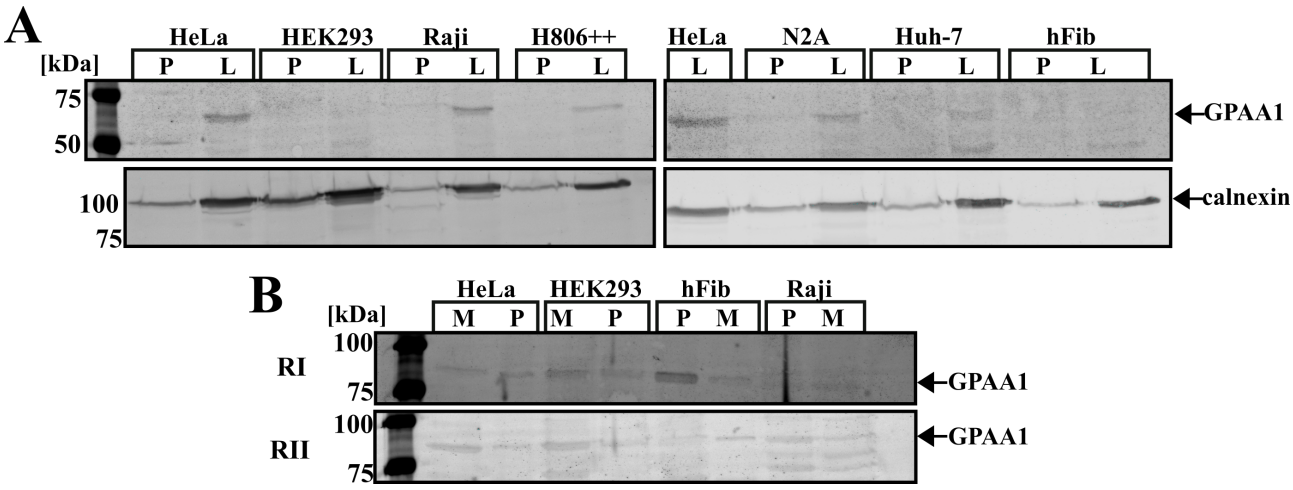

Figure 16: Analysis of endogenous GPAA1 levels in different human and murine cell lines A) 50 µg of whole cell lysates of different cell lines were separated by two different SDS-PAGE, transferred to PVDF-membranes and analysed with α-GPAA1 (sc-373710) antibody. To compare quantification intensities, the same HeLa lysate sample was loaded on both blots. Furthermore, the endogenous ER resident protein calnexin was used as a control for solubilisation of ER proteins. L, whole cell lysate; P, non-solubilised proteins; hFib, human fibroblasts; H806, mouse embryonic fibroblasts; N2A, mus musculus brain neuroblastoma N2A; A549, adenocarcinomic human alveolar basal epithelial cell line; Huh-7, hepatocarcinoma cell line; HeLa, cervix carcinoma cell line; HEK293, human embryonic kidney cell line; Raji, lymphoblast-like cell line. **B)** 50 µg of membrane fractions from selected cell lines of A) were compared with each other. Two biological replicates are shown and were used for quantification. M, membrane fraction; P, non-solubilised proteins after membrane fraction.

5.4.3 Design of gRNAs for genomic GPAA1 loci

To design guide RNAs (gRNA), the genomic context of the GPAA1 loci on chromosome 8 was retrieved from Ensembl and a search query containing partially the C-terminal end of GPAA1 exon 12, and a short sequence of the 3'UTR was designed and used as input for the gRNA prediction tool CRISPR Design (http://crispr.mit.edu/) from the Zhang lab (MIT, USA). The top 9 candidates and their orientation on the genomic sequence are shown in figure 17. The top 3 candidates were selected, their detailed location in the genomic loci determined (figure 17B) and their capability to induce double strand breaks was assessed. For this, HeLa cells were double transfected with the vector containing the coding sequence for the Cas9 molecule (hCas9) and the vector containing any of the three gRNAs (MLM3636-gRNA#1-3). As a control, wild-type cells were used. After 72 hours, genomic DNA was extracted and a fragment, containing the C-terminal part of the genomic GPAA1 loci (as depicted in figure 17B), was amplified. PCR fragments from wild-type and gRNA transfected cells were heterodimerised (1:1 ratio) and cut at positions containing a base pair mismatch. All gRNA-candidates, as seen in figure 18A), successfully introduced a double strand break, and gRNA#1 was selected for the CRISPR/Cas9 generation of a HeLa cell line containing C-terminal tagged GPAA1.

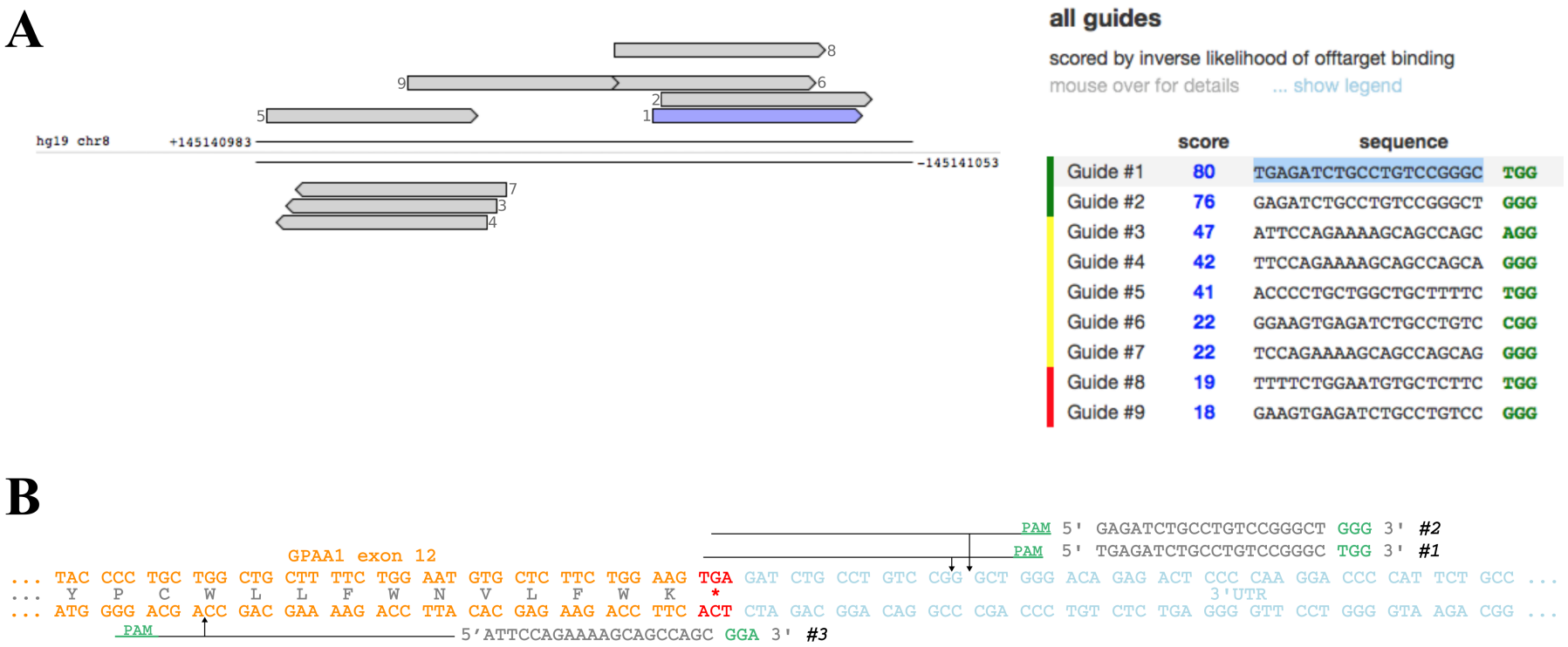

Figure 17: Predicted guide RNAs and their position in the genomic loci of GPAA1 A) Results of the gRNA prediction tool CRISPR Design (http://crispr.mit.edu/) for the C-terminal part of last exon of the GPAA1 loci. Shown are top 9 guide (g)RNA-candidates, their location and orientation in the genomic context. For in detail results of genomic off targets, see figure 31 for Guide#1, figure 32 for Guide#2 and figure 33 for Guide#3. **B)** Position on a base per base sequence and the corresponding amino acids of gRNA-candidates #1, #2, and #3. Shown are the C-terminal part of GPAA1 (in orange), the stop codon (in red), the 3'-UTR, the gRNA sequences, and the exact position where Cas9 is expected to introduce the double strand break (arrow). PAM, protospacer adjacent motif sequence.

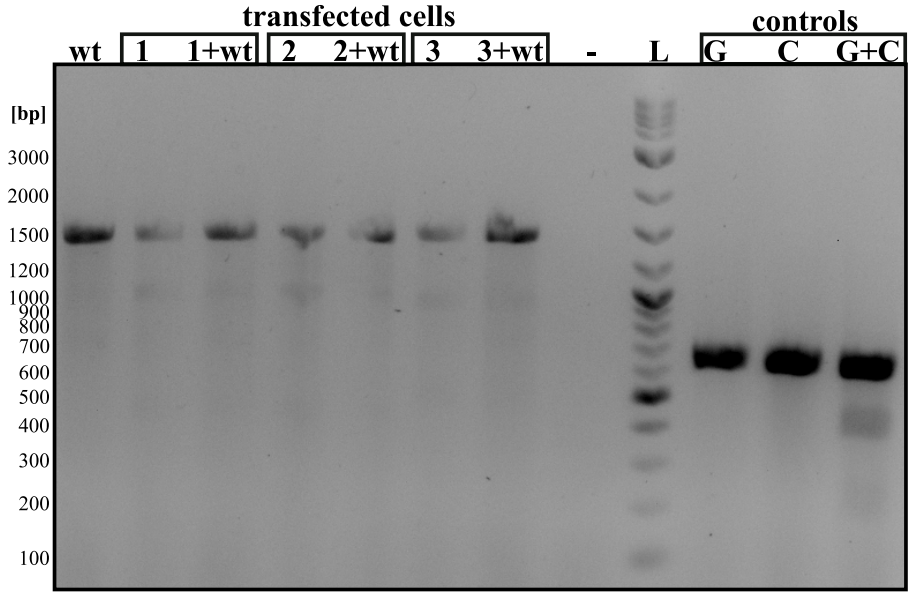

Figure 18: Assessment of gRNA-candidates capability to introduce DNA double strand breaks HeLa cells were transfected for 72 hours with a vector containing either gRNA#1, #2, or #3. Genomic DNA was extracted and a fragment, containing the C-terminal part of the genomic GPAA1 loci (as depicted in figure 17B), amplified. PCR fragments from wild-type (wt) and gRNA transfected cells were mixed in a 1:1 ratio, heated up to create single stranded DNA fragments which then were allowed to form DNA-heteroduplexes by stepwise temperature reduction. Employing the fact that specific nuclease exist that cut mismatched double stranded DNA, such as the result of an error in the double strand break repair mechanism, the surveyor mutation detection kit was used according to manufactures instruction. Expected fragment sizes: 1350nt for GPAA1 fragment (digestion products at 905nt, 445nt) and 633nt for surveyor mutation detection Kit controls G and C (digestion products at 400nt, 200nt). L, ladder; -, negative control; G/C/G+C, positive controls from the kit.

5.4.4 Generation and selection of specific HeLaΔS1PL cell line containing endogenous C-terminal tagged GPAA1

HelaΔS1PL were triple transfected (gRNA#1, Cas9, and donor plasmid containing the to be inserted tag sequence) for 72 hours. Serial diluted cells were seeded into 96 wells and propagated until 6-well format was reached. At this point cells were harvested, genomic DNA was extracted and success of tag integration was determined for each single cell clone via PCR (see figure 19A). Clones containing one band at 1527nt were expected to represent a successful homozygous tag integration, while one band at 1350nt defined a wild-type clone. Samples with two bands at the respective heights were termed to reflect a heterozygous integration, containing wild-type and tagged allele of GPAA1. Out of 55 clones tested, 14 were determined to be heterozygous for tag insertion (25%), while two clones (#76, #39) were homozygous (3.6%). The screening results of #76 and #39 as examples for a homozygous insertion and #18 for a wild type are displayed in figure 19B). Sequencing of all three clones confirmed the integration for #76 and #39 (see figure 19C). HeLaΔS1PL GPAA1#76 was selected as mutant cell line of choice for further validation experiments.

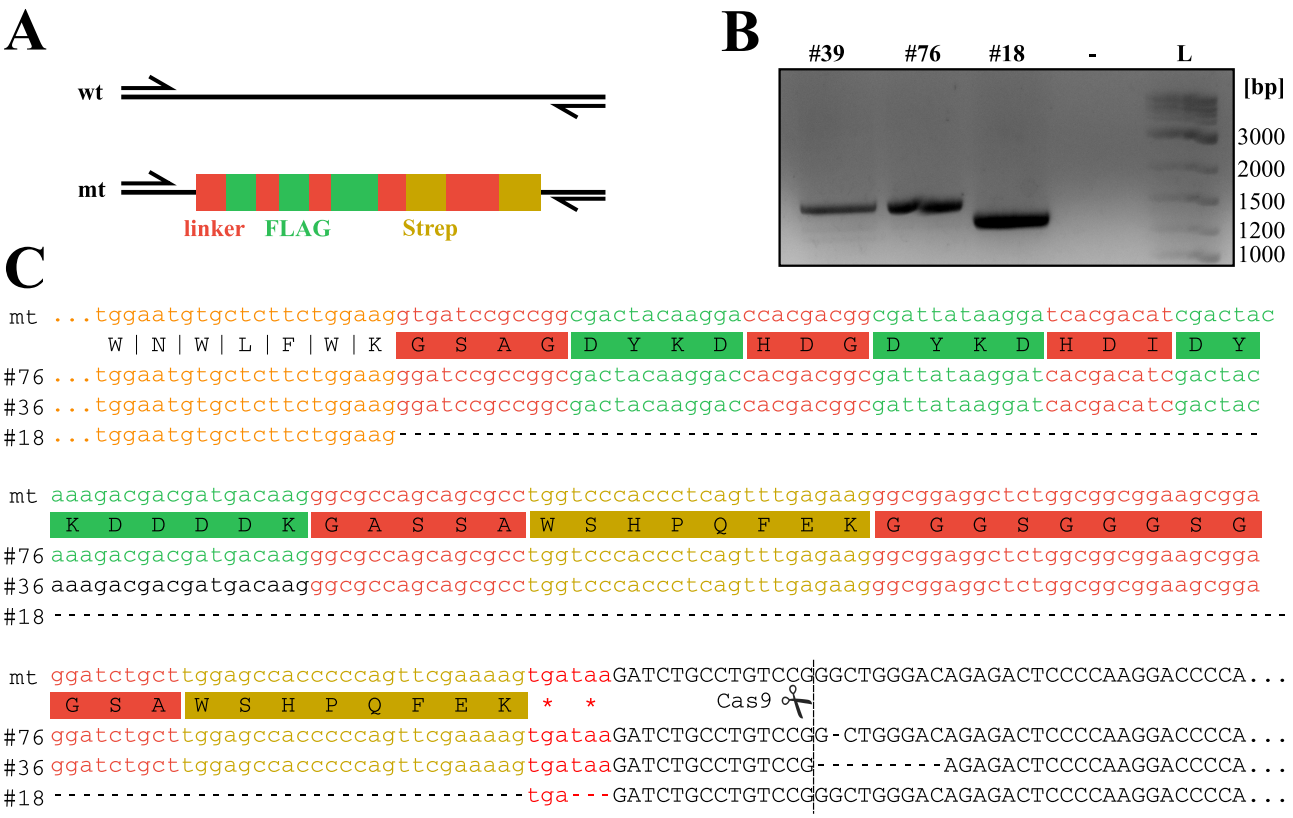

Figure 19: CRISPR mediated C-terminal tagging of endogenous GPAA1 A) Schematic drawing of a PCR on genomic DNA to determine positive insertions of the 3xFLAG-Twin-Strep tag. Cells without insertion of the tag are coded with wild type (wt) and successful integration with mutant (mt). Primer positions are decoded with black arrows. Expected sizes: wt=1350, mt=1527nt **B)** PCR results of three single cell clones derived from gRNA#1 transfected HeLaΔS1PL cells displayed homozygous integration of the tag (#39/76) or a wt allele (#18). **C)** Sequencing results of B) showed variability in the 3'-UTR, closely to the Cas9 cleavage site. Inserted sequence is colour coded according to A) and contains a double stop codon (red).

5.4.5 Characterisation of HeLaΔS1PL GPAA1#76

Functionality of the integrated 3xFLAG-Twin-Strep tag in the HeLaΔS1PL GPAA1#76 clone was assessed in the following. After a FLAG-IP it was possible to co-IP the transamidase subunits PIGS and PIGK (see figure 20A), indicating an integration of GPAA1-$(FLAG)_3$ into the transamidase complex. Furthermore, a pull-down experiment with streptactin-beads proved successful in enrichment of GPAA1 (see figure 20B). To verify that the C-terminal tag did not interfered with the actual attachment of GPI-anchors to proteins containing the respective GPI-anchor attachment sequence, the cell surface localisation of the GPI-anchored protein CD59 was determined via cell surface biotinylation. No difference was observed for the endogenous (see figure 20D) and overexpressed CD59 (see figure 20C/E).
To rule out that the two internal streptags unspecifically interact with neutravidin beads, thus rendering them incompatible with the biotin-click protocol (see figure 14), an experiment was performed where HeLaΔS1PL GPAA1#76 were labelled with pacSph and clicked in lysate with Alexa-647-N_3 (see figure 21B). No signal was observed in the eluted fraction after neutravidin-beads enrichment, while the in gel fluorescence showed the respective signal for GPAA1.

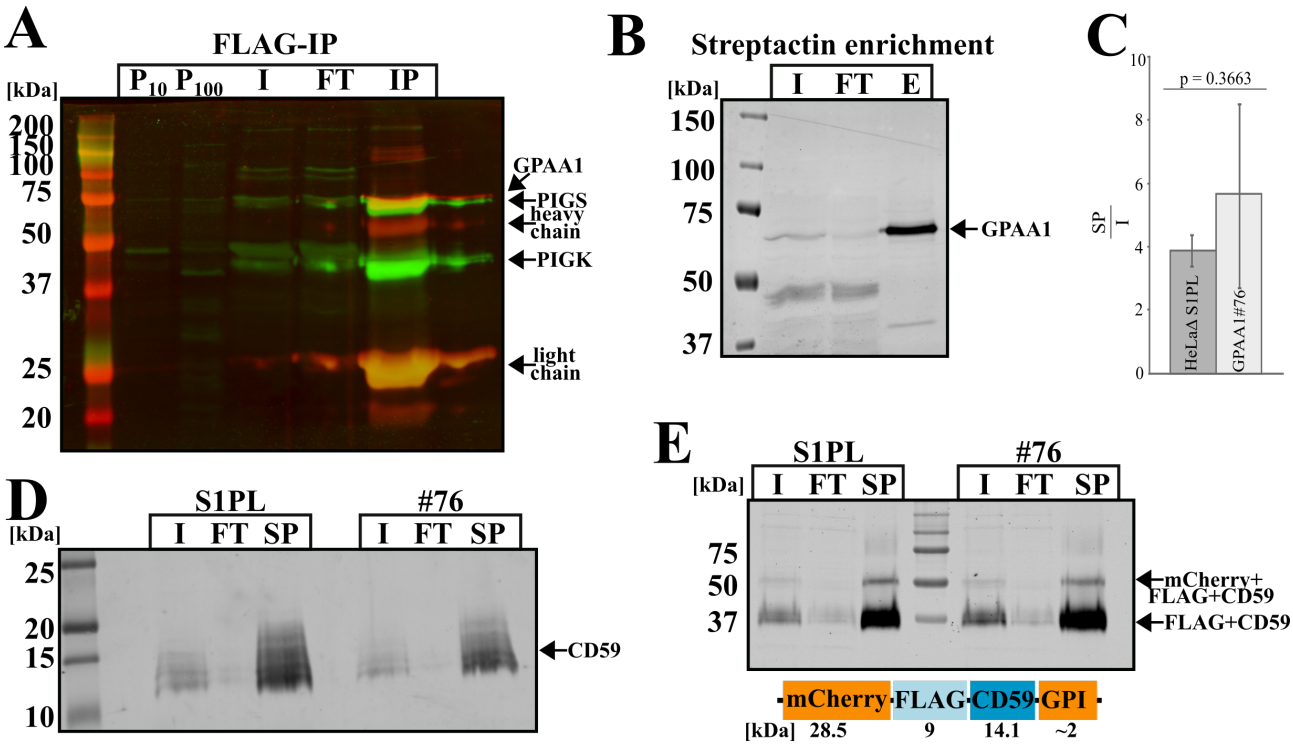

Figure 20: Validation of tag integration and functionality of the transamidase complex in HeLaΔS1PL GPAA1#76 A) FLAG-IP of endogenous C-terminal $(FLAG)_3$-tagged GPAA1 from $5x10^7$ HeLaΔS1PL GPAA1#76 pre-cleared (P_{10}=10.000g for 20min, P_{100}=100.000g for 20min) whole cell lysate. The blot was sequentially developed with antibodies against GPAA1 and PIGS/K. I, input sample; FT, flow-through sample; IP, proteins enriched via FLAG beads. **B)** Streptactin enrichment of GPAA1 from $2x10^7$ whole cell lysate. Samples were bound to streptactin-beads and incubated over night, before being eluted with 3mM biotin. E, enriched fraction after elution and MeOH-$CHCl_3$ precipitation. **C)** Ratios of quantified signal intensities $\frac{SP}{I}$ of three biological replicates from E are shown and were tested for significant differences between groups by way of a two-sided T-test. **D)** Endogenous CD59 expression levels in $3x10^5$ HeLaΔS1PL and HeLaΔS1PL GPAA1#76 cells as detected by surface biotinylation. SP, enriched fraction containing biotinylated protein. **E)** Construct from [55] was used to assess differences of CD59 cell surface recruitment in $3x10^5$ HeLaΔS1PL and HeLaΔS1PL GPAA1#76 via surface biotinylation.

When replacing the neutravidin-beads with streptactin-beads, strong signals were obtained for in-gel fluorescenc as well as for western blot (see figure 21A). According to the streptactin protocol, before loading the sample on the beads, the chemicals from the click reaction are to be removed via several MeOH precipitation steps. To validate the necessity of these washing steps, samples were precipitated not at all, once, twice or three times (see figure 21C/D). No difference was observed between one and three times, while the signal intensity without any washing step appeared to be lower. Furthermore, compared to the overexpressed experiments where 2 µM pacSph was the limit with regards to cell viability, in the HeLaΔS1PL GPAA1#76 cell line, 3 and 5 µM could be used without any major increase in cell mortality (data not shown). A final experiment with 5 µM pacSph and one MeOH washing step provided a clear and strong signal for in-gel fluorescenc as well as for western blot (see figure 21E).

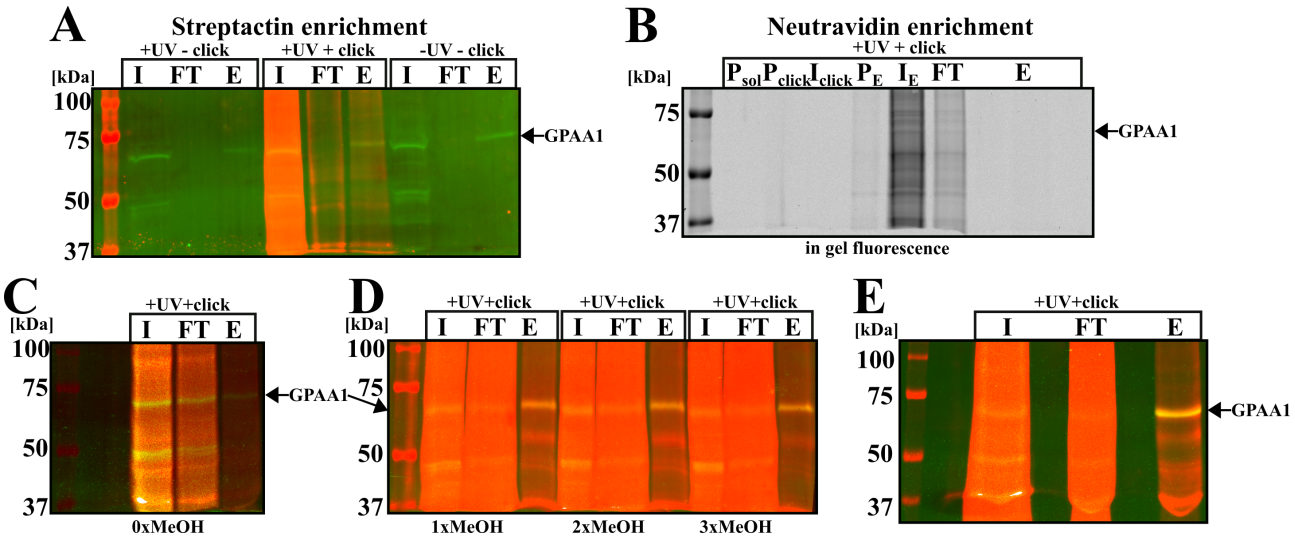

Figure 21: Alexa-647-N_3 click in HeLaΔS1PL GPAA1#76 whole cell lysate A) Alexa-647-N_3 click in 4x10^6 whole cell lysate and enrichment via streptactin-beads. I, input sample; FT, flow-through sample; E, proteins enriched via streptactin-beads; red, in gel fluorescence; green, α-FLAG antibody. **B)** In-gel fluorescence of Alexa-647-N_3 click in 2x10^7 whole cell lysate and enrichment via Neutravidin-beads. P_{sol}, non-solubilised pellet; P_{click}, non-solubilised pellet before click reaction; P_E, non-solubilised pellet before the sample was given on the beads; I_{click}, lysate before click reaction; I_E, solubilised sample before mixing with neutravidin-beads; FT, sample bound by beads; E, bead eluate after enrichment. **C/D)** Alexa-647-N_3 click in 2x10^7 whole cell lysate was precipitated zero to three times, before being loaded on streptacin-beads. **E)** One time precipitation of Alexa-647-N_3 clicked whole cell lysate (2x10^7) and enrichment with streptactin-beads.

5.4.6 Enrichment of endogenous transamidase complex in native lipid environment from HelaΔS1PL GPAA1#76

HelaΔS1PL GPAA1#76 were harvested and the transamidase complex was, surrounded by its native lipid environment, enriched via styrene maleic anhydride (SMA) co-polymer. Following this approach, it was possible for the first time, to co-IP all transamidase subunits (for GPAA1/PIGT/U/K see figure 22A, for GPAA1/PIGS/PIGK see figure 22B).

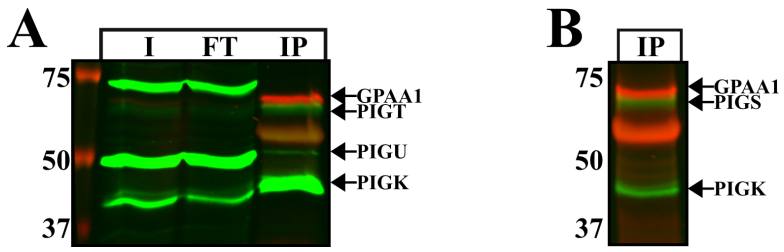

Figure 22: Purification of endogenous transamidase complex using styrene maleic anhydride (SMA) co-polymer A) 8x10^6 HelaΔS1PL GPAA1#76 cells were seeded, solubilised via SMA and enriched over FLAG-beads. Blot was sequentially developed with rabbit α-PIGU/K/T and mouse α-DDDKK antibodies. I, input sample before IP; FT, proteins not bound to beads; IP, proteins enriched via FLAG beads. **B)** Same as in A, but developed with rabbit α-PIGS und α-PIGK.

In a proof-of-principle experiment, it was possible to detect via mass spectrometry lipids from endogenous transamidase complexes enriched via FLAG-IP from SMA treated HeLaΔS1PL GPAA1#76

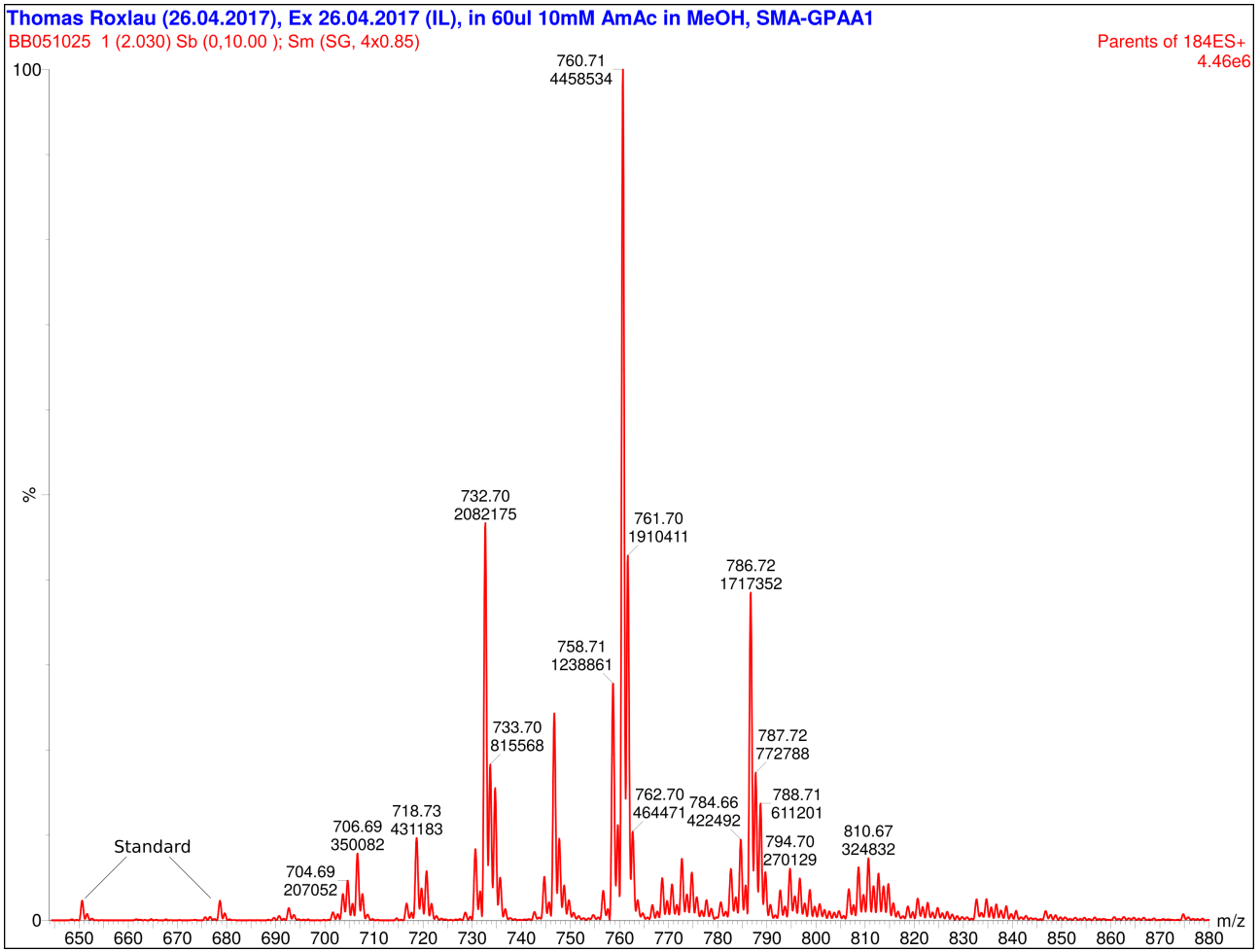

Figure 23: Mass spectrometric analysis of lipids derived via FLAG-enrichment of endogenous GPAA1 using styrene maleic anhydride (SMA) co-polymer Mass spectrometric spectra from lipids extracted from a FLAG-beads IP from HelaΔS1PL GPAA1#76 cells. Data produced jointly with Iris Leibrecht and Christian Lüchtenborg.

membrane fractions (see figure 23). Comparing the amplitude of the standards at 650 and 678 m/z with the amplitudes of the rest of the spectra shows the substantial amount of lipids extracted.

5.4.7 Separation of transamidase subunits via different protein gel systems

Having verified the functionality of the CRISPR/Cas9 inserted tag, the next target was to find a way to assess labelling specificity for all transamidase subunits in one experiment and on the same protein gel. PIGS, PIGT, and GPAA1 should be, as depicted in figure 24A and according to their predicted molecular weight (PIGT: 65.1 kDa, UniProt: Q969N2, PIGS: 61.65, Uni-Prot: Q96S52, GPAA1: 67.623, UniProt: O43292), size-wise closely matched and it is already difficult to successfully separate a 3kDa difference. Furthermore, the the tag sequence (see figure 19C) is to be added upon the GPAA1 molecular weight. According to the ExPASy tool *compute pI/Mw* (https://web.expasy.org/cgi-bin/compute_pi/pi_tool), an additional molecular weight of 6.245 kDa attributes to an overall 71.868 kDa for GPAA1. Theoretical, PIGT should be separated by 6.78 kDa from GPAA1 and by 3.45 kDa from PIGS. Furthermore, the other two subunits PIGS (45.252 kDa, UniProt: Q92643) and PIGU (50.052 kDa, UniProt: Q9H490) should also to be resolved on the same protein gel. The commercial kits NuPAGE^{TM} 4-12% Bis-Tris protein gel (see figure 24B), NuPAGE^{TM} 7% Tris-Acetate protein gel (see figure 24C) and the Bolt^{TM} 8% Bis-Tris plus gel (see figure 24E) from ThermoFischer were procured and tested together with a hand cast 18x16cm Tris-Glycine protein gel (figure 24D). For the experiment, 1x10^{7} HeLaΔS1PL GPAA1#76-cells were harvested, the transamidase subunits enriched via FLAG-IP and separated on the different gel systems. To analyse their characteristics, the height of the different marker bands as well as the distance between 37-50 kDa and 50-75 kDa bands was measured with a ruler and are displayed in table 12. Here the Bolt^{TM} 8% Bis-Tris plus gel showed the highest resolution as it focussed bands more than all other commercial gel systems (0.1 cm against 0.2-0.3cm) and provided the highest distance between the 50-75 kDa marker bands (1.4 cm against 0.95-1.05 cm) on an 8x8 cm gel. Contrary to the theoretical expectations, not GPAA1 with its higher molecular weight was to be detected closest to the 75 kDa marker band, but PIGT. PIGS is seen on the expected height. While the NuPAGE^{TM} 4-12% Bis-Tris protein gel showed a separation between the PIGS and GPAA1 band, no separation was detectable between GPAA1 and PIGT. The NuPAGE^{TM} 7% Tris-Acetate protein gel failed to separate any of the bands and only the Bolt^{TM} 8% Bis-Tris plus gel showed the potential to differentiate between all three bands. The space in-between the bands of PIGT/S and GPAA1 was not deemed to be sufficient for a successful separation, knowing that p24 and the p24-pacSph metabolite complex show a different SDS-PAGE running behaviour. A manually casted 18x16 cm 8% Tris-Glycine gel was chosen to analyse the change in separation behaviour when the maximal separation distance was increased (previously 8x8 cm). Even though the distance between the 50-75 kDa marker bands increased from the 1.4 cm of the Bolt^{TM} 8% Bis-Tris plus gel to 3.1 cm, the sharpness of bands decreased as the marker width range increased from 0.1 cm to 0.3-0.65 cm (see figure 24D). Furthermore, no differentiation between the GPAA1 and PIGS signal was observed.
Additionally, separation properties of manually cast 8x8 cm 7% and 10% Tris-Glycine gels were compared directly with each other. If the 37 kDa protein marker band nearly reached the end of the separation gel (not shown), no difference in separation capabilities were observed and it was not possible to create distinct bands for PIGS, PIGT and GPAA1.
Therefore, the approach was changed and the samples were loaded on a 2D-gel electrophoresis system (see figure 24F). Even though a nice separation was observed for different unspecific proteins, no signal at all for any of the transamidase subunits could be detected. Therefore, the

decision was taken to go for a traditional approach by splitting samples on two different gels, to detect PIGT, GPAA1, and PIGS on different gels without overlapping signals.

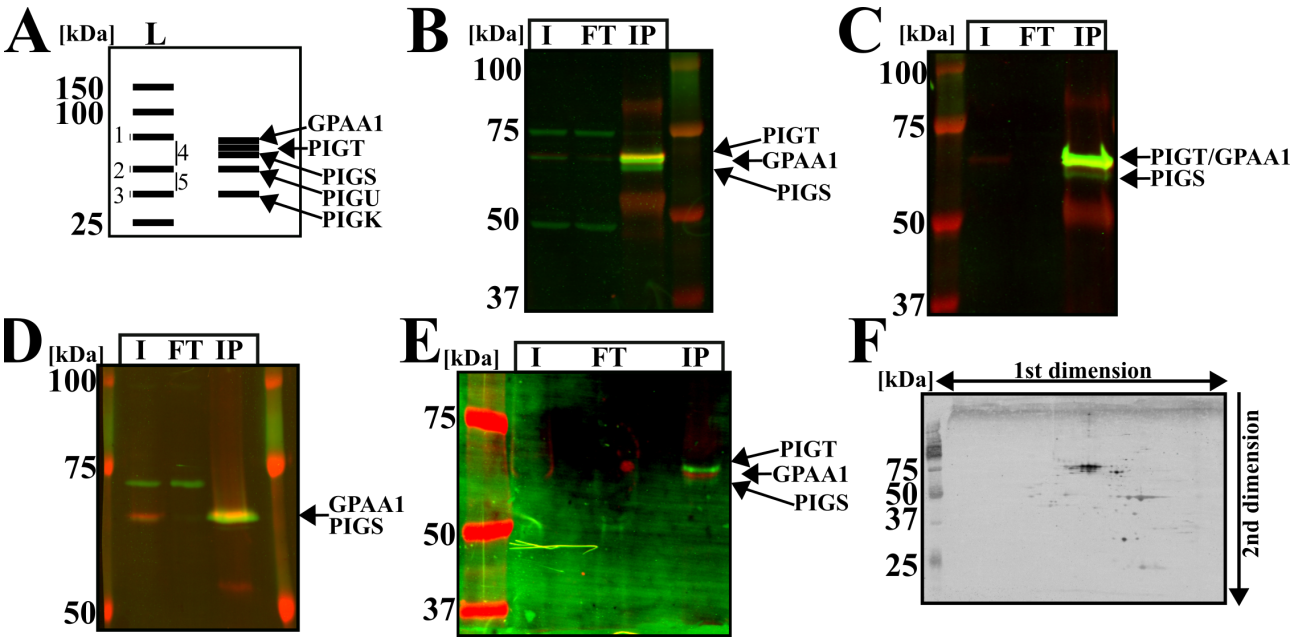

Figure 24: Separation of transamidase subunits GPAA1, PIGS and PIGT A) Schematic view of expected protein transamidase subunit sizes and distances (1-5) to be measured to analyse the separation properties of the different gel systems. **B)** FLAG-IP loaded on a NuPAGE™ 4-12% Bis-Tris protein gel. **C)** NuPAGE™ 7% Tris-Acetate protein gel. **D)** Hand cast 18x16 cm 8% Tris-Glycine protein gel. **E)** Bolt™ 8% Bis-Tris Plus Gel. **F)** 2D-gel electrophoresis of overexpressed PIGK/T/S and GPAA1. Samples were first separated on an IPG-strip in the first dimension, before being transfered from the IPG-strip to an SDS-PAGE to resolve he second dimension.

Table 12: Separation of transamidase subunits on different gel systems

corresponding figure	gel system	marker width [cm]	distance between marker bands [cm]	
			37-50 kDa	50-75 kDa
24B	NuPAGE™ 4-12% Bis-Tris	0.2	0.9	0.95
24C	NuPAGE™ 7% Tris-Acetate	0.2-0.3	0.8	1.05
24D	8% Tris-Glycine (18x16cm)	0.3-0.65	1.6[1]	3.1
24E	Bolt™ 8% Bis-Tris Plus	0.1	0.9	1.4

[1] not shown in figure 24D

5.5 Endogenous transamidase subunits protein-lipid interactions

5.5.1 pacChol and pacSph labelling characteristics of endogenous transamidase subunits in HeLaΔS1PL GPAA1#76

After verification of endogenous tagged GPAA1 functionality in the HeLaΔS1PL GPAA1#76 cell line and the decision to detect all different transamidase subunits on two different blots, labelling experiments were conducted to analyse specificity of protein-lipid interactions in the transamidase complex. Whole cell lysate was labelled with pacSph and enriched via biotin-N_3. Without biotin-N_3 click reaction, no transamidase subunit showed any enrichment (see figure 25A-C). On

the other hand, only GPAA1 showed substantial enrichment when subjected to a click reaction The same experiment was repeated with cell lysates from membrane fractions obtained from cells labelled with pacChol(see figure 25B) and pacSph (see figure 25C). In both experiments, only for GPAA1 labelling was observable. To summarise, strong labelling signals could be observed for GPAA1 with both, pacSph and pacChol.
To analyse if the observed labelling results correlate with the occurrence of cholesterol (CRAC/-CARC) binding sites, the amino acid sequences for the transamidase subunits were retrieved from UniProt and used as input samples for the ScanProsite tool. The search terms for cholesterol binding sites (CRAC: [LV]-X(1,5)-Y-X(1,5)-[KR], CARC: [KR]-X(1,5)-[YF]-X(1,5)-[LV]) were retrieved from the literature [104] and the search term ([VITL]-X(2)-[VITL][VITL]-X(2)-[VITL][FWY]) for the sphingolipid binding motif was retrieved from [15],[16]. All sequences that did correspond to one of the binding motifs (see table 13) were considered a hit, when at least one amino acid was located inside a transmembrane domain (TMD). When retrieving the protein sequence of PIGU, no data with respect to the orientation of the N- and C-terminal part (lumenal or cytosolic) was provided by UniProt. The results are displayed in figure 26. CARC cholesterol binding motifs could be detected for the TMD of PIGT, both PIGS TMDs, the TMDs five and six of GPAA1 and TMDs two, seven and eight of PIGU. CRAC binding motifs were detected in the first TMD of GPAA1, the PIGK TMD and TMD three of PIGU. The sphingolipid binding motif of GPAA1 is located in TMD four, and a partially covered binding motif is present in TMD eight of PIGU. The specific PIGU region with a similarity to a conserved sequence in long-chain fatty acid elongases [105], was determined to be between the TMDs four and five. Experimentally, GPAA1 showed labelling for pacChol and pacSph which fits also with the specific motifs found in the *in silico* screen. Even though a cholesterol binding motif was suggested for PIGK/U and PIGT, no labelling was detected in the *in vivo* experiments. As prime candidate for a protein-sphingolipid interaction, only GPAA1 was assessed in the following experiments.

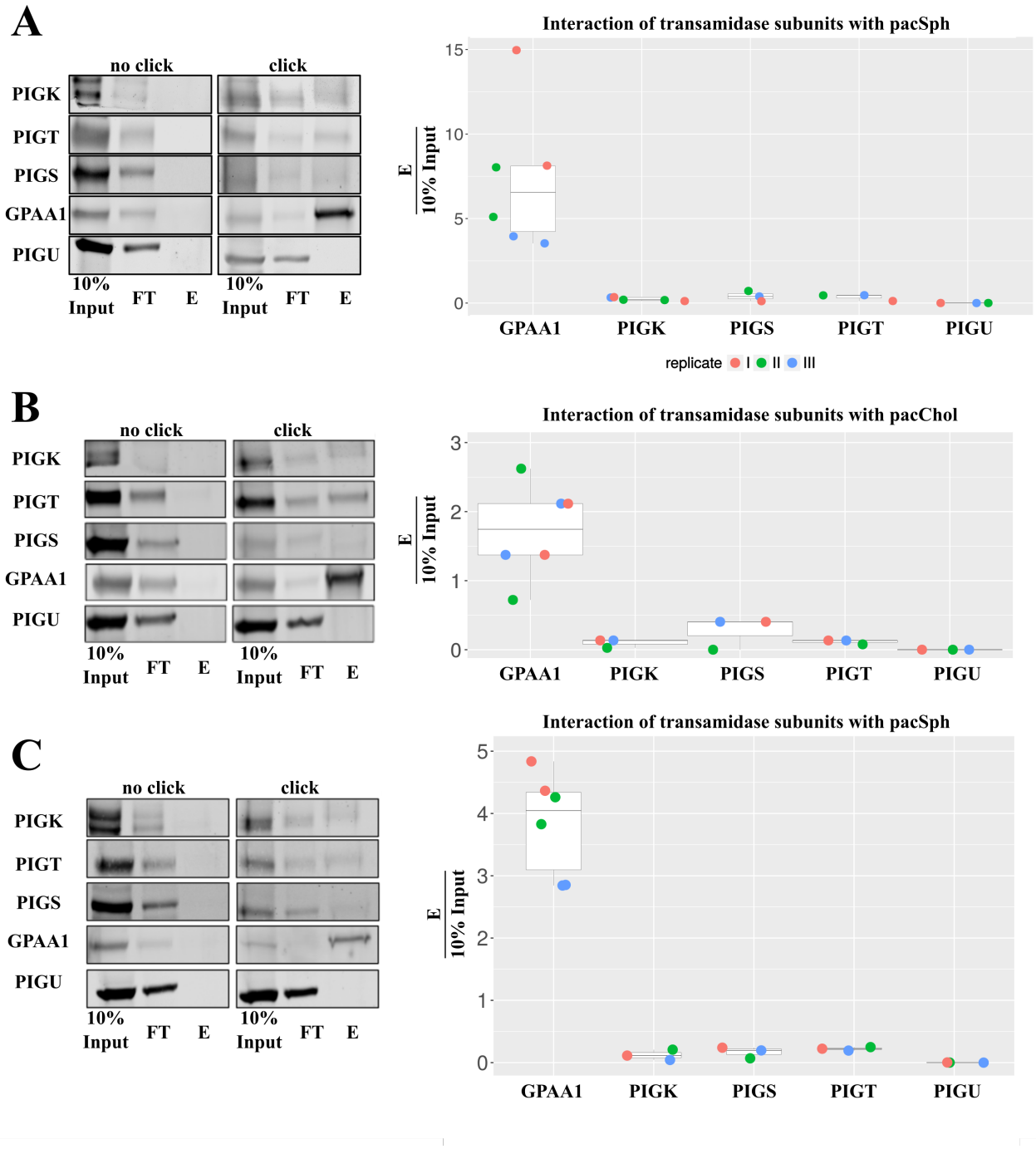

Figure 25: Lipid interactions of transamidase subunits 1x10^7 HeLaΔS1PL GPAA1#76 were seeded, labelled for 4 hours with 6 µM pacSph or for 30 Minutes with 10 µM pacChol, harvested and protein-lipid complexes were enriched by attachment of biotin to the azide group of the bifunctional lipid via a CuAAC reaction. Western blot signal intensities of three biological replicates were measuered and the interaction between the lipid and the specific transamidase subunit was determined by the ratio between the enriched fraction (E) and the 10% Input sample. Shown on the left are the results of one representative experiment. On the right are the results of the data quantification displayed (n=3). Labellings were either performed in whole cell lysates (**A**) or in membrane fractions (**B/C**).

Table 13: *In silico*[1] identification of protein lipid interaction motifs in the mammalian transamidase complex subunits.

	CRAC[2]			CARC[3]			Sphingolipid binding motif[4]		
gene	position	sequence	TMD[5]	position	sequence	TMD[5]	position	sequence	TMD[5]
PIGK	66 - 74	Lsv...Yrsvk.R	N	54 - 62	Rfwfn.Yrh...V	N	274 - 392	LwaLIimVF	N
	381 - 392	Vffkt.YgikhmK	Y	122 - 128	Rs....Yevt..V	N			
				193 - 200	Krr...Ynel..L	N			
				248-257	Rytf..Yvlef.L	N			
PIGS	66 - 74	Lsv...Yrsvk.R	N	17 - 29	KraalfFaavaiV	Y			
	94 - 101	Lk....Ykmki.K	N	37 - 46	Kttet.Yras..L	Y			
	331 - 341	LahsplYiqd..K	N	43 - 54	Raslp.YsqisgL	N			
	507 - 518	Llhll.YfpddqK	N	81 - 87	Klp...Ftv...V	N			
				103 - 112	Rfqka.Yrra..L	N			
				222 - 233	Ksslg.YeitfsL	N			
				252 - 262	RryvqpFlna..L	N			
				367 - 374	Kt....Ynasv.L	N			
				384 - 395	Rvmev.FlaqlrL	N			
				518 - 527	Kfai..Yiplf.L	Y			
PIGT	63 - 71	Vsh...Yrlfp.K	N	60 - 68	RegvshYr....L	N	130 - 138	LsnVLsgIF	N
	76 - 83	Lisk..Ysl...R	N	67 - 73	Rl....Fpka..L	N	238 - 246	LrqTLsvVF	N
	171 - 178	Lr....Yavlp.R	N	95 - 104	Rtr...YwgppfL	N			
	358 - 365	Vsg...Yglq..K	N	209 - 220	RlfhtsYhsqa.V	N			
	368 - 379	Lstll.YnthpyR	N	262 - 268	Rm....Fsrt..L	N			
	386 - 394	LdtvpwYl....R	N	312 - 321	RktyaiYdl...L	N			
	498 - 507	VsdgsnYfv...R	N	356 - 363	Ryvsg.Yg....L	N			
	538 - 549	VcygsfYnllt.R	Y	379 - 386	Ra....Fpvll.L	N			
				394 - 400	Rl....Yvht..L	N			
				441 - 451	Kvsiq.Feral.L	N			
				507 - 515	Rl....YtepllV	N			
PIGU	201 - 210	Vpgll.Yllq..R	Y	16 - 24	Raal..Frss..L	N	368 - 376	LfpVLwhLW	Y
	207 - 218	Llqrq.YipvkmK	Y	21 - 32	RsslaeFiser.V	N			
	344 - 353	Vwnhl.Yrfl..R	N	104 - 113	Kvv...FkkqklL	N			
	400 - 411	Llisd.YfyaflR	N	139 - 146	Kvalf.Yl....L	N			
	401 - 412	LisdyfYaflr.R	Y	176 - 186	Kgsa..FlsaifL	Y			
	416 - 425	Lthgl.Ylta..K	N	210 - 215	Rq....Yip...V	N			
				327 - 335	Ks....YptvgdV	Y			
				350 - 358	RflrniFv....L	Y			
				411 - 420	Rrey..Ylthg.L	N			
GPAA1	99 - 110	Vglev.YtqsfsR	N	171 - 181	Rgqi..YwakdiV	N	464 - 472	VvlTLlaIY	Y
	124 - 134	NVsgtnvYgil..R	N	178 - 184	Kdiv..Fl....V	N			
				326 - 335	Rqyk..Ydlva.V	N			
				337 - 349	KalegmFrklnhL	N			
				352 - 362	RlhqsfFlyl..L	N			
				499 - 510	KlvaliYlalq.L	Y			
				541 - 550	Rtl...YaallvL	Y			

[1] *In silico* determination of cholesterol and sphingolipid binding sequences of transamidase subunits. Amino acid sequences of subunits were derived from UniProt (see appendix 8.5 for full sequences) and used with the ScanProsite tool (http://prosite.expasy.org/scanprosite/) to identify possible cholesterol[104] and sphingolipid[15],[16] interacting sites.

Search queries: [2]CRAC: [LV]-X(1,5)-Y-X(1,5)-[KR]; [3]CARC: [KR]-X(1,5)-[YF]-X(1,5)-[LV]; [4]sphingolipid binding motif: [VITL]-X(2)-[VITL][VITL]-X(2)-[VITL][FWY]. Capital characters denote essential amino acids of the binding motifs as defined in the search queries. Not essential characters are displayed in lower case.

[5] Only sequences containing at least one amino acid inside a trans membrane domain (TMD) were considered and are displayed in the schematic drawing (see figure 26).

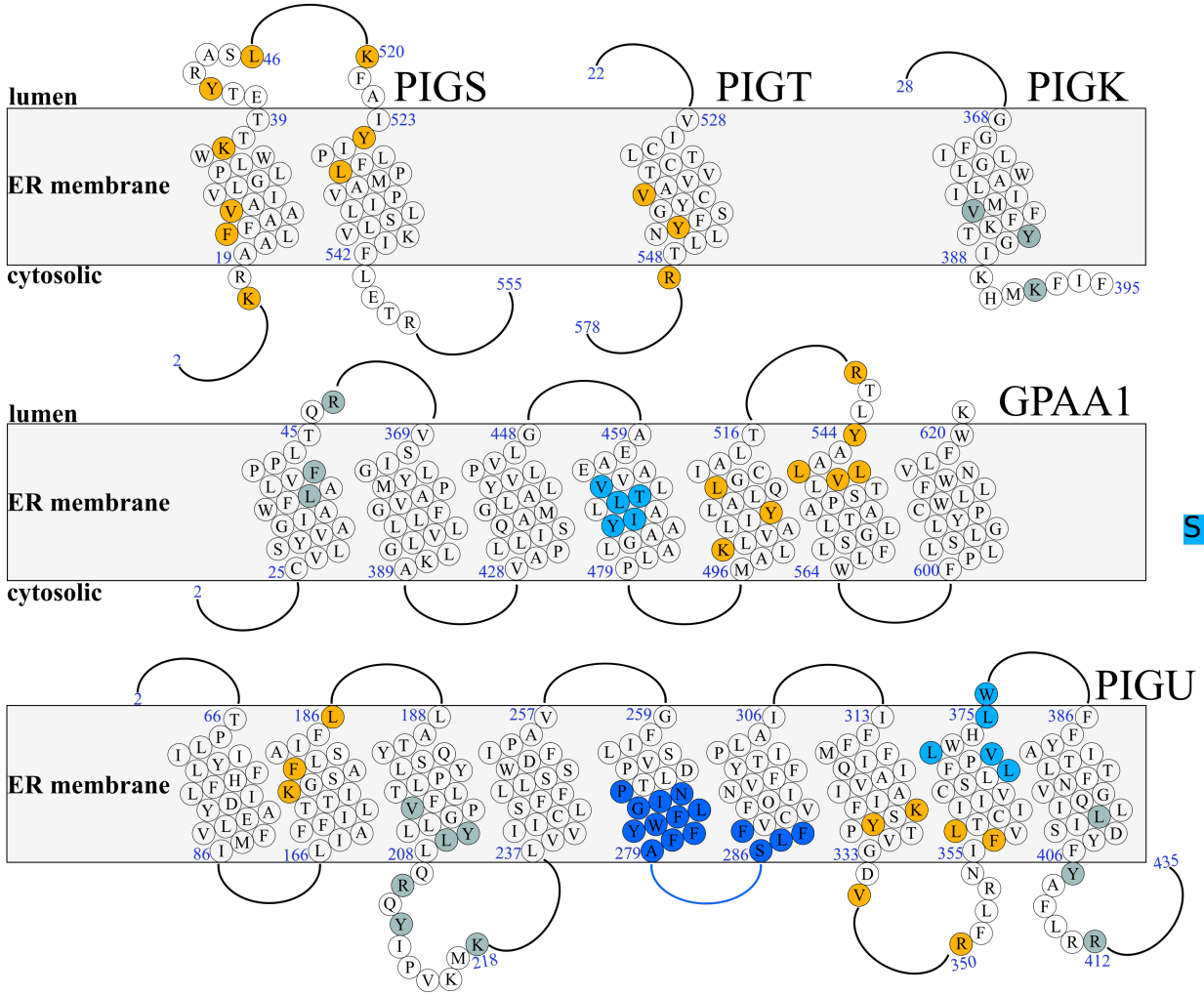

Figure 26: *In silico* determination of cholesterol and sphingolipid binding sequences of trans-amidase subunits. Amino acid sequences of subunits (PIGK/S/T/U and GPAA1) were derived from UniProt (see appendix 8.5 for full sequences) and used as inputs for the ScanProsite tool (http://prosite.expasy.org/scanprosite/). Search term for cholesterol[104] (CRAC/CARC) binding sequences ([LV]-X(1,5)-Y-X(1,5)-[KR]/[KR]-X(1,5)-[YF]-X(1,5)-[LV]) were derived from[104]. Hits taken into account required at least one amino acid of the motif to be located in a transmembrane domain. The complete list of hits are displayed in table 13. The sphingolipid binding sequence (search term: [VITL]-X(2)-[VITL][VITL]-X(2)-[VITL][FWY]) was derived from[15],[16]. For PIGU, no sequence information was available regarding the lumenal/cytosolic orientation of the molecule. Dark blue defines the section hypothesised to be responsible for recognition of long-chain fatty acids in GPI[105].

5.5.2 Inhibition of pacSph labelling of endogenous GPAA1 in HeLaΔS1PL GPAA1#76

HeLaΔS1PL GPAA1#76 were labelled with pacSph and different specific inhibitors (PPMP/FB1/D609) of the sphingolipid pathway (see figure 27A) to determine the specific experimental settings and functionality of these inhibitors. PPMP inhibits glucosylceramide synthase, FB1 acts on the ceramide synthase and D609 reduces sphingomyelin synthase activity.
Different concentrations (8/20/41 µM) of PPMP showed a strong decrease of pacGlucCer metabolites on TLC level (see figure 27 C). For the analysis of the influence of PPMP on GPAA1-pacSph metabolite interactions, cells were labelled with 4 µM pacSph and 25 µM PPMP for 4 hours, clicked in lysate of membrane fractions with biotin-N_3 and enriched over Neutravidin-beads (see figure 27E). No interaction was observed in pacSph labelled cells without click. Samples that were subjected to click reactions showed interactions with GPAA1 independent of PPMP presence. When quantifying the signal intensities of three biological replicates, no difference between either group (pacSph or pacSph + PPMP) was detectable ($p=0.7895$, see figure 27G). Furthermore, mass spectrometric analysis of inhibition via lipidomics[103] (see figure 28B), did not show any significant differences in lipid composition of the sphingolipid pathway due to high variability in-between the 3 replicates. To find the optimal experimental conditions for FB1, different concentrations and pre-incubation times where tested:

- pre-incubation: 4 hours with 75/150 µM FB1, labelling 0.5 µM pacSph 4 hours (not shown)
- pre-incubation: 15 hours with 25/50/150 µM FB1, labelling 4 µM pacSph 4 hours (not shown)
- pre-incubation: 16 hours with 25/50/150 µM FB1, labelling 4 µM pacSph 4 hours (not shown)
- pre-incubation: 16 hours with 25/50/100 µM FB1, labelling 1 µM pacSph for 1 or 4 hours (see figure 27B)

None of these 4 hours settings (to be directly comparable with the PPMP experiment) provided satisfying results with regards to reduction and reproducibility of the sought after inhibitory effect and therefore did not allow for a 1:1 comparison with the PPMP results achieved at four hours. Furthermore, in all experimental settings it was not possible to achieve a complete inhibition of the pacSph metabolic pathway. Therefore, the choice was made to switch from 4 hours pacSph labelling with 1 µM to 1 hour labelling (see figure 27B). Here FB1 was able to increase the amount of pacSph compared to cells without inhibitor present. Furthermore, nearly no levels or only low levels of the pacSph metabolites glucosylceramide (GlucCer), sphingomyelin (SM) and ceramide (Cer) were detectable. Interestingly, only the bands depicting long chained variants of Cer and SM disappeared, while the short chain-variants seemed to be, even though on lower level than compared to the control, unaffected. For the analysis of the influence of FB1 on GPAA1-pacSph metabolite interactions, cells were pre-incubated with 100 µM FB1 for 16 hours, labelled for 1 hour with 1 µM pacSph in presence of 100 µM FB1, clicked in lysate of membrane fractions with biotin-N_3 and enriched over Neutravidin-beads (see figure 27D). Here a significant reduction of enriched GPAA1-pacSph metabolite complexes between cells with or without FB1 was observed ($p=0.0313$, see figure 27F). As with PPMP, the high variability of the three samples of FB1 did not allow for a reliable quantification with lipidomics, but showed a significant decrease in sphingomyelin levels ($p<0.0001$, see figure 28A).

As displayed in figure 27A, after successfully employing the inhibitors FB1 and PPMP, the next step was to test for a potential contribution of sphingomyelin (SM) to the protein-lipid interaction.

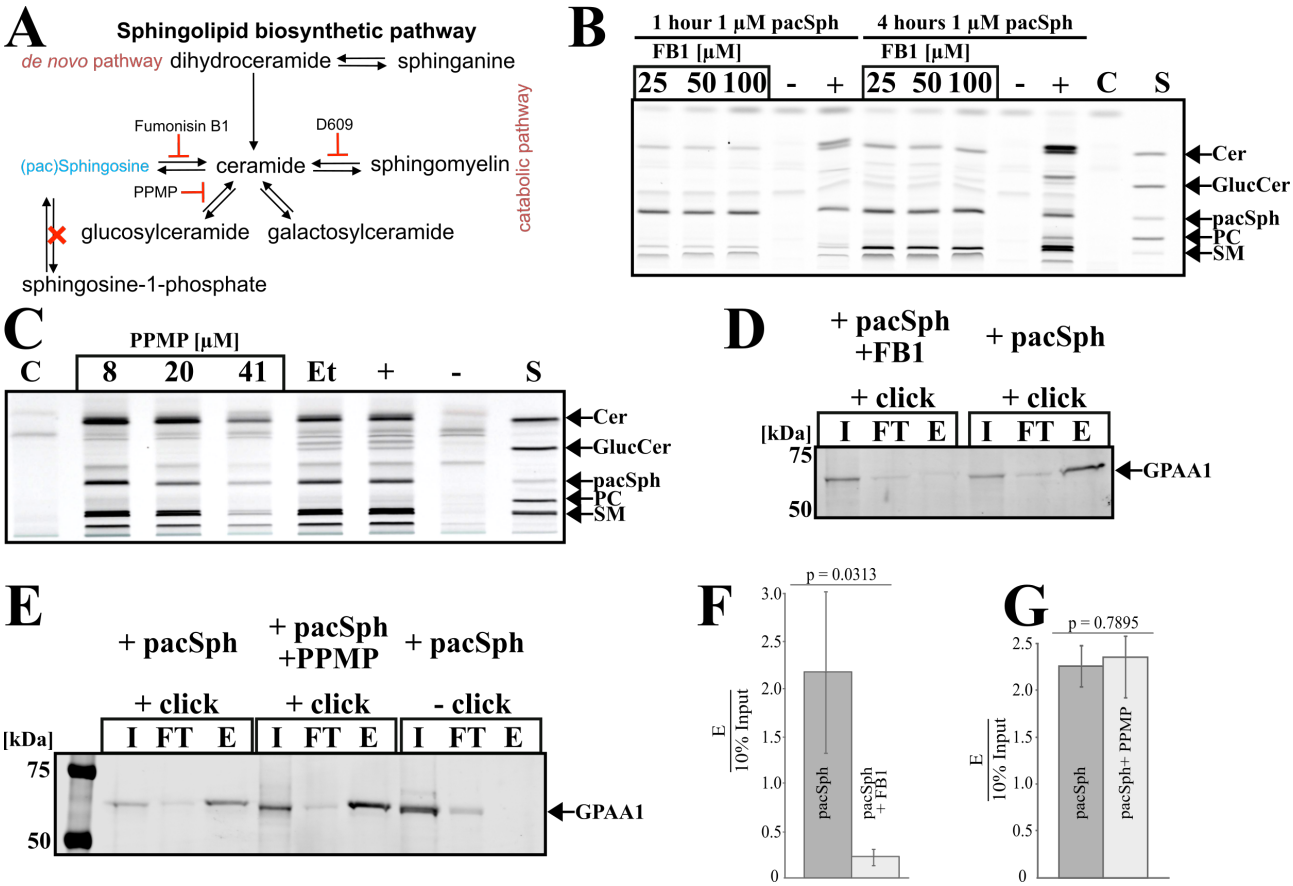

Figure 27: Analysis of the effect of specific inhibitors of the pacSph metabolism on GPAA1-sphingolipid interactions in HeLaΔS1PL GPAA1#76 cells via TLC and western blotA) Simplified schematic view of the sphingolipid biosynthetic pathway, the entry point of pacSph (blue), sites of actions of the inhibitors (PPMP/FB1/D609) and the in HeLaΔS1PL cell line knocked out part of the pathway (red cross). **B)** Cells were pre-incubated with the ceramide synthase inhibitor Funmonisin B_1 (FB1) for 16 hours, before being labelled with 1 µM pacSph for 1 or 4 hours. C, c3-azido-7-hydroxcoumarin only; +, pacSph only; -, labelling media only; S, standard mix containing pacCer, pacGlucCer, pacPC, pacSph, and clickSM. **C)** Cells were labelled with 4 µM pacSph and different concentrations (8/20/41 µM) of glucosylceramide synthase inhibitor D-threo-PPMP (PPMP) for 4 hours and detected via 3-azido-7-hydroxycoumarin. Et, EtOH control. **D)** $1x10^7$ cells were seeded, pre-incubated with 100 µM FB1 for 16 hours and labelled for 1 hour with 1 µM pacSph in presence of 100 µM FB1. Shown is one representative blot of three biological replicates. I, Input; FT, flow-through; E, enriched fraction. **E)** $1x10^7$ cells were seeded, labelled for 4 hours with 4 µM pacSph and 25 µM PPMP. Shown is one representative blot of three biological replicates. **F/G)** Ratio between E and I signal intensities of three biological replicates from D/E) are shown. Error bars represents the standard deviation. T-test was used to test for differences between groups.

Therefore, different conditions with the SM inhibitor D609 were tested, but none of them showed any decrease in SM concentrations:

- pre-incubation: 1/4 hour with 25/50 µM D609; labelled: 4 hours with 4 µM (see figure 28C)
- pre-incubation: 1 hours with 187.5/375 µM D609; labelled: 0.5/4 µM pacSph (not shown)
- pre-incubation: 4 hours with 375 µM D609 and 4 hours labelling with 0.5/2 µM pacSph (not shown)
- pre-incubation: 15 hours with 250 µM D609 and 4 hours labelling with 4 µM pacSph (not shown)
- no pre-incubation: 250/375 µM D609 labelled with 1 µM pacSph for 1 hour (not shown)

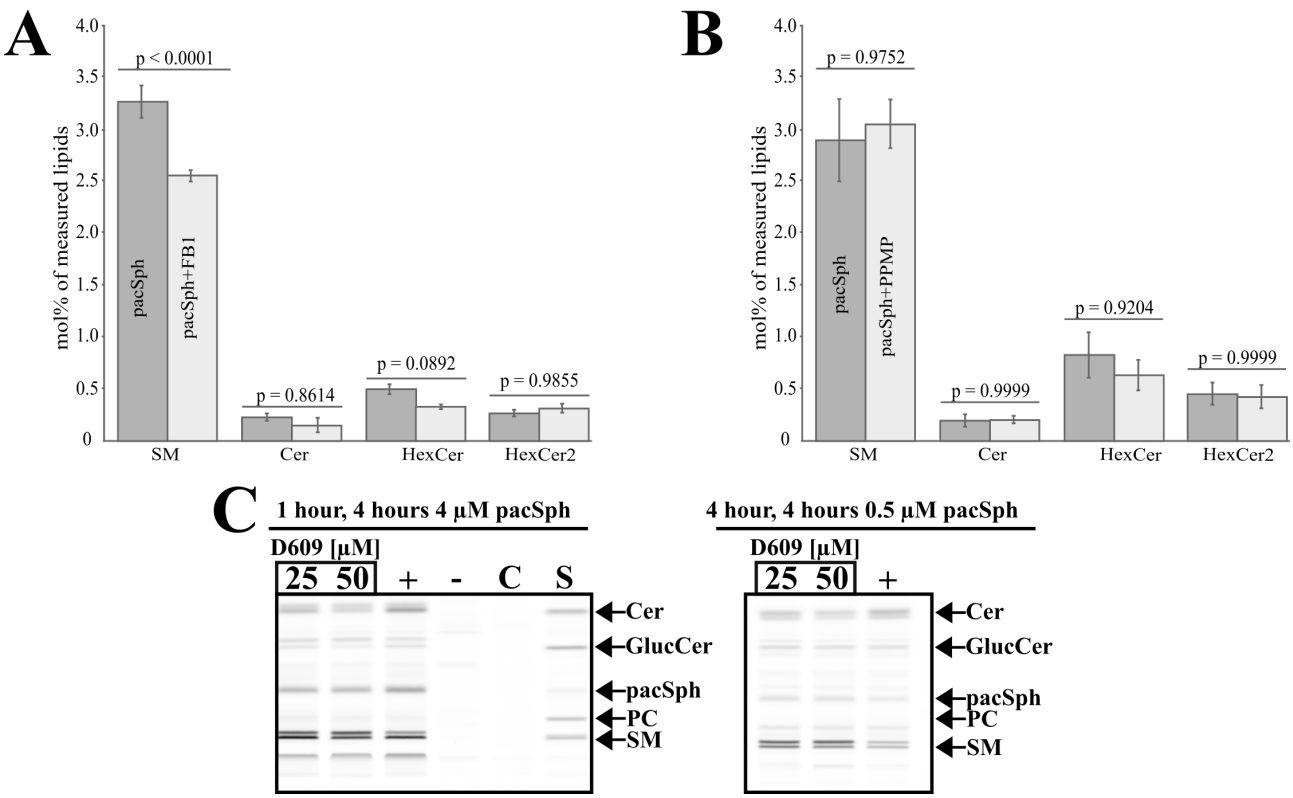

Figure 28: Analysis of the effect of specific inhibitors of the pacSph metabolism on GPAA1-sphingolipid interactions in HeLaΔS1PL GPAA1#76 cells via mass spectrometry and TLC Shown are sphingolipids measured via mass spectrometry, displayed as mol% of total measured lipids, of cells treated with **A)** FB1 and **B)** PPMP (see figure 27). Data produced jointly with Iris Leibrecht and Christian Lüchtenborg. Group differences were analysed via one-way ANOVA and Tukey's honestly significant difference post hoc test. SM, sphingomyelin; Cer, ceramide; HexCer, hexoyslceramide, contains measurments of glucosyl- und galactosylceramides; HexCer2, lactosylceramide. **C)** Cells were pre-incubated for one or four hours with 20/50 µM of spingomyelin synthase inhibitor D609, before being subjected to 4 hours of pacSph labelling. C, c3-azido-7-hydroxcoumarin only; +,= pacSph only; -, labelling media only; S, standard mix containing pacCer, pacGlucCer, pacPC, pacSph, and clickSM.

To summarise, GPAA1-pacSph metabolite interaction could be inhibited through the ceramide synthase inhibitor FB1, while the glucosylceramide synthase inhibitor PPMP did not interfere with the interaction. The sphingomyelin synthase inhibitor D609 proved unable to decrease SM concentrations in any of the tested conditions and additional experiments were suspended.

6 Discussion

The aim of this thesis was to establish an experimental setup to analyse protein lipid interactions of the transamidase complex, which is responsible for GPI-anchor attachment. Two approaches were tested and the experimental setup will be briefly described and the implications of the results will be discussed. The first approach contained transiently transfection of four of the transamidase subunits (PIGK/T/S, GPAA1), experimental optimisation of solubilisation parameters (temperature, duration of cell lysis, detergent of choice), best method for analysing transamidase subunits on a gel system as well as detection of sphingolipid-protein interactions through bifunctional pacSph via click-reactions. The second approach shifted from an over-expression to an endogenous system containing tagged GPAA1, while keeping variations to the rest of the work flow (pacSph, click-reaction) to a minimum.

6.1 Analysis of protein-lipid interactions of the transamidase complex via transient expression

6.1.1 Optimisation of experimental parameters of transient expression and solubilisation of transamidase subunits

In a first approach, transient expression of four transamidase subunits (PIGK/T/S, GPAA1) was conducted and a concentration dependent solubilisation efficiency was determined for GPAA1 (see figure 7), the prime candidate for a sphingolipid protein interaction [16, 85]. GPAA1 contains seven TMDs and therefore hosts, compared to PIGK/T with one TMD and PIGS with two TMDs, an increased amount of hydrophobic amino acids which might play a role in its selectivity for certain solubilisation parameters. The fifth subunit PIGU, which in contrast to GPAA1 did not show up in a screen for sphingolipid protein interactions[16], might have shown comparable characteristics due to its hypothetical nine TMDs (see figure 26), but due to a non-functional cDNA the experiments could not be performed during the course of this work.
To generate reproducible and stable western blot signals, the best conditions for solublisation of GPAA1 were determined by analysis of different detergents (Triton-X-100, Nonident-P40, OG, CHAPS). Of these, the non-ionic detergent Nonident P40 was selected as the candidate of choice (figure 8). The other non-ionic detergent Triton-X-100, chemically nearly identical with Nonident P40 (which is not to be confused with the detergent NP-40) proved to be the second best detergent in this experiment. These findings match protocols used in literature, where NP-40[105, 106], Nonident-P40 [51, 52], digitonin [51, 52], Triton-X-100[16] were used. Furthermore, detergent free lysis via sonication[85] proved efficient. With this setting, it was possible to immunoprecipitate all tested subunits (see figure 9A), as well as Co-IP all subunits with the exception of PIGU (see e.g. figure 9B). This one might be due to the disruptive characteristics of Nonident P40 and Triton-X-100, and aligns well with reports where mild detergents such as digitonin are needed to Co-IP all subunits, indicating a tightly associated core complex containing PIGK/T/S and GPAA1, as well as a loosely attached PIGU[52, 105].

6.1.2 Optimisation of experimental parameters of click reactions to detect GPAA1-lipid complexes in transiently transcfected HeLaΔS1PL cells

GPAA1-sphingolipid interactions have been shown before in HeLa cells labelled with [^{3}H]-photo-Sph precursor[16] and in HeLaΔS1PL cells labelled with pacSph[85]. Surprisingly, labeling HeLaΔS1PL cells with pacSph and a subsequent click reaction with Alexa-647-N_3 on proteins bound to FLAG-beads did not result in the expected GPAA1-lipid complex signal in in-gel fluorescence and subsequent western blot analysis (figure 10B). The reason for the discrepancy with published data might be due to a combination of the high hydrophobicity of the seven TMDs of GPAA1 and the interference of the click reaction reagents with the GPAA1-pacSph metabolite complex binding to FLAG-beads as biotin-N_3 enrichment via neutravidin beads (see figure 4F-G in [85] and figure 14 of this work) provided results in agreement with[85]. This behaviour might be characteristic for GPAA1, as the positive control p24 (not shown in this experiment, but visible in figure 11) did worked as expected in Alexa-647-N_3 click reaction of proteins bound to FLAG-beads (see figure 6 of article [18]). Repeating the same experiment, but performing the click reaction in whole cell lysate (see protocol 4.13.1.2) before IP with FLAG-beads, resulted in the expected detection of the GPAA1-pacSph metabolite complex (see figure 10C). To increase the reproducibility and signal intensity of the click reaction, the influence of the two detergents known best to solubilise GPAA1, Triton-X-100 and Nonident P40, were compared with regards to their influence on labelling efficiency (see figure 10D). Triton-X-100 showed a clear superior result, which was in line with a similar analysis of click reaction parameters [107], and compensated for the slightly lower GPAA1 solubilisation efficiency.

6.1.3 Analysis of sphingolipid binding kinetics in HeLaΔS1PL cells transiently transfected with GPAA1

The cell line HeLaΔS1PL[18] was selected to study protein-sphingolipid interactions. Previous experiments performed in the Brügger group have shown a time dependent increase of GPAA1 labelling with [^{3}H]-photo-Sph over time, with a sharp rise in the first 15-30 minutes. Based on these data, it was hypothesised that the prime candidate for an interaction with GPAA1 might be ceramide, the first metabolite of sphingosine (see figure 1). Based on this assumption, a time course to assess GPAA1 labelling kinetics with pacSph was performed and provided similar results (see figure 11A/C). TLC analysis of pacSph metabolism (see figure 11D) depicted pacSph and pacCer to be the most abundant sphingolipid species during the first two hours. Therefore, a certain uncertainty exists regarding the question which one of these species is incorporated in the GPAA1-lipid complex. The observed kinetics of the pacSph metabolism in HeLaΔS1PL cells are in line with data of the same cell line[18]. When analysing the signal intensity of all available metabolites for each given point in time, it is to be observed that over time the overall signal intensity increases (see figure 10B). This indicates, that a constant influx of extracellular pacSph takes place and the observed sphingolipid kinetics do not depict the actual intracellular metabolic conversion rates. When labelling continuously with pacSph, it is not possible to correlate a specific GPAA1-lipid complex signal at a given time point to a specific sphingolipid. Therefore, the idea was to reduce the overall signal intensity and even out the variation in temporal signal intensity (as seen in figure 11B) through a pulse chase experiment (see figure 12C/D). The temporal resolution of different pacSph metabolites aligned now with the ones observed in [85], but still did not allow for matching a certain time period with a specific metabolite. Furthermore, the available level of sphingolipid fed into the cell did not prove sufficient for detection of

protein-lipid complexes on western blot level (see figure 13). Additionally, the binding kinetics of continuous labelling with pacSph and detection via Alexa-647-N_3 (see figure 11C) were verified in a second methodological setup via attachment of biotin-N_3 to the cross-linked pacSph metabolites (see figure 14B) similar to the approach in [85]. Here it was seen that the labelling kinetics of GPAA1 did not differ at all from p24, which is known to interact specifically with sphingomyelin 18[15]. Therefore it should show different labelling kinetics than GPAA1, which is suspected to interact with ceramide or a lipid in the early stages of the spingolipid biosynthetic pathway.
On another note, the transient transfection of GPAA1 in HeLaΔS1PL cells limited the available labelling conditions compared to transfection with p24. When higher levels of pacSph (e.g. >3 µM) were administered to cells transfected with GPAA1, an increased cell mortality (e.g. > 50%, data not shown) was observed at prolonged labelling periods (e.g. >4 hours). Reducing pacSph concentrations allowed for labelling times up to 6 hours, but led to variations in the signal intensity for Alexa-647-N_3 detection. When cells were transfected with p24, none of these limitations applied (not shown). In contrast, mouse embryonic fibroblasts (MEFs) did not show any susceptibility to even harsher labelling conditions[85]. In future experiments, a careful analysis of suitable experimental parameters (amount of GPAA1-plasmid DNA transfected, variation of labelling time and concentration of pacSph) could be carried out to address these issues. A Co-IP of transamidase complex subuits via transiently expressed GPAA1 (see figure 9B) or PIGT (not shown) showed the capability to pull-down transamidase subunits, but lacking signal intensity compared to GPAA1. This difference might be due to artificial DDK epitope tags for the primary IP targets, while the subunits were detected via endogenous epitopes. Furthermore, when analysing the intracellular localisation of HeLaΔS1PL cells transiently expressing GPAA1 via immunofluorescence microscopy (not shown), a cytosolic accumulation of GPAA1 was observed. Expected would be a localisation in the ER. This accumulation in the cytosol has also been reported in studies of tumor tissue with overexpression of GPAA1[108, 109]. This indicates that the amount of plasmid DNA required for repeatable and detectable expression levels of GPAA1 on western blot level (see figure 8) introduced a high amount of GPAA1 not incorporated into the transamidase complex and breaking its stoichiometric composition in Co-IP experiments. Therefore, the results obtained with a transient expression system do not provide reliable information about the real lipid environment of the transamidase complex. Therefore, the decision was made to move forward and establish an experimental system to work with the endogenous transamidase complex.

6.1.4 Separation of transamidase subunits via different protein gel systems

Another step for validation of this experimental setup was to assess whether all transamidase subunits (see section 5.4.7) can be analysed on one SDS-page to circumvent variability of signal quantification between the same sample in one experiment. For this, different PAGE-systems were evaluated, but none of them allowed for a clear separation of all subunits. As depicted in figure 24A, the subunits PIGT (65.1 kDa), PIGS (61.65 kDa) and GPAA1 (67.623 kDa endogenous, with FLAG-tag 71.87 kDa) are supposed to be difficult to separate. The gel system closest to achieve this would have been the 8% Bis-Tris plus gel, but the requirement of having a high resolution between 37-75 kDa and especially in the region between 60-75 kDa were not fulfilled to a satisfactory extent. Therefore, an attempt was made to separate the region between 60-75 kDa in the vertical as well as the horizontal dimension via 2D-gel electrophoresis. After establishing a robust protocol, it was not possible to detect any signal of the transamidase subunits (see figure 24F). Based on the isoelectric points of PIGS/T and GPAA1 it should have been possible, in combination with the slightly different molecular weight, to distinguish between these subunits. As

high hydrophobicity of transmembrane regions can lead to precipitation events occurring under the high voltage during the isoelectrical focussing in the IPG-strip, in certain conditions (e.g. grand average of hydropathy (GRAVY) scores >0.5) a blue native PAGE is superior to isoelectric focusing [110]. When calculating the scores of the transamidase subunits (see table 14), only PIGU breached this threshold and GPAA1 came close to it (0.4). But as the calculation of the theoretical GRAVY score did not account for post-translational modifications, this values might have been off and the high hydrophobicity of the transmembrane regions might have led to precipitation events occurring under the high voltage during the isoelectrical focussing in the IPG-strip, thus preventing transfer to the second dimension. A possible solution for this problem could have been to change the first dimension separation system to blue native PAGE or by using ionic detergents (e.g. SDS, 16-BAC or CTAB)[110, 111]. Instead of spending further time consuming work to optimise SDS-PAGE based separation of the transamidase subunits, the decision was taken to go for a traditional approach by splitting samples on different gels to detect PIGS/T and GPAA1 on two different gels.

Table 14: Structural features of the transamidase complex subunits for 2D-gel electrophoresis

Name	UniProtID	isoelectric point[1,2]	grand average hydropathy (GRAVY) score[2,3]
GPAA1	O43292	8.19	0.40
PIGK	Q92643	5.76	-0.22
PIGT	Q969N2	8.68	-0.12
PIGS	Q96S52	6.05	-0.06
PIGU	Q9H490	7.74	0.92

[1]computationally derived values: www.web.expasy.org/compute_pi/
[2]input sequences are listed in Appendix 8.5.
[3]computationally derived GRAVY score: www.bioinformatics.org/sms2/protein_gravy

6.2 Analysis of lipid protein interactions of the endogenous transamidase complex

Two approaches for the development of a system to study the endogenous transamidase complex were followed. The first one was based on IP of endogenous subunits via an antibody specific for GPAA1, while the second one relied on a CRISPR/Cas9 guided cell line generation containing C-terminal tagged GPAA1.

6.2.1 IP of the endogenous transamidase complex

Coupling the anti-GPAA1 antibody (sc-373710) with CNBr-beads allowed for enrichment of the endogenous GPAA1, but was not efficient to Co-IP transamidase subunits besides PIGS (see figure 15A). Increasing the amount of cells by the power of ten did not change this outcome (see figure 15B). Instead, a limitation in the binding capacity of the CNBr-beads, when compared to FLAG-beads in IP of GPAA1-DDK, was observed (see figure 15C). Repetitive usage of the same set of CNBr-beads over the course of multiple experiments might have led to reduced binding capacities of these bead due to the following reasons: First, the elution of the proteins might have been incomplete. Second, the heavy chain of the antibody was detectable with increasing signal intensity in each experiment, while the GPAA1 signal intensity decreased. Third, the manual

washing steps of the beads might have led to decreased bead volume.
To be able to handle even higher amounts of cellular material without the mentioned limitations of the CNBr-beads, the antibody was coupled to a NHS-column. But as this did not provide a functional coupling (see figure 15D), the decision was taken to go directly for the generation of a cell line containing C-terminal tagged GPAA1.

6.2.2 CRISPR/Cas9 guided cell line generation containing C-terminal tagged GPAA1

When comparing tissue specific GPAA1 expression listed in the human protein atlas (HPA) project (see figure 30 in the appendix), the cervix is generally one of the tissues with a higher than average expression of GPAA1. Data from the tissue-specific gene expression and regulation (TiGER) database, even though quite outdated with a time stamp from 2008, points in a similar direction (see figure 29 in the appendix). An up to date reference is the EMBL-EBI Expression Atlas which and can be found at (https://www.ebi.ac.uk/gxa/home). There, the search term GPAA1 lists over 33 different experiments that assessed GPAA1 expression levels in different tissues and cell lines and classifies the cervix as a tissue with high expression (based on the same GTEx dataset used in the HPA). The already available sphingosine-1-phosphate lyase deficient HeLa cell line (HeLaΔS1PL[18]) in our lab and the results of the GPAA1 protein level screening (see figure 16 and table 11) set the rational to use HeLaΔS1PL as the cell line for the genomic integration of a C-terminal tag for GPAA1.
Having decided on a cell line, CRISPR/Cas9 was chosen as the technique of choice for generation of a cellular model to study sphingolipid interactions within the endogenous transamidase complex. Respective gRNAs were designed (see figure 17) and tested with regards to their capabilities to introduce DNA double strand breaks (see figure 18). In this process it is to be noted that DNA extracted from cells transfected with the gRNAs in question and not heterodimerised with wild-type extracts showed respective fragments of the heterodimerised samples after treatment with the surveyor nuclease. This is explained by the fact that the transfection reagent Fugene does not have a 100% transfection efficiency in HeLa cells and therefore there will always be a mixture between cells transfected and cells corresponding to the wild-type. After having all plasmids ready (plasmid containing the gRNAs, the homology sequence containing the to be inserted tag, the plasmid containing the human codon optimised Cas9), cells were transfected for 72 hours and single cell clones were created by serial dilution into 96 well plates as described in [88]. Out of 55 clones tested, 14 were determined to be heterozygous for tag insertion (25%), while two clones (#76, #39) were homozygous (3.6%). This aligns with previously reported low efficiency of homology directed repair (< below 10% of modified alleles) integration of genomic material[112]. Additionally, it is to be noted that in over 60 years of propagation of HeLa cells a lot of genomic variations did occur and the copy number of the majority of the loci is 3 or higher[113]. Therefore, the generation of two homozygous clones can be seen as a good achievement considering the methodology used. Maybe an increase in transfection efficiency by reducing the amount of plasmids to two (gRNAs/Cas9 on the same plasmid) or even to one (gRNA, homology sequence, Cas9 on the same plasmid) plasmid might be helpful. Furthermore, reduction of off-targets could be achieved by switching to a Cas9 nickase system[114]. For further experiments, the clone HeLaΔS1PL#76 was selected as it contained only a one nucleotide mismatch in the 3'UTR region, compared to a deletion of 9 nucleotides in the 3'UTR of HeLaΔS1PL#39 (see figure 19). It might be noted, that this genomic alteration could potentially influence the localisation/expression levels of GPAA1 [115, 116], but for the purpose of this project and the projection of 27/146 off-targets being located in genes (see figure 31) it seemed reasonable to only test for the integrity

of the transamidase complex and its functionality.
The arrival of the GPI-anchor protein CD59 at the plasma membrane was used previous as a model to determine transamidase complex activity[117]. Therefore, a comparison between HeLaΔS1PL and HeLaΔS1PL#76 was conducted to assess the function of the transamidase complex (see figure 20C-E). No difference in the cell surface arrival of basal and transient expressed CD59 was observed, thus indicating no substantial interference of the C-terminal tag with the function of GPAA1 and the transamidase complex. Having verified the non-interference of the introduced 3xFLAG and 2xStrep-tag, the suitability to enrich the transamidase complex was successfully assessed via FLAG- (see figure 20A and figure 24B-E) and streptactin-beads (see figure 20B). Furthermore, the complex constituted out of PIGK/T/S and GPAA1 (see figure 20A/B) and thus showed a result comparable to the outcome of transient transfection (see figure 9B and [47]) and endogenous IP (see figure 15A). While in the transient expression experiment it was not possible to Co-IP or express PIG-U (see section 6.1.1), the use of SMA to extract endogenous tagged GPAA1 within its native lipid environment showed a faint Western signal of PIG-U in the enriched fraction (see figure 22A) located at the predicted height of around 50 kDa. This did not correspond to literature reported SDS-Page running behaviour of around 38 kDa[105], but was in agreement with manufactures informations (α-PIGU antibody, see table 3). The experiment showing the 38 kDa band of PIGU was based on Co-IP of whole cell extract of mammalian cells transiently transfected with the yeast homologue of PIGK with a SDS sample buffer containing 6 M urea[105, 118]. The addition of urea might have resulted in a more complete denaturation of PIGU[105], thus providing more opportunities for SDS to interact with the respective amino acids. This has been shown to be specifically important for transmembrane containing proteins and might determine the appearance or magnitude of ”gel shifting”, a term describing the fact that the formal molecular weight might not correspond to the actual migration on the SDS-PAGE[119]. Therefore, the discrepancy between results observed in this thesis and the literature might be due to the absence of urea in the sample loading buffer, affecting the migration pattern of PIGU. This does not affect the overall outcome, which is the ability to extract from the HeLaΔS1PL GPAA1#76 cell line the complete transamidase complex in its native lipid environment with SMA. In a proof-of-principle experiment, it was ascertained that SMALP extracted from FLAG-beads mixed with a SMA whole cell lysate of HeLaΔS1PL GPAA1#76 cells allowed for detection of lipids via mass spectrometry (see figure 23), but similar physiochemical properties of SMA and the endogenous lipids incorporated in the SMALP nanodisc did not allow for a separation between SMA and the incorporated lipids, thus indicating that further experiments are required to establish a lipid extraction method taking into account the characteristics of SMA. In the future, due to the 3xFLAG-Twin-Strep tag, this system might also provide structural information via single particle cryo-electron microscopy as it was already shown for other SMA extracted proteins[74]. This is of special interest, because nowadays no structures are available depicting the whole complex and how all of the subunits intervene in the process of GPI-anchor attachment.
Finally, HeLaΔS1PL GPAA1#76 cells were assessed for their compatibility with different click-reaction protocols (Alexa-N_3 and biotin-N_3 click reaction in whole cell lysate) and verified the protein lipid interaction seen in the transient transfection experiments as described above.
Summarising, HeLaΔS1PL GPAA1#76 contains the C-terminal 3xFLAG-Twin-Strep tag and GPAA1 can be purified over either of them. The knock-in did not influence the function of the transamidase complex as measured by CD59 cell surface expression levels and is compatible with different click protocols.

6.2.3 Protein-Lipid interactions of the endogenous transamidase complex

To assess potential lipid interactions of the transamidase complex subunits, the model cell line HeLaΔS1PL GPAA1#76 was subjected to continuous labelling with the bifunctional lipids, pacChol and pachSph and detection via biotin-N_3.

6.2.3.1 Interactions of cholesterol with the endogenous transamidase complex Of the subunits of the transamidase complex, only GPAA1 showed a strong labelling signal (see figure 25B). This matches with the two detected CARC binding motifs in the TMDs 5 and 6 of GPAA1 (see table 13 and figure 26). Weak signals for PIGK/T/S (see figure 25B) were visible, but were not reliable quantifiable. This does not match with the *in silico* predicted cholesterol binding motifs, where PIGK/S/T/U seemed to contain either CRAC- or CARC-motifs or both. As seen in table 13, the amount of cholesterol binding motifs inside of TMDs is much smaller than binding motifs located outside of TMDs. It has been shown that proteins exist that use exposed cholesterol binding motifs to interact with cholesterol containing liposomes[120]. As the transamidase complex is not being thought of having interactions of such type, the focus was set on motifs which have at least one amino acid inside of the TMD. A mass spectrometry–based profiling of sterol-binding proteins in HeLa cells identified over 250 cholesterol-binding proteins and the follow up pathway analysis identified the "GPI-anchor synthesis" as one of the top 5 KEGG pathway matches and one of the top 12 of biological function networks as assessed via the DAVID gene ontology server [121]. All transamidase subunits in this experiment were seen to interact with cholesterol in the following quantifiable order: GPAA1=PIGS=PIGT~PIGS>PIGU. This contradicts somehow the results of this thesis, where the observed signal of GPAA1 clearly dominates over the weak signals for PIGK/T/S. This discrepancy can be explained through the missing validation of the results and the high sensitivity of mass spectrometry in[121]. Especially the latter one might provide false positive results for the members of the inner core complex PIGK/T/S, which are in close proximity to the cholesterol binding protein GPAA1. This aligns well with a model where PIGK/T and GPAA1 are part of a closely associated inner core complex inside of the transamidase complex[46]. This results further indicate, that some sort of spatial arrangement into specific lipid domains occurs, where specifically cholesterol surrounds the inner core complex. Lipid analysis of SMALPs containing endogenous transamidase complex via mass spectrometry might provide the key to verify this assumption and allow a closer look at the exact lipid environment surrounding the transamidase complex inside the ER membrane.

6.2.3.2 Interactions of sphingolipids with the endogenous transamidase complex Of the subunits of the endogenous transamidase complex, only GPAA1 showed a strong labelling signal (see figure 25A/C) and aligns well with the results of transiently expression of GPAA1 in HelaΔS1PL cells, as presented in this thesis and in[16, 85]. In a proteomic profiling of protein-sphingolipid complexes[85], endogenous GPAA1 has been identified as an interaction partner for sphingolipids in MEFΔS1PL cells[85]. Under the stringent criteria applied in this screen (4x fold increase in spectral counts between treated and untreated cells) PIGK/PIGS/PIGT showed no observable enrichment in any of the three biological replicates, while PIGU was not part of the 2098 annotated hits[85]. As PIGU came up in the *in silico* screen with a partial sphingolipid binding motif, this one is most likely a false positive as the last amino acid tryptophan (W) in the binding motif is outside of the TMD and therefore lacks probably the properties to accommodate the respective sphingolipid head group[15]. This characteristic of one or more amino acids being

outside of the TMD, is generally seen in nearly all motifs (CRAC, CARC, sphingolipid) residing in the TMDs of PIGU. When PIGU was discovered in 2003, it was suspected that PIGU might be responsible for recognition of long-chain fatty acids in GPI[105]. 15 years later, this hypothesised function was reaffirmed by a bioinformatic screen that found a membrane-embedded domain conserved in the GPI-anchor synthesis pathway of the proteins PIGB/M/U/W/V/Z[122]. This Bind-GPILA("bind GPI lipid anchor) motif is consistently available throughout the GPI-anchor synthesis pathway and comprises out of a stretch of 10 TMDs[122]. Comparing this with the annotation retrieved from UniProt, which is also referenced as source data of the article, reveals that only 9 TMDs are annotated for PIGU and it was suggested that a signal peptide sequence was wrongly assigned and should have been a TMD in reality[122]. This might have resulted in annotation of two more CARC motifs (see 6.2.3.1) in the hypothetical TMD1, but would not have changed the outcome of the experimental results.

The subset of specific sphingolipid species interacting with the transamidase complex were to be elucidated by selective inhibition of enzymes involved in the sphingolipid metabolism (see figure 27A). Fumonisin B_1 (FB1) inhibits ceramide synthases[123, 124] and was used to investigate if sphingosine or one of its downstream metabolites are engaged in the interaction with GPAA1. The decrease of labelling intensity (see figure 27B/D/F) indicates that the primary interaction partner of GPAA1 is not a sphingosine. Mass spectrometry analysis of the actual lipid composition of this experiment showed only a significant decrease in sphingomyelin levels and a trend towards decreased hexosylceramides, while ceramides and lactosylceramides showed no difference (see figure 28). Independent of the FB1 concentrations used and variations of different pre-incubation and labelling times, it was never possible to achieve a nearly complete reduction of ceramide levels as seen in MEFΔS1PL cells[85]. The intriguing observation was, that HeLaΔS1PL GPAA1#76 cells treated with FB1 displayed a reduction of sphingomyelin and ceramide containing long chain length fatty acids, comparable to the HeLaΔS1PLΔCerS2 cell line[125], which is characterised by its knock-out of the ceramide synthase 2 (CerS2). CerS2 (next to CerS4 and CerS3) is specifically involved in the synthesis of ceramides containing fatty acid chain lengths (C20-C26), while CerS6 (next to CerS5) is required for generation of ceramides containing short chained fatty acids (C14-C16)[126]. During the generation of the HeLaΔS1PL cell line, a slight, but not significant increase of sphingolipids containing short chain fatty acids and a significant decrease in long chain fatty acids was reported [18]. CerS6 came up as a differentially regulated protein during a proteomic comparison between HeLa and HeLaΔS1PL, but was classified as a false-positive hit based on western blot expression levels[18]. An in-depth analysis of the influence of FB1 on fatty acid chain length in HeLaΔS1PL GPAA1#76 cell line treated with FB1 compared to untreated cells (not shown) demonstrated a nearly 50% decrease of ceramide 42:2,2 (two-sided t-test, p=0.0006) and a trend for an increase of ceramide 34:1,2. The latter one might be due to high variability of drug efficacy and low sample number (n=3). This would indicate either a difference in the set of ceramide synthases active in the HeLaΔS1PL based cell line HeLaΔS1PL GPAA1#76 or a difference in expression levels of specific ceramide synthases with a respective interference on FB1 activity, as literature reports indicate that in some cases of increased levels of ceramide synthases FB1 might not display its inhibitory effect and even result in elevated ceramide levels [127]. Additionally, there might be an unkown specificity of FB1 to respective ceramide synthases, but this has not been investigated so far. In summary, the FB1 experiment indicates that the specific interaction partner of GPAA1 is not sphingosine, but one of its downstream metabolites and probably one containing long chain fatty acids. To verify this, there might be additional experiments required, employing different specific CerS inhibitors in combination with additional inhibitors downstream of the sphingosine metabolite ceramide.

The second inhibitor investigated was PPMP which acts on the glucosylceramide synthase. Here, no interference with GPAA1 labelling was observed (see figure 27E/G). This might be due to no significant changes in the lipid profile (see figure 28B) as detected by mass spectrometry. The low number (n=3) and intra experiment variability of the samples (two showing the same trend, one the opposite) did not allow to attain statistical significance. When taking the TLC results (see figure 27C) in consideration, PPMP showed a complete reduction of glucosylceramide and therefore eliminates glucosylceramide as an interaction partner of GPAA1.
The third inhibitor assessed was D609, which has been shown in different literature sources to inhibit sphingomyelin synthase (SMS)[128, 129, 130] in a dose dependent manner[131, 132]. D609 was proven to inhibit SMS1 with a two fold higher specificity than SMS2[130]. For example, incubation times of two hours with 50 µM D609 were sufficient to block sphingomyelin synthesis in HeLa cells[129]. Pre-incubation with 50 µM D609 for over 6-24 hours did not result in unbearable cell toxicity[133]. Furthermore, HeLa cells with transfection stress and 4 hours of 200 µM D609 did not die due to cell toxicity[134]. 300 µM D609 over 16 hours of pre-incubation did not increase mortality of mouse myoblasts[135]. The inhibition of SMS via D609 has been shown to increase intracellular ceramide concentrations, to induce cell cycle arrest and apoptosis[136, 137]. In this thesis, different concentrations of D609 (with/without pre-incubation time) together with pacSph were assessed for their ability to inhibit SMS and to remove sphingomyelin as a potential interaction partner of GPAA1. Unfortunately, none of the tested concentrations showed a reproducible reductionof cellular SM levels. Either the cell toxicity was not tolerated by the cells and up to 90% died (not shown), or there was no effect measurable on sphingomyelin levels detected via TLC (see figure 28C). When using 375 µM for 4 hours with 0.5 µM pacSph without pre-incubation time, a reduction of sphingomyelin was observed, but due to the overall low intensity on TLC level due to low lipid quantities, this could not be used as a suitable experiment for the biotin-N_3 click reaction. A theoretical possibility for this behaviour could be, that the increased level of intracellular ceramide due to reduced channelling into sphingomyelin and the continuously inflow of ceramide through pacSph passed the threshold of intracellular ceramide concentrations and activated the pro-apoptotic signalling of ceramide[138].
In the future, the treatment of the generated HeLaΔS1PL GPAA1 # 76 cell line with respective inhibitors and mass spectrometric analysis of SMALPs containing the endogenous transamidase complex would help to get insights into lipid interactions of the transamidase complex.

7 References

[1] SJ Singer and Garth L Nicolson. The fluid mosaic model of the structure of cell membranes. *Membranes and Viruses in Immunopathology; Day, SB, Good, RA, Eds*, pages 7–47, 1972.

[2] Kai Simons and Julio L. Sampaio. Membrane organization and lipid rafts, Oct 2011.

[3] Donald Voet, Judith G Voet, and Charlotte W Pratt. *Fundamentals of biochemistry : life at the molecular level*. Hoboken, N.J. : John Wiley & Sons, 3rd ed. edition, 2008.

[4] Gerrit van Meer and Sandra Hoetzl. Sphingolipid topology and the dynamic organization and function of membrane proteins. *FEBS letters*, 584:1800–5, May 2010.

[5] Michael A. J. Ferguson, Gerald W. Hart, and Taroh Kinoshita. Glycosylphosphatidylinositol anchors, 2015.

[6] Kazuyuki Kitatani, Jolanta Idkowiak-Baldys, and Yusuf A. Hannun. The sphingolipid salvage pathway in ceramide metabolism and signaling. *Cellular signalling*, 20:1010–8, Jun 2008.

[7] Gerrit van Meer, Dennis R. Voelker, and Gerald W. Feigenson. Membrane lipids: where they are and how they behave. *Nature reviews. Molecular cell biology*, 9:112–24, Feb 2008.

[8] Philippe F. Devaux and Roger Morris. Transmembrane asymmetry and lateral domains in biological membranes. *Traffic (Copenhagen, Denmark)*, 5:241–6, Apr 2004.

[9] Manish Sud, Eoin Fahy, Dawn Cotter, Alex Brown, Edward A. Dennis, Christopher K. Glass, Alfred H. Jr Merrill, Robert C. Murphy, Christian R. H. Raetz, David W. Russell, and Shankar Subramaniam. Lmsd: Lipid maps structure database. *Nucleic acids research*, 35:D527–32, Jan 2007.

[10] Eoin Fahy, Manish Sud, Dawn Cotter, and Shankar Subramaniam. Lipid maps online tools for lipid research. *Nucleic acids research*, 35:W606–12, Jul 2007.

[11] Jacques Fantini, Coralie Di Scala, Luke S. Evans, Philip T. F. Williamson, and Francisco J. Barrantes. A mirror code for protein-cholesterol interactions in the two leaflets of biological membranes. *Scientific reports*, 6:21907, Feb 2016.

[12] U. Coskun, M. Grzybek, D. Drechsel, and K. Simons. Regulation of human EGF receptor by lipids. *Proceedings of the National Academy of Sciences*, 108(22):9044–9048, may 2011.

[13] Kathy Pfeiffer, Vishal Gohil, Rosemary A. Stuart, Carola Hunte, Ulrich Brandt, Miriam L. Greenberg, and Hermann Schagger. Cardiolipin stabilizes respiratory chain supercomplexes. *The Journal of biological chemistry*, 278:52873–80, Dec 2003.

[14] Mei Zhang, Eugenia Mileykovskaya, and William Dowhan. Cardiolipin is essential for organization of complexes iii and iv into a supercomplex in intact yeast mitochondria. *The Journal of biological chemistry*, 280:29403–8, Aug 2005.

[15] F-Xabier Contreras, Andreas M Ernst, Per Haberkant, Patrik Björkholm, Erik Lindahl, Basak Gönen, Christian Tischer, Arne Elofsson, Gunnar von Heijne, Christoph Thiele, and o. Molecular recognition of a single sphingolipid species by a protein's transmembrane domain. *Nature*, 481(7382):525, 2012.

[16] Patrik Björkholm, Andreas M Ernst, Moritz Hacke, Felix Wieland, Britta Brügger, and Gunnar von Heijne. Identification of novel sphingolipid-binding motifs in mammalian membrane proteins. *Biochimica et Biophysica Acta (BBA)-Biomembranes*, 1838(8):2066–2070, 2014.

[17] Morihisa Fujita, Reika Watanabe, Nina Jaensch, Maria Romanova-Michaelides, Tadashi Satoh, Masaki Kato, Howard Riezman, Yoshiki Yamaguchi, Yusuke Maeda, and Taroh Kinoshita. Sorting of gpi-anchored proteins into er exit sites by p24 proteins is dependent on remodeled gpi. *The Journal of cell biology*, 194:61–75, Jul 2011.

[18] Mathias J Gerl, Verena Bittl, Susanne Kirchner, Timo Sachsenheimer, Hanna L Brunner, Christian Lüchtenborg, Cagakan Özbalci, Hannah Wiedemann, Sabine Wegehingel, Walter Nickel, et al. Sphingosine-1-phosphate lyase deficient cells as a tool to study protein lipid interactions. *PloS one*, 11(4):e0153009, 2016.

[19] Taroh Kinoshita and Morihisa Fujita. Biosynthesis of gpi-anchored proteins: special emphasis on gpi lipid remodeling. *Journal of lipid research*, 57:6–24, Jan 2016.

[20] R. A. Brodsky, S. M. Jane, E. F. Vanin, H. Mitsuya, T. R. Peters, T. Shimada, M. E. Medof, and A. W. Nienhuis. Purified gpi-anchored cd4daf as a receptor for hiv-mediated gene transfer. *Human gene therapy*, 5:1231–9, Oct 1994.

[21] Samuel Dolezal, Shanterian Hester, Pamela S. Kirby, Allison Nairn, Michael Pierce, and Karen L. Abbott. Elevated levels of glycosylphosphatidylinositol (gpi) anchored proteins in plasma from human cancers detected by c. septicum alpha toxin. *Cancer biomarkers : section A of Disease markers*, 14:55–62, Jan 2014.

[22] Yoshitaka Fujihara and Masahito Ikawa. Gpi-ap release in cellular, developmental, and reproductive biology. *Journal of lipid research*, 57:538–45, Apr 2016.

[23] Consortium UniProt. Uniprot: a hub for protein information. *Nucleic acids research*, 43:D204–12, Jan 2015.

[24] Taroh Kinoshita. Biosynthesis and deficiencies of glycosylphosphatidylinositol. *Proceedings of the Japan Academy. Series B, Physical and biological sciences*, 90:130–43, 2014.

[25] Emanuela Manea. A step closer in defining glycosylphosphatidylinositol anchored proteins role in health and glycosylation disorders. *Molecular genetics and metabolism reports*, 16:67–75, Sep 2018.

[26] Malcolm F. Howard, Yoshiko Murakami, Alistair T. Pagnamenta, Cornelia Daumer-Haas, Bjorn Fischer, Jochen Hecht, David A. Keays, Samantha J. L. Knight, Uwe Kolsch, Ulrike Kruger, Steffen Leiz, Yusuke Maeda, Daphne Mitchell, Stefan Mundlos, John A. 3rd Phillips, Peter N. Robinson, Usha Kini, Jenny C. Taylor, Denise Horn, Taroh Kinoshita, and Peter M. Krawitz. Mutations in pgap3 impair gpi-anchor maturation, causing a subtype of hyperphosphatasia with mental retardation. *American journal of human genetics*, 94:278–87, Feb 2014.

[27] Jatin K. Nagpal, Santanu Dasgupta, Sana Jadallah, Young K. Chae, Edward A. Ratovitski, Antoun Toubaji, George J. Netto, Toby Eagle, Aviram Nissan, David Sidransky, and Barry Trink. Profiling the expression pattern of gpi transamidase complex subunits in human cancer. *Modern pathology : an official journal of the United States and Canadian Academy of Pathology, Inc*, 21:979–91, Aug 2008.

[28] Viktoria Koroknai, Szilvia Ecsedi, Laura Vizkeleti, Timea Kiss, Istvan Szasz, Andrea Lukacs, Orsolya Papp, Roza Adany, and Margit Balazs. Genomic profiling of invasive melanoma cell lines by array comparative genomic hybridization. *Melanoma research*, 26:100–7, Apr 2016.

[29] Yoshiko Murakami, Uamporn Siripanyaphinyo, Yeongjin Hong, Yuko Tashima, Yusuke Maeda, and Taroh Kinoshita. The initial enzyme for glycosylphosphatidylinositol biosynthesis requires pig-y, a seventh component. *Molecular biology of the cell*, 16:5236–46, Nov 2005.

[30] R. Watanabe, K. Ohishi, Y. Maeda, N. Nakamura, and T. Kinoshita. Mammalian pig-l and its yeast homologue gpi12p are n-acetylglucosaminylphosphatidylinositol de-n-acetylases essential in glycosylphosphatidylinositol biosynthesis. *The Biochemical journal*, 339 (Pt 1):185–92, Apr 1999.

[31] Yoshiko Murakami, Uamporn Siripanyapinyo, Yeongjin Hong, Ji Young Kang, Sonoko Ishihara, Hideki Nakakuma, Yusuke Maeda, and Taroh Kinoshita. Pig-w is critical for inositol acylation but not for flipping of glycosylphosphatidylinositol-anchor. *Molecular biology of the cell*, 14:4285–95, Oct 2003.

[32] M. Anand, J. S. Rush, S. Ray, M. A. Doucey, J. Weik, F. E. Ware, J. Hofsteenge, C. J. Waechter, and M. A. Lehrman. Requirement of the lec35 gene for all known classes of monosaccharide-p-dolichol-dependent glycosyltransferase reactions in mammals. *Molecular biology of the cell*, 12:487–501, Feb 2001.

[33] Vladimir Saudek. Cystinosin, mpdu1, sweets and kdelr belong to a well-defined protein family with putative function of cargo receptors involved in vesicle trafficking. *PloS one*, 7:e30876, 2012.

[34] Hisashi Ashida, Yeongjin Hong, Yoshiko Murakami, Nobue Shishioh, Nakaba Sugimoto, Youn Uck Kim, Yusuke Maeda, and Taroh Kinoshita. Mammalian pig-x and yeast pbn1p are the essential components of glycosylphosphatidylinositol-mannosyltransferase i. *Molecular biology of the cell*, 16:1439–48, Mar 2005.

[35] Ji Young Kang, Yeongjin Hong, Hisashi Ashida, Nobue Shishioh, Yoshiko Murakami, Yasu S. Morita, Yusuke Maeda, and Taroh Kinoshita. Pig-v involved in transferring the second mannose in glycosylphosphatidylinositol. *The Journal of biological chemistry*, 280:9489–97, Mar 2005.

[36] Y. Hong, Y. Maeda, R. Watanabe, K. Ohishi, M. Mishkind, H. Riezman, and T. Kinoshita. Pig-n, a mammalian homologue of yeast mcd4p, is involved in transferring phosphoethanolamine to the first mannose of the glycosylphosphatidylinositol. *The Journal of biological chemistry*, 274:35099–106, Dec 1999.

[37] M. Takahashi, N. Inoue, K. Ohishi, Y. Maeda, N. Nakamura, Y. Endo, T. Fujita, J. Takeda, and T. Kinoshita. Pig-b, a membrane protein of the endoplasmic reticulum with a large lumenal domain, is involved in transferring the third mannose of the gpi anchor. *The EMBO journal*, 15:4254–61, Aug 1996.

[38] Y. Hong, Y. Maeda, R. Watanabe, N. Inoue, K. Ohishi, and T. Kinoshita. Requirement of pig-f and pig-o for transferring phosphoethanolamine to the third mannose in glycosylphosphatidylinositol. *The Journal of biological chemistry*, 275:20911–9, Jul 2000.

[39] Nobue Shishioh, Yeongjin Hong, Kazuhito Ohishi, Hisashi Ashida, Yusuke Maeda, and Taroh Kinoshita. Gpi7 is the second partner of pig-f and involved in modification of glycosylphosphatidylinositol. *The Journal of biological chemistry*, 280:9728–34, Mar 2005.

[40] Barbara W. Taron, Paul A. Colussi, Jill M. Wiedman, Peter Orlean, and Christopher H. Taron. Human smp3p adds a fourth mannose to yeast and human glycosylphosphatidylinositol precursors in vivo. *The Journal of biological chemistry*, 279:36083–92, Aug 2004.

[41] Taroh Kinoshita, Morihisa Fujita, and Yusuke Maeda. Biosynthesis, remodelling and functions of mammalian gpi-anchored proteins: recent progress. *Journal of biochemistry*, 144:287–94, Sep 2008.

[42] Yew Kwang Toh, Neelagandan Kamariah, Sebastian Maurer-Stroh, Manfred Roessle, Frank Eisenhaber, Sharmila Adhikari, Birgit Eisenhaber, and Gerhard Grüber. Structural insight into the glycosylphosphatidylinositol transamidase subunits PIG-k and PIG-s from yeast. *J Struct Biol.*, 173(2):271–281, 2011.

[43] Stephen E. Maxwell, Sandhya Ramalingam, Louise D. Gerber, Larry Brink, and Sidney Udenfriend. An active carbonyl formed during glycosylphosphatidylinositol addition to a protein is evidence of catalysis by a transamidase. *J Biol Chem.*, 270(33):19576–19582, 1995.

[44] Taroh Kinoshita. Enzymatic mechanism of GPI anchor attachment clarified. *Cell Cycle.*, 13(12):1838–1839, 2014.

[45] Birgit Eisenhaber, Sebastian Maurer-Stroh, Maria Novatchkova, Georg Schneider, and Frank Eisenhaber. Enzymes and auxiliary factors for GPI lipid anchor biosynthesis and post-translational transfer to proteins. *Bioessays*, 25(4):367–385, 2003.

[46] Birgit Eisenhaber, Stephan Eisenhaber, Toh Yew Kwang, Gerhard Grüber, and Frank Eisenhaber. Transamidase subunit GAA1/GPAA1 is a m28 family metallo-peptide-synthetase that catalyzes the peptide bond formation between the substrate protein's omega-site and the GPI lipid anchor's phosphoethanolamine. *Cell Cycle*, 13(12):1912–1917, 2014.

[47] Kazuhito Ohishi, Kisaburo Nagamune, Yusuke Maeda, and Taroh Kinoshita. Two subunits of glycosylphosphatidylinositol transamidase, GPI8 and PIG-t, form a functionally important intermolecular disulfide bridge. *J Biol Chem*, 278(16):13959–13967, 2003.

[48] K. Kodukula, R. Micanovic, L. Gerber, M. Tamburrini, L. Brink, and S. Udenfriend. Biosynthesis of phosphatidylinositol glycan-anchored membrane proteins. design of a simple protein substrate to characterize the enzyme that cleaves the cooh-terminal signal peptide. *The Journal of biological chemistry*, 266:4464–70, Mar 1991.

[49] S. Mayor, A. K. Menon, and G. A. Cross. Transfer of glycosyl-phosphatidylinositol membrane anchors to polypeptide acceptors in a cell-free system. *The Journal of cell biology*, 114:61–71, Jul 1991.

[50] D. K. Sharma, J. Vidugiriene, J. D. Bangs, and A. K. Menon. A cell-free assay for glycosylphosphatidylinositol anchoring in african trypanosomes. demonstration of a transamidation reaction mechanism. *The Journal of biological chemistry*, 274:16479–86, Jun 1999.

[51] Saulius Vainauskas, Yusuke Maeda, Henry Kurniawan, Taroh Kinoshita, and Anant K. Menon. Structural requirements for the recruitment of gaa1 into a functional glycosylphosphatidylinositol transamidase complex. *J Biol Chem*, 277(34):30535–30542, 2002.

[52] Saulius Vainauskas and Anant K. Menon. Endoplasmic reticulum localization of gaa1 and PIG-t, subunits of the glycosylphosphatidylinositol transamidase complex. *J Biol Chem*, 280(16):16402–16409, 2005.

[53] Natalia Sikorska, Leticia Lemus, Auxiliadora Aguilera-Romero, Javier Manzano-Lopez, Howard Riezman, Manuel Muniz, and Veit Goder. Limited er quality control for gpi-anchored proteins. *The Journal of cell biology*, 213:693–704, Jun 2016.

[54] Morihisa Fujita, Yusuke Maeda, Moonjin Ra, Yoshiki Yamaguchi, Ryo Taguchi, and Taroh Kinoshita. Gpi glycan remodeling by pgap5 regulates transport of gpi-anchored proteins from the er to the golgi. *Cell*, 139:352–65, Oct 2009.

[55] Anne-Sophie Rivier, Guillaume A Castillon, Laetitia Michon, Masayoshi Fukasawa, Maria Romanova-Michaelides, Nina Jaensch, Kentaro Hanada, and Reika Watanabe. Exit of gpi-anchored proteins from the er differs in yeast and mammalian cells. *Traffic*, 11(8):1017–1033, 2010.

[56] Nina Jaensch, Ivan R. Jr Correa, and Reika Watanabe. Stable cell surface expression of gpi-anchored proteins, but not intracellular transport, depends on their fatty acid structure. *Traffic (Copenhagen, Denmark)*, 15:1305–29, Dec 2014.

[57] Yusuke Maeda, Yuko Tashima, Toshiaki Houjou, Morihisa Fujita, Takehiko Yoko-o, Yoshifumi Jigami, Ryo Taguchi, and Taroh Kinoshita. Fatty acid remodeling of gpi-anchored proteins is required for their raft association. *Molecular biology of the cell*, 18:1497–506, Apr 2007.

[58] Yuko Tashima, Ryo Taguchi, Chie Murata, Hisashi Ashida, Taroh Kinoshita, and Yusuke Maeda. Pgap2 is essential for correct processing and stable expression of gpi-anchored proteins. *Molecular biology of the cell*, 17:1410–20, Mar 2006.

[59] Charles Roduit, F. Gisou van der Goot, Paolo De Los Rios, Alexandre Yersin, Pascal Steiner, Giovanni Dietler, Stefan Catsicas, Frank Lafont, and Sandor Kasas. Elastic membrane heterogeneity of living cells revealed by stiff nanoscale membrane domains. *Biophysical journal*, 94:1521–32, Feb 2008.

[60] Riya Raghupathy, Anupama Ambika Anilkumar, Anirban Polley, Parvinder Pal Singh, Mahipal Yadav, Charles Johnson, Sharad Suryawanshi, Varma Saikam, Sanghapal D. Sawant, Aniruddha Panda, Zhongwu Guo, Ram A. Vishwakarma, Madan Rao, and Satyajit Mayor. Transbilayer lipid interactions mediate nanoclustering of lipid-anchored proteins. *Cell*, 161:581–594, Apr 2015.

[61] Christophe Tribet, Roland Audebert, and Jean-Luc Popot. Amphipols: polymers that keep membrane proteins soluble in aqueous solutions. *Proceedings of the National Academy of Sciences*, 93(26):15047–15050, 1996.

[62] Irfan Prabudiansyah, Ilja Kusters, Antonella Caforio, and Arnold J.M. Driessen. Characterization of the annular lipid shell of the sec translocon. *Biochimica et Biophysica Acta (BBA) - Biomembranes*, 1848(10):2050–2056, oct 2015.

[63] Jonas M Dörr, Stefan Scheidelaar, Martijn C Koorengevel, Juan J Dominguez, Marre Schäfer, Cornelis A van Walree, and J Antoinette Killian. The styrene–maleic acid copolymer: a versatile tool in membrane research. *European Biophysics Journal*, 45(1):3–21, 2016.

[64] Dov Lichtenberg, Hasna Ahyayauch, and Felix M. Goni. The mechanism of detergent solubilization of lipid bilayers. *Biophysical journal*, 105:289–99, Jul 2013.

[65] ThermoFisherScientific. Detergents for cell lysis and protein extraction (source: https://www.thermofisher.com/de/de/home/life-science/protein-biology/protein-biology-learning-center/protein-biology-resource-library/pierce-protein-methods/detergents-cell-lysis-protein-extraction.html), 2018.

[66] D. A. Brown and E. London. Structure and function of sphingolipid- and cholesterol-rich membrane rafts. *The Journal of biological chemistry*, 275:17221–4, Jun 2000.

[67] E. London and D. A. Brown. Insolubility of lipids in triton x-100: physical origin and relationship to sphingolipid/cholesterol membrane domains (rafts). *Biochimica et biophysica acta*, 1508:182–95, Nov 2000.

[68] Ulrich H. N. Durr, Ronald Soong, and Ayyalusamy Ramamoorthy. When detergent meets bilayer: birth and coming of age of lipid bicelles. *Progress in nuclear magnetic resonance spectroscopy*, 69:1–22, Feb 2013.

[69] Timothy H. Bayburt and Stephen G. Sligar. Membrane protein assembly into nanodiscs. *FEBS letters*, 584:1721–7, May 2010.

[70] Minmin Xue, Lisheng Cheng, Ignacio Faustino, Wanlin Guo, and Siewert J. Marrink. Molecular mechanism of lipid nanodisk formation by styrene-maleic acid copolymers. *Biophysical journal*, 115:494–502, Aug 2018.

[71] Rodrigo Cuevas Arenas, Bartholomäus Danielczak, Anne Martel, Lionel Porcar, Cécile Breyton, Christine Ebel, and Sandro Keller. Fast collisional lipid transfer among polymer-bounded nanodiscs. *Scientific Reports*, 7:45875, April 2017.

[72] Ashley R. Long, Catherine C. O'Brien, Ketan Malhotra, Christine T. Schwall, Arlene D. Albert, Anthony Watts, and Nathan N. Alder. A detergent-free strategy for the reconstitution of active enzyme complexes from native biological membranes into nanoscale discs. *BMC biotechnology*, 13:41, May 2013.

[73] Jana Broecker, Bryan T. Eger, and Oliver P. Ernst. Crystallogenesis of membrane proteins mediated by polymer-bounded lipid nanodiscs. *Structure (London, England : 1993)*, 25:384–392, Feb 2017.

[74] Vincent Postis, Shaun Rawson, Jennifer K. Mitchell, Sarah C. Lee, Rosemary A. Parslow, Tim R. Dafforn, Stephen A. Baldwin, and Stephen P. Muench. The use of smalps as a novel membrane protein scaffold for structure study by negative stain electron microscopy. *Biochimica et biophysica acta*, 1848:496–501, Feb 2015.

[75] German G. Sgro and Tiago R. D. Costa. Cryo-em grid preparation of membrane protein samples for single particle analysis. *Frontiers in molecular biosciences*, 5:74, 2018.

[76] SR Tonge and BJ Tighe. Responsive hydrophobically associating polymers: a review of structure and properties. *Advanced drug delivery reviews*, 53(1):109–122, 2001.

[77] Sarah C. Lee, Tim J. Knowles, Vincent L. G. Postis, Mohammed Jamshad, Rosemary A. Parslow, Yu-Pin Lin, Adrian Goldman, Pooja Sridhar, Michael Overduin, Stephen P. Muench, and Timothy R. Dafforn. A method for detergent-free isolation of membrane proteins in their local lipid environment. *Nature protocols*, 11:1149–62, Jul 2016.

[78] David J. K. Swainsbury, Stefan Scheidelaar, Nicholas Foster, Rienk van Grondelle, J. Antoinette Killian, and Michael R. Jones. The effectiveness of styrene-maleic acid (sma) copolymers for solubilisation of integral membrane proteins from sma-accessible and sma-resistant membranes. *Biochimica et biophysica acta*, 1859:2133–2143, Oct 2017.

[79] Andrew F. Craig, Emily E. Clark, Indra D. Sahu, Rongfu Zhang, Nick D. Frantz, M. Sameer Al-Abdul-Wahid, Carole Dabney-Smith, Dominik Konkolewicz, and Gary A. Lorigan. Tuning the size of styrene-maleic acid copolymer-lipid nanoparticles (smalps) using raft polymerization for biophysical studies. *Biochimica et biophysica acta*, 1858:2931–2939, Nov 2016.

[80] Anne Grethen, Abraham Olusegun Oluwole, Bartholomäus Danielczak, Carolyn Vargas, and Sandro Keller. Thermodynamics of nanodisc formation mediated by styrene/maleic acid (2:1) copolymer. *Scientific Reports*, 7(1):11517, September 2017.

[81] Juan J. Dominguez Pardo, Jonas M. Dorr, Aditya Iyer, Ruud C. Cox, Stefan Scheidelaar, Martijn C. Koorengevel, Vinod Subramaniam, and J. Antoinette Killian. Solubilization of lipids and lipid phases by the styrene-maleic acid copolymer. *European biophysics journal : EBJ*, 46:91–101, Jan 2017.

[82] Victoria Schmidt and James N. Sturgis. Modifying styrene-maleic acid co-polymer for studying lipid nanodiscs. *Biochimica et biophysica acta*, 1860:777–783, Mar 2018.

[83] Per Haberkant and Joost C. M. Holthuis. Fat & fabulous: bifunctional lipids in the spotlight. *Biochimica et biophysica acta*, 1841:1022–30, Aug 2014.

[84] Hartmuth C. Kolb, M. G. Finn, and K. Barry Sharpless. Click chemistry: Diverse chemical function from a few good reactions. *Angewandte Chemie (International ed. in English)*, 40:2004–2021, Jun 2001.

[85] Per Haberkant, Frank Stein, Doris Höglinger, Mathias J Gerl, Britta Brügger, Paul P Van Veldhoven, Jeroen Krijgsveld, Anne-Claude Gavin, and Carsten Schultz. Bifunctional sphingosine for cell-based analysis of protein-sphingolipid interactions. *ACS chemical biology*, 11(1):222–230, 2015.

[86] Howard C. Hang, John P. Wilson, and Guillaume Charron. Bioorthogonal chemical reporters for analyzing protein lipidation and lipid trafficking. *Acc. Chem. Res.*, 44(9):699–708, September 2011.

[87] Valery V. Fokin. Click imaging of biochemical processes in living systems. *ACS Chem. Biol.*, 2(12):775–778, December 2007.

[88] Mathieu Dalvai, Jeremy Loehr, Karine Jacquet, Caroline C Huard, Céline Roques, Pauline Herst, Jacques Côté, and Yannick Doyon. A scalable genome-editing-based approach for mapping multi-protein complexes in human cells. *Cell reports*, 13(3):621–633, 2015.

[89] Michael Ratz, Ilaria Testa, Stefan W. Hell, and Stefan Jakobs. Crispr/cas9-mediated endogenous protein tagging for resolft super-resolution microscopy of living human cells. *Scientific reports*, 5:9592, Apr 2015.

[90] Eric S. Lander. The heroes of crispr. *Cell*, 164:18–28, Jan 2016.

[91] F. Ann Ran, Patrick D. Hsu, Jason Wright, Vineeta Agarwala, David A. Scott, and Feng Zhang. Genome engineering using the crispr-cas9 system. *Nature protocols*, 8:2281–2308, Nov 2013.

[92] Oguz Kanca, Hugo J. Bellen, and Frank Schnorrer. Gene tagging strategies to assess protein expression, localization, and function in drosophila. *Genetics*, 207:389–412, Oct 2017.

[93] F. J. Mojica, C. Diez-Villasenor, E. Soria, and G. Juez. Biological significance of a family of regularly spaced repeats in the genomes of archaea, bacteria and mitochondria., Apr 2000.

[94] Francisco J. M. Mojica, Cesar Diez-Villasenor, Jesus Garcia-Martinez, and Elena Soria. Intervening sequences of regularly spaced prokaryotic repeats derive from foreign genetic elements. *Journal of molecular evolution*, 60:174–82, Feb 2005.

[95] Kasey Rodgers and Mitch McVey. Error-prone repair of dna double-strand breaks. *Journal of cellular physiology*, 231:15–24, Jan 2016.

[96] Mireille Betermier, Pascale Bertrand, and Bernard S. Lopez. Is non-homologous end-joining really an inherently error-prone process? *PLoS genetics*, 10:e1004086, Jan 2014.

[97] Takayasu Mikuni, Jun Nishiyama, Ye Sun, Naomi Kamasawa, and Ryohei Yasuda. High-throughput, high-resolution mapping of protein localization in mammalian brain by in vivo genome editing. *Cell*, 165:1803–1817, Jun 2016.

[98] Lina Yi, Gunes Bozkurt, Qiubai Li, Stanley Lo, Anant K. Menon, and Hao Wu. Disulfide bond formation and n-glycosylation modulate protein-protein interactions in gpi-transamidase (gpit). *Scientific reports*, 8:45912, Apr 2017.

[99] NEB. Crispr/cas9 & targeted genome editing: New era in molecular biology. NEB expressions Issue I, 2014.

[100] Ulrich K Laemmli. Cleavage of structural proteins during the assembly of the head of bacteriophage t4. *nature*, 227:680–685, 1970.

[101] D Wessel and Ulf-Ingo Flügge. A method for the quantitative recovery of protein in dilute solution in the presence of detergents and lipids. *Analytical biochemistry*, 138(1):141–143, 1984.

[102] Prashant Mali, Luhan Yang, Kevin M Esvelt, John Aach, Marc Guell, James E DiCarlo, Julie E Norville, and George M Church. Rna-guided human genome engineering via cas9. *Science*, 339(6121):823–826, 2013.

[103] Cagakan Ozbalci, Timo Sachsenheimer, and Britta Brugger. Quantitative analysis of cellular lipids by nano-electrospray ionization mass spectrometry. *Methods in molecular biology (Clifton, N.J.)*, 1033:3–20, 2013.

[104] Jacques Fantini and Francisco J. Barrantes. How cholesterol interacts with membrane proteins: an exploration of cholesterol-binding sites including crac, carc, and tilted domains, 2013.

[105] Yeongjin Hong, Kazuhito Ohishi, Ji Young Kang, Satoshi Tanaka, Norimitsu Inoue, Jun-ichi Nishimura, Yusuke Maeda, and Taroh Kinoshita. Human pig-u and yeast cdc91p are the fifth subunit of gpi transamidase that attaches gpi-anchors to proteins. *Molecular biology of the cell*, 14(5):1780–1789, 2003.

[106] Kazuhito Ohishi, Norimitsu Inoue, Yusuke Maeda, Junji Takeda, Howard Riezman, and Taroh Kinoshita. Gaa1p and gpi8p are components of a glycosylphosphatidylinositol (GPI) transamidase that mediates attachment of GPI to proteins. *Mol Biol Cell*, 11(5):1523–1533, 2000.

[107] Yinliang Yang, Xiaomeng Yang, and Steven H. L. Verhelst. Comparative analysis of click chemistry mediated activity-based protein profiling in cell lysates. *Molecules (Basel, Switzerland)*, 18:12599–608, Oct 2013.

[108] Jenny C. Ho, Siu Tim Cheung, Mohini Patil, Xin Chen, and Sheung Tat Fan. Increased expression of glycosyl-phosphatidylinositol anchor attachment protein 1 (gpaa1) is associated with gene amplification in hepatocellular carcinoma. *International journal of cancer*, 119:1330–7, Sep 2006.

[109] G. Chen, S. Y. Li, H. Y. Cai, and F. Y. Zuo. Enhanced expression and significance of glycosylphosphatidylinositol anchor attachment protein 1 in colorectal cancer. *Genetics and molecular research : GMR*, 13:499–507, Jan 2014.

[110] Lutz A. Eichacker, Bernhard Granvogl, Oliver Mirus, Bernd Christian Muller, Christian Miess, and Enrico Schleiff. Hiding behind hydrophobicity. transmembrane segments in mass spectrometry. *The Journal of biological chemistry*, 279:50915–22, Dec 2004.

[111] Ralf J. Braun, Norbert Kinkl, Monika Beer, and Marius Ueffing. Two-dimensional electrophoresis of membrane proteins. *Analytical and bioanalytical chemistry*, 389:1033–45, Oct 2007.

[112] Addgene. Crispr 101: A desktop resource. Created and Compiled by Addgene (2nd Edition), May 2017.

[113] David Mittelman and John H. Wilson. The fractured genome of hela cells. *Genome biology*, 14:111, Apr 2013.

[114] Atsushi Satomura, Ryosuke Nishioka, Hitoshi Mori, Kosuke Sato, Kouichi Kuroda, and Mitsuyoshi Ueda. Precise genome-wide base editing by the crispr nickase system in yeast. *Scientific Reports*, 7(1):2095, May 2017.

[115] Christine Mayr and David P. Bartel. Widespread shortening of 3'utrs by alternative cleavage and polyadenylation activates oncogenes in cancer cells. *Cell*, 138:673–84, Aug 2009.

[116] Christine Mayr. Evolution and biological roles of alternative 3'utrs. *Trends in cell biology*, 26:227–237, Mar 2016.

[117] J. Yu, S. Nagarajan, J. J. Knez, S. Udenfriend, R. Chen, and M. E. Medof. The affected gene underlying the class k glycosylphosphatidylinositol (gpi) surface protein defect codes for the gpi transamidase. *Proceedings of the National Academy of Sciences of the United States of America*, 94:12580–5, Nov 1997.

[118] K. Ohishi, N. Inoue, and T. Kinoshita. Pig-s and pig-t, essential for gpi anchor attachment to proteins, form a complex with gaa1 and gpi8. *The EMBO journal*, 20:4088–98, Aug 2001.

[119] Arianna Rath, Mira Glibowicka, Vincent G. Nadeau, Gong Chen, and Charles M. Deber. Detergent binding explains anomalous sds-page migration of membrane proteins. *Proceedings of the National Academy of Sciences of the United States of America*, 106:1760–5, Feb 2009.

[120] Richard M. Epand. Cholesterol and the interaction of proteins with membrane domains. *Progress in lipid research*, 45:279–94, Jul 2006.

[121] Jonathan J. Hulce, Armand B. Cognetta, Micah J. Niphakis, Sarah E. Tully, and Benjamin F. Cravatt. Proteome-wide mapping of cholesterol-interacting proteins in mammalian cells. *Nature methods*, 10:259–64, Mar 2013.

[122] Birgit Eisenhaber, Swati Sinha, Wing-Cheong Wong, and Frank Eisenhaber. Function of a membrane-embedded domain evolutionarily multiplied in the gpi lipid anchor pathway proteins pig-b, pig-m, pig-u, pig-w, pig-v, and pig-z. *Cell cycle (Georgetown, Tex.)*, 17:874–880, 2018.

[123] E. Wang, W. P. Norred, C. W. Bacon, R. T. Riley, and A. H. Jr Merrill. Inhibition of sphingolipid biosynthesis by fumonisins. implications for diseases associated with fusarium moniliforme. *The Journal of biological chemistry*, 266:14486–90, Aug 1991.

[124] A. H. Jr Merrill, G. van Echten, E. Wang, and K. Sandhoff. Fumonisin b1 inhibits sphingosine (sphinganine) n-acyltransferase and de novo sphingolipid biosynthesis in cultured neurons in situ. *The Journal of biological chemistry*, 268:27299–306, Dec 1993.

[125] Daniela Ostkotte. Lipidomic characterization of ceramide synthase kockout cells and identification of very-long chain sphingolipid interacting proteins. Master's thesis, Faculty of bioscience, Ruprecht-Kalrs-Universität Heidelberg, 2016.

[126] Michal Levy and Anthony H. Futerman. Mammalian ceramide synthases. *IUBMB life*, 62:347–56, May 2010.

[127] Sujoy Lahiri, Hyejung Park, Elad L. Laviad, Xuequan Lu, Robert Bittman, and Anthony H. Futerman. Ceramide synthesis is modulated by the sphingosine analog fty720 via a mixture of uncompetitive and noncompetitive inhibition in an acyl-coa chain length-dependent manner. *The Journal of biological chemistry*, 284:16090–8, Jun 2009.

[128] Marimuthu Subathra, Asfia Qureshi, and Chiara Luberto. Sphingomyelin synthases regulate protein trafficking and secretion. *PloS one*, 6:e23644, 2011.

[129] Qiang Dai, Jihua Liu, Jun Chen, David Durrant, Thomas M. McIntyre, and Ray M. Lee. Mitochondrial ceramide increases in uv-irradiated hela cells and is mainly derived from hydrolysis of sphingomyelin. *Oncogene*, 23:3650–8, Apr 2004.

[130] Klazien Huitema, Joep van den Dikkenberg, Jos F. H. M. Brouwers, and Joost C. M. Holthuis. Identification of a family of animal sphingomyelin synthases. *The EMBO journal*, 23:33–44, Jan 2004.

[131] C. Luberto and Y. A. Hannun. Sphingomyelin synthase, a potential regulator of intracellular levels of ceramide and diacylglycerol during sv40 transformation. does sphingomyelin synthase account for the putative phosphatidylcholine-specific phospholipase c? *The Journal of biological chemistry*, 273:14550–9, Jun 1998.

[132] C. Luberto, D. S. Yoo, H. S. Suidan, G. M. Bartoli, and Y. A. Hannun. Differential effects of sphingomyelin hydrolysis and resynthesis on the activation of nf-kappa b in normal and sv40-transformed human fibroblasts. *The Journal of biological chemistry*, 275:14760–6, May 2000.

[133] Jerry E. Chipuk, Gavin P. McStay, Archana Bharti, Tomomi Kuwana, Christopher J. Clarke, Leah J. Siskind, Lina M. Obeid, and Douglas R. Green. Sphingolipid metabolism cooperates with bak and bax to promote the mitochondrial pathway of apoptosis. *Cell*, 148:988–1000, Mar 2012.

[134] Yongqiang Deng, Felix E. Rivera-Molina, Derek K. Toomre, and Christopher G. Burd. Sphingomyelin is sorted at the trans golgi network into a distinct class of secretory vesicle. *Proceedings of the National Academy of Sciences of the United States of America*, 113:6677–82, Jun 2016.

[135] Min Park, Vincent Kaddai, Jianhong Ching, Kevin T. Fridianto, Ryan J. Sieli, Shigeki Sugii, and Scott A. Summers. A role for ceramides, but not sphingomyelins, as antagonists of insulin signaling and mitochondrial metabolism in c2c12 myotubes. *The Journal of biological chemistry*, 291:23978–23988, Nov 2016.

[136] Rao Muralikrishna Adibhatla, J. F. Hatcher, and A. Gusain. Tricyclodecan-9-yl-xanthogenate (d609) mechanism of actions: a mini-review of literature. *Neurochemical research*, 37:671–9, Apr 2012.

[137] T. Yabu, H. Shiba, Y. Shibasaki, T. Nakanishi, S. Imamura, K. Touhata, and M. Yamashita. Stress-induced ceramide generation and apoptosis via the phosphorylation and activation of nsmase1 by jnk signaling. *Cell death and differentiation*, 22:258–73, Feb 2015.

[138] Thomas D. Mullen and Lina M. Obeid. Ceramide and apoptosis: exploring the enigmatic connections between sphingolipid metabolism and programmed cell death. *Anti-cancer agents in medicinal chemistry*, 12:340–63, May 2012.

[139] Xiong Liu, Xueping Yu, Donald J. Zack, Heng Zhu, and Jiang Qian. Tiger: a database for tissue-specific gene expression and regulation. *BMC bioinformatics*, 9:271, Jun 2008.

8 Appendix

8.1 Sequences: GPAA1 genomic context

Genomic sequence of GPAA1 including exons, introns, start/stop codons and 3'UTR

>8 dna:chromosome chromosome:GRCh38:8:144082610:144086216:1 GTCTCTGGGACCGGAAGTGCGGGCGAG
CGCGGGTCCCCGGGTCTGACAGGAGCAGCCTGTGGGCACCGCGGCGGTAGTTGGAGGCGGGAGAGGGTCCGTAGCC
GCGCCGCCCTGCCCCGCC ATG GGCCTCCTGTCGGACCCGGTTCGCCGGCGCGCGCTCGCCCGCCTAGTGCTGCGCCT-
CAACGCGCCGTTGTG GTGAGGACAGGGCCCGGGGAGGCGGGGACCCGAGGGCCCTGGGCTCGCGCCGGCGGCCCCA
TGCGCGGTCCCCATCGAGGGCCGGGGCCGCTCCAGCTGCTCGCGCCCCTCCGGCTGCTCGCGCCCTTCCGCTCCTGCC
CTCTGGAAGCACTGAGGGTATCAGGCCCAGGCTTAGGGCTCGGGTCCGGCGTCCCGATGCAGGACTCCGGGTTTAG
GTCTCCCAGACCCGCGCGATCGACCCCGGGTGCGGAGGTTGTGGCCTCGGGTCGGCGTCTGAGGACCCGCTGACGCT
CCGGTGCCCCTCCGTCCTCTCTCACAG CGTGCTGAGCTACGTGGCGGGCATCGCCTGGTTCTTGGCGCTGGTTTTCC
CGCCGCTGACCCAGCGCACTTACATGTCGGAGAACGCCATGGGCTCCACCATGGTGGAGGAGCAGTTTGCGGGCGG
AGACCGTGCCCGGGCTTTTGCCCGGGACTTCGCCGCCCACCGCAAGAAGTCGGG GTGAGCGGCAGAGCAGGGCGTA
TGGGGCGAGCAGTGGTGGCTAAGGCCGGGGAGCTCTGCTCAGAGGCTCCCTTCGTGTCTGCAG GGCTCTGCCAGTG
GCCTGGCTTGAACGGACGATGCGGTCAGTAGGGCTGGAGGTCTACACGCAGAGTTTCTCCCGGAAACTGCCCTTCCC
AGATGAGACCCACGAGCGCTAT GTACTGGGGGAGTGGGGTGTGCCTGGGCCCAGAAAGCACCTTGGAGGGAGGGG
TCTGGGCTGGGTATCACCTTGCGGGGGTGTCATGGGGCCAGGAAGCTCAGTGGGAGGGAAATCCCTGGTGGGCACT
GGAGGGCTAGGAAAGTTGTGGGGGGCCCTTCAGCCCCCTACCACAAAGTTACACTGAGGCTCCCCCCACCGATGCTG
CATACAG ATGGTGTCGGGCACCAACGTGTACGGCATCCTGCGGGCCCCGCGTGCTGCCAGCACCGAGTCGCTTGTG
CTCACCGTGCCCTGTGGCTCTGACTCTACCAACAGCCAGGCTGTGGGGCTGCTGCTGGCACTGGCTGCCCACTTCCG
GG GTGAGTCTCAGGGCTGCTGGCCGTGGAGGGGTTTGGTCAGTGCCCCAGACCCTGCTGATCCTGCTTCTGGCCTCC
AG GGCAGATTTATTGGGCCAAAGATATCGTCTTCCTGGTAACAGAACATGACCTTCTGGGCACTGAGGCTTGGCTT
GAAGCCTACCACGATGTCAATGTCACTG GTAGGTTCTCTTGTCCTGCCTGCCCTGGTCCCCCTCTCAGGGTCACTGT
CCTCACCACGTCCTCCATTAGCACTCATTCACTTGCTCCTACAG GCATGCAGTCGTCTCCCCTGCAGGGCCGAGCTG
GGGCCATTCAGGCAGCCGTGGCCCTGGAGCTGAGCAGTGATGTGGTCACCAGCCTCGATGTGGCCGTGGAGGGGCT
TAACGGGCAGCTGCCCAACCTTGACCTGCTCAATCTCTTCCAGACCTTCTGCCAGAAAGGGGGCCTGTTGTGCACGC
TTCAGGGCAAG GTGGGGCTGCCTGCCTGCCTGAGGGCTGAAGGGCACAGGGTCTGTGGGAGGGGCTGTCTCATCCT
GTCCTGCACCTCTAAAG CTGCAGCCCGAGGACTGGACATCATTGGATGGACCGCTGCAGGGCCTGCAGACACTGCT
GCTCATGGTTCTGCGGCAGGCCTCCGGCCGCCCCCACGGCTCCCATGGCCTCTTCCTGCGCTACCGTGTGGAGGCCCT
AACCCTGCGTGGCATCAATAGCTTCCGCCAGTACAAGTATGACCTGGTGGCAGTGGGCAA GTAAGTAGTCTCTGGT
CCCCCCTTTCCATGCCCAGGATGGGGTCTAGCTGGAGCGGAGTGGGGGATGGCCTGGTGGCTCTGGCCAGCCGTGAA
CCTGCCCCACACCTGACAG GGCTTTGGAGGGCATGTTCCGCAAGCTCAACCACCTCCTGGAGCGCCTGCACCAGTCC
TTCTTCCTCTACTTGCTCCCCGGCCTCTCCCGCTTCGTCTCCATCGGCCTCTACATGCCCGCTGTCGGCTTCTTGCTC
CTGGTCCTTGGTCTCAAG ATATCCTCTGCCCCTTGCCATCTACCTGTGACCAGCCTCCAGTCTCCTCAACTCTAGGC
TGGGGAGAGTCTTCCATCCTGATGGGGGGTGGGGTACGGGGGTGAGCCCTGGGTCCCCCTCTGGGCAGATCCCGTTA
CACCTCTTGTTGGGGTCCTTGATTGGGCTAC GCTCTGGAACTGTGGATGCAGCTGCATGAGGCTGGAATGGGCCTT
GAGGAGCCCGGGGGTGCCCCTGGCCCCAGTGTACCCCTTCCCCCATCACAG GTGATGGCACCCCCTTCTGTTGTTGG
AATGGGCTTCTGGGGTCTGACTGGTGTTTAGTGTTGCAACTTAGCCTCAGCTGGTGGGATGGTGGTGGTCTTTGGG
GATCCCCTGGCCCCAGGGTCCATCTCCAAGAGCCTGTGTGCCCTGCAG GGTGTGGGGCTGGCCTCGCTCGTGGCACC
TCTGCTGATCTCACAGGCCATGGGACTGGCCCTCTATGTCCTGCCAGTGCTGGGCCAACACGTTGCCACCCAGCACT
TCCCAGTGGCAGAGGCTGAGGCTGTGGTGCTGACACTGCTGGCGATTTATGCAGCTGGCCTGGCCCTGCCCCACAAT
ACCCACCG GTAAGAGGCTGGGCTGGTTGTTGGGGGCAGGGGTAGAGGTCCCCTGGACATGCAGACAGCTTGTGGGT
TGCCTCTGAGTCCTTTGTCTTACAG GGTGGTAAGCACACAGGCCCCAGACAGGGGCTGGATGGCACTGAAGCTGGT
AGCCCTGATCTACCTAGCACTGCAGCTGGGCTGCATCGCCCTCACCAACTTCTCACTGGGCTTCCTGCTGGCCACCA
CCATGGTGCCCACTGCTGCGCTTGCCAAGCCTCATGGGCCCCG GTATGTATGGATCAGCCCCACTTCCCCCAATGCC
TGTGCCCTCATCACAGACCGCACCCTCATTCAGTAGCCCTTTCCCCCAACCTGGTGCCCATGCCCCCACCATGGAGCC
TACCTTGATGTTGCTTCTCCACCCAG GACCCTCTATGCTGCCCTGCTGGTGCTGACCAGCCCGGCAGCCACGCTCCT

TGGCAGCCTGTTCCTGTGGCGGGAGCTGCAGGAGGCGCCACTGTCACTGGCCGAGGGCTGGCAGCTCTTCCTGGCAG
CGCTAGCCCAGGGTGTGCTGGAGCACCACACCTACGGCGCCCTGCTCTTCCCACTGCTGTCCCTGGGCCTCTACCCCT
GCTGGCTGCTTTTCTGGAATGTGCTCTTCTGGAAG TGA GATCTGCCTGTCCGGGCTGGGACAGAGACTCCCCAAGG
ACCCCATTCTGCCTCCTTCTGGGGAAATAAATGAGTGTCTGTTTCAGCAGCTA

8.2 GPAA1 RNA expression in different tissues

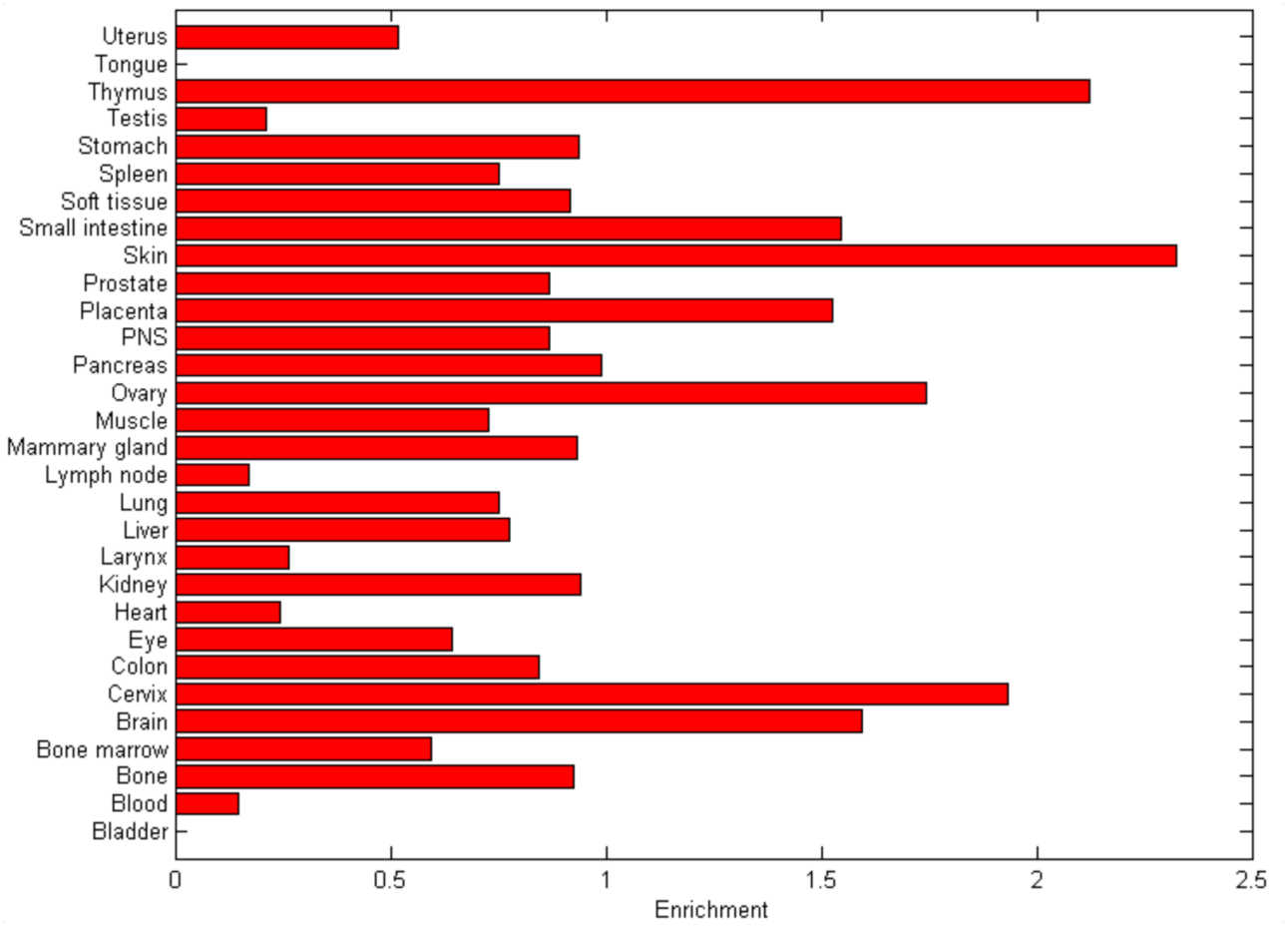

Figure 29: Overview of GPAA1 in the tissue-specific gene expression and regulation (TiGER) database TiGER is a database developed by the Bioinformatics Lab at Wilmer Eye Institute of Johns Hopkins University. The database contains tissue-specific gene expression profiles or expressed sequence tag (EST) data, cis-regulatory module (CRM) data, and combinatorial gene regulation data. Legend adapted from http://bioinfo.wilmer.jhu.edu/tiger/. Last publication for this database is from the year 2008[139].

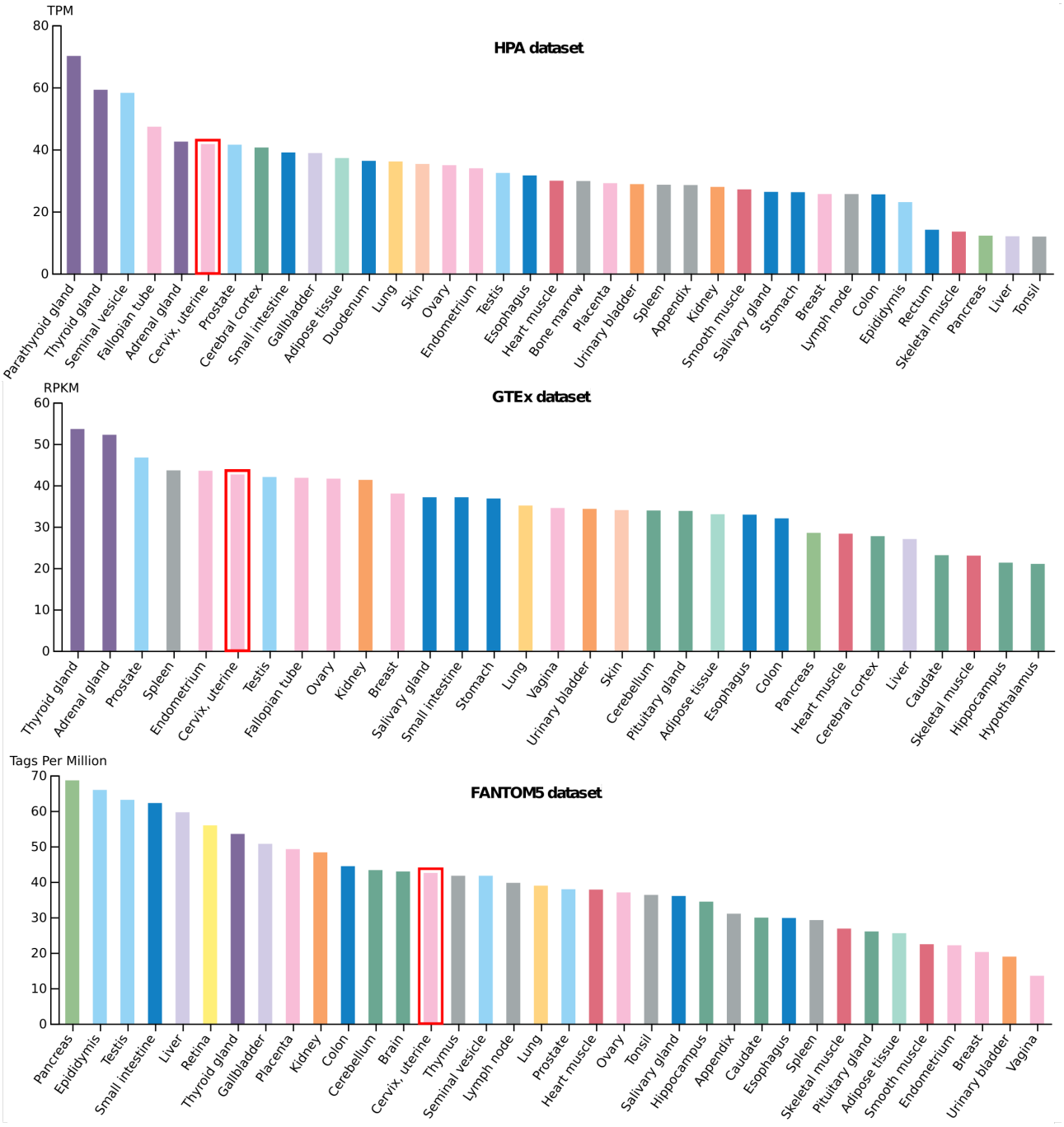

Figure 30: Tissue specific RNA expression overview of the Human Protein Atlas Project RNA expression overview shows RNA-data from three different sources: Human Protein Atlas (HPA) RNA-seq data (https://www.proteinatlas.org/), RNA-seq data from the Genotype-Tissue Expression project (http://www.gtexportal.org/) and data from the Cap Analysis of Gene Expression project FANTOM5 (http://fantom.gsc.riken.jp/5/). TPM= transcripts per million, RPKM= reads per kilobase per million mapped reads. Figure and figure legend adapted from HPA.

8.3 gRNA Design

guide #1 quality score: 80

guide sequence: TGAGATCTGCCTGTCCGGGC **TGG**
on-target locus: chr8:+145141025
number of offtarget sites: 146 (27 are in genes)

top 20 genome-wide off-target sites — show all exonic

sequence	score	mismatches	UCSC gene	locus
CGAGGGCTGCCGGTCCGGGCAGG	0.4	4MMs [1:5:6:12]	NM_014918	chr15:-101791500
TGTCATCTCCCAGTCCGGGCAAG	0.4	4MMs [3:4:9:12]	NM_003344	chr7:-129592367
TGAGATGAGTCTGTCCGGGACAG	0.4	4MMs [7:8:10:20]	NM_001145023	chr17:+45915384
TGAGGTCTGCCTGTCCCGCCAGG	0.4	3MMs [5:17:19]	NM_020795	chr17:+7318251
AGGGATCTACCTGTCCAGGCCAG	0.4	4MMs [1:3:9:17]	NM_153021	chr2:+28800970
AGAGATCTGAGTGTCCGGGTAGG	0.4	4MMs [1:10:11:20]	NR_073461	chr17:+37826775
GGAGAACTGGCTCTCCGGGCTAG	0.3	4MMs [1:6:10:13]	NM_207360	chr6:+149772204
CGAGGTCTGCGTGTCCGGTCTGG	0.3	4MMs [1:5:11:19]	NM_001198551	chr11:-32452268
TGACCTCTGCCTGTCCTGGTGAG	0.3	4MMs [4:5:17:20]	NM_001038618	chr17:+80430555
TCAGTGCTGCCTGTGCGGGCGAG	0.2	4MMs [2:5:6:15]	NR_038865	chr19:+3611351
TGAGATCCGGGTGTGCGGGCTGG	0.2	4MMs [8:10:11:15]	NM_174869	chrX:-153053501
GGAGATGTGCCTGTCCAGGACAG	0.2	4MMs [1:7:17:20]	NM_001080824	chr2:+85049174
CGAGACCTGCCCCTCCGGGCTGG	0.2	4MMs [1:6:12:13]	NM_016333	chr16:-2812349
ACAGATCTGCCTGGCCAGGCAGG	0.1	4MMs [1:2:14:17]	NM_138578	chr20:+30252710
TGAGCTCCGCCTGCCCTGGCCAG	0.1	4MMs [5:8:14:17]	NM_148960	chr1:-43201514
TGAGATGCCCCTGCCCGGGCTGG	0.1	4MMs [7:8:9:14]	NM_018306	chr3:+12776090
TGAGCTCTGACTGCCCCGGCCAG	0.1	4MMs [5:10:14:17]	NM_022572	chr2:+219204621
TGAGATGAGCCTCTCAGGGCAGG	0.1	4MMs [7:8:13:16]	NM_003953	chr1:+167759690
TGAGCTCTGCACGGCCGGGCCGG	0.1	4MMs [5:11:12:14]	NM_004218	chr19:+8468552
TGAGCTCTGCCGGTCCCAGCAGG	0.1	4MMs [5:12:17:18]	NM_153278	chr11:-62748567
TGAGATCGGCACGGCCGGGCAAG	0.1	4MMs [8:11:12:14]	NM_017617	chr9:+139393828
TGAAAACTGCCTGTCTGGCCGGG	0.1	4MMs [4:6:16:19]	NM_031475	chr1:+6520751
TGAGACTTGCCGGTCTGGGCAGG	0.1	4MMs [6:7:12:16]	NM_001122671	chr9:-131597727
TGAGCTCTGCCTGCCCTGCCAGG	0.0	4MMs [5:14:17:19]	NR_046317	chr20:+61976923
TGAGTTCTGCCTGGCGGGGAAGG	0.0	4MMs [5:14:16:20]	NM_001139457	chrX:-152989124
TGAGATCGGCCTGACCTTGCAGG	0.0	4MMs [8:14:17:18]	NR_026709	chr19:-7827965

Figure 31: Detailed results for gRNA#1, Results derived from the gRNA prediction tool CRISPR Design (http://crispr.mit.edu/) from the Zhang lab (MIT, USA) for the c-terminal part of GPAA1 exon 12 in its genomic context. For the full sequence of the genomic context, see appendix 8.1. Overview of the results are displayed in figure 17.

guide #2 quality score: 76

guide sequence: GAGATCTGCCTGTCCGGGCT GGG
on-target locus: chr8:+145141026
number of offtarget sites: 162 (27 are in genes)

top 20 genome-wide off-target sites ☑ show all exonic

sequence	score	mismatches	UCSC gene	locus
GAGAACTGGCTCTCCGGGCTAGG	0.8	3MMs [5:9:12]	NM_207360	chr6:+149772205
GCGCGCTGCCTGGCCGGGCTTGG	0.6	4MMs [2:4:5:13]	NM_024426	chr11:-32457177
GAGGTCTGCGTGTCCGGTCTGGG	0.6	3MMs [4:10:18]	NM_001198551	chr11:-32452267
GCCACCTGCCTGCCCGGGCTTGG	0.6	4MMs [2:3:5:13]	NM_005886	chr16:+57789452
GAGCCCTCCCTGCCCGGGCTGAG	0.6	4MMs [4:5:8:13]	NM_022553	chr6:-33218670
CAGGTCGGCCGGTCCGGGCTGGG	0.6	4MMs [1:4:7:11]	NM_001174164	chr7:-128001335
GTGCTCTTCCTGTCCGGGGTTGG	0.5	4MMs [2:4:8:19]	NM_025109	chr17:-34866514
GAGAGCTCACAGTCCGGGCTAAG	0.5	4MMs [5:8:9:11]	NM_001009991	chr6:+159181707
GGGTTCTGCCTGGCCGAGCTCAG	0.2	4MMs [2:4:13:17]	NM_012116	chr19:-45293297
GAGGTCGGCCAGTCCGGGGTCGG	0.2	4MMs [4:7:11:19]	NM_031485	chr19:-48956123
GAGACCAGCCTGCCCGGGCCTGG	0.2	4MMs [5:7:13:20]	NM_001025100	chr18:-74844596
GATATCAGCCTCTCCGGGATGGG	0.2	4MMs [3:7:12:19]	NM_030957	chr19:+8657076
GAGTGCTGCCTGGCTGGGCTTGG	0.2	4MMs [4:5:13:15]	NM_004646	chr19:+36332995
GGGATCTACCTGTCCAGGCCAGG	0.1	4MMs [2:8:16:20]	NM_153021	chr2:+28800971
GGGATCTGCACGTGCGGGCTGAG	0.1	4MMs [2:10:11:14]	NM_144997	chr17:+17119712
GAGATCTGAGTGTCCGGGTAGGG	0.1	4MMs [9:10:19:20]	NR_073461	chr17:+37826776
GAGTTCTCCCTGTGCGTGCTCGG	0.1	4MMs [4:8:14:17]	NR_026887	chr19:-33794477
GAGATCCGGGTGTGCGGGCTGGG	0.1	4MMs [7:9:10:14]	NM_174869	chrX:-153053500
GAGACCTGCCTCCCAGGGCTGGG	0.1	4MMs [5:12:13:15]	NM_080869	chr20:-43752715
GAGGCCTGCCTGTTCTGGCTGGG	0.0	4MMs [4:5:14:16]	NM_001005914	chr3:+50307999
GAGATCAGCCTGTCTGCGGTGAG	0.0	4MMs [7:15:17:19]	NM_004560	chr9:-94487350
GAGATCAGCCAGTCAGGCCTTGG	0.0	4MMs [7:11:15:18]	NM_000029	chr1:-230845656
CAGATGTGCCTGTGCGGCCTCAG	0.0	4MMs [1:6:14:18]	NM_001001851	chr10:-7618739
GAGTTCTGCCTGTGTGTGCTGGG	0.0	4MMs [4:14:15:17]	NM_001010867	chr1:+228363915
GAGGTCTGCCTGTCCCGCCAGGG	0.0	4MMs [4:16:18:20]	NM_020795	chr17:+7318252
GAGATGTGCCTGTCCAGGACAGG	0.0	4MMs [6:16:19:20]	NM_001080824	chr2:+85049175

Figure 32: Detailed results for gRNA#2, Results derived from the gRNA prediction tool CRISPR Design (http://crispr.mit.edu/) from the Zhang lab (MIT, USA) for the c-terminal part of GPAA1 exon 12 in its genomic context. For the full sequence of the genomic context, see appendix 8.1. Overview of the results are displayed in figure 17.

guide #3 quality score: 47

guide sequence: ATTCCAGAAAAGCAGCCAGC AGG
on-target locus: chr8:-145140987
number of offtarget sites: 392 (23 are in genes)

top 20 genome-wide off-target sites ☑ show all exonic

sequence	score	mismatches	UCSC gene	locus
ATTCCAGTCGAGCAGCCAGCAGG	1.3	3MMs [8:9:10]	NM_144666	chr11:-6566271
GTTTCAGAACAGCAGCCAGTGGG	0.7	4MMs [1:4:10:20]	NM_005184	chr19:-47113051
AACCCAGAACAGCAGCCAGATGG	0.6	4MMs [2:3:10:20]	NM_152286	chr9:+140444905
TTTCAAAACAAGCAGCCAGCTGG	0.6	4MMs [1:5:7:9]	NM_022569	chr4:+116034819
AATCCATTAAAGCAGCCAGGAAG	0.5	4MMs [2:7:8:20]	NM_001018111	chr7:-131187953
AATTCAGAGAAGCAGCCAGAAGG	0.4	4MMs [2:4:9:20]	NM_015058	chr13:-42142151
ATTACAGAATCACAGCCAGCCAG	0.4	4MMs [4:10:11:12]	NR_047655	chr2:+97272802
ATGCAAGAAAAGCAGCAAGGGAG	0.3	4MMs [3:5:17:20]	NM_001159597	chr2:-231033
CTTCCAGGATAGCAGTCAGCCAG	0.3	4MMs [1:8:10:16]	NM_001258310	chr12:-6666546
AGTCCAGAAGAGGAGCCAGAAGG	0.2	4MMs [2:10:13:20]	NM_006825	chr12:-106633813
TTTACAGAAACGCATCCAGCAAG	0.2	4MMs [1:4:11:15]	NM_005228	chr7:+55273519
AGTCCAGGAAAGCAGCCACACAG	0.2	4MMs [2:8:19:20]	NR_027300	chr19:-10157135
ATCCGGGAAAAGCAGCCGGCTGG	0.2	4MMs [3:5:6:18]	NR_015441	chr16:-2653312
ATTCAAAAAATGCAACCAGCAGG	0.1	4MMs [5:7:11:15]	NM_030955	chr5:-33534951
ACTCCAGAACAGCAGAAAGCGGG	0.1	4MMs [2:10:16:17]	NM_001135190	chr11:-72396299
ATACAAGAAAAGCATTCAGCTAG	0.1	4MMs [3:5:15:16]	NR_072984	chr10:-81852300
ATACAAGAAAAGCATTCAGCTAG	0.1	4MMs [3:5:15:16]	NR_036537	chr2:+130724143
ATTCCGGAACAGCAGGTAGCAAG	0.1	4MMs [6:10:16:17]	NM_001004128	chr1:-180151404
GTTCCAGAAAAACCTCCAGCAGG	0.0	4MMs [1:12:14:15]	NM_018190	chr4:-122754444
ATTCCAGAGAAGTATCCAACAGG	0.0	4MMs [9:13:15:19]	NM_005074	chr6:+25820038
ATTCCACAAAAGAAGCCTTCAGG	0.0	4MMs [7:13:18:19]	NM_020854	chr18:-59941288
ATTCCAGAAAGGCAGGAATCAAG	0.0	4MMs [11:16:17:19]	NM_207398	chr1:+89614926

Figure 33: Detailed results for gRNA#3, Results derived from the gRNA prediction tool CRISPR Design (http://crispr.mit.edu/) from the Zhang lab (MIT, USA) for the c-terminal part of GPAA1 exon 12 in its genomic context. For the full sequence of the genomic context, see appendix 8.1. Overview of the results are displayed in figure 17.

8.4 Sequences: Homology Arms

Left Homology Arm: poly(A) for restriction enzyme binding 5'-NdeI/3'-NgoMIV
AAAAAAAACATATGCACGTTGCCACCCAGCACTTCCCAGTGGCAGAGGCTGAGGCTGTGGTGCTGACACTGCTGGC
GATTTATGCAGCTGGCCTGGCCCTGCCCCACAATACCCACCGGTAAGAGGCTGGGCTGGTTGTTGGGGGCAGGGGT
AGAGGTCCCCTGGACATGCAGACAGCTTGTGGGTTGCCTCTGAGTCCTTTGTCTTACAGGGTGGTAAGCACACAGG
CCCCAGACAGGGGCTGGATGGCACTGAAGCTGGTAGCCCTGATCTACCTAGCACTGCAGCTGGGCTGCATCGCCCT
CACCAACTTCTCACTGGGCTTCCTGCTGGCCACCACCATGGTGCCCACTGCTGCGCTTGCCAAGCCTCATGGGCCCC
GGTATGTATGGATCAGCCCCACTTCCCCCAATGCCTGTGCCCTCATCACAGACCGCACCCTCATTCAGTAGCCCTTT
CCCCCAACCTGGTGCCCATGCCCCCACCATGGAGCCTACCTTGATGTTGCTTCTCCACCCAGGACCCTCTATGCTGC
CCTGCTGGTGCTGACCAGCCCGGCAGCCACGCTCCTTGGCAGCCTGTTCCTGTGGCGGGAGCTGCAGGAGGCGCCAC
TGTCACTGGCCGAGGGCTGGCAGCTCTTCCTGGCAGCGCTAGCCCAGGGTGTGCTGGAGCACCACACCTACGGCGCC
CTGCTCTTCCCACTGCTGTCCCTGGGCCTCTACCCCTGCTGGCTGCTTTTCTGGAATGTGCTCTTCTGGAAGGGATC
CGCCGGCAAAAAAAA

Right Homology Arm: poly(A) for restriction enzyme binding 5'-BstBI/3'-EcoRI necessary for in frame insertion of thr strep tag and second STOP codon
TTCGAAAAGTGATAAGATCTGCCTGTCCGGGCTGGGACAGAGACTCCCCAAGGACCCCATTCTGCCTCCTTCTGGGG
AAATAAATGAGTGTCTGTTTCAGCAGCTATTTGAGCTCCTGGCCCGCTGTCCGTGTAGGGCCCCAGGGCATGGGGG
TGAGAAGCCTCTGTCTGCAGGGCTTGGCATTCCTCACACCTCCTCCCTGGCAAGGGCTGCTGTAGTCCACTTACTGG
GTAGCATTCCTGCCGACCAGGGCTCTGCTGCTGCATCAGGTGCACTCTCAGCCCTGGCGGGTGCCATGCAGGCTCAG
AGGGCTGTGTGCATTGCTCTGTGGTACTGTGCCAGGAGCGGTGCTGGGAAGGAGAATACACCATAGCCATGGTTTG
AGGGCCTGCCAGGAGCTGAGGCACCCAGAAACCACCTAACACCATCTTTACTGCTAGGACTGAGGCTGGAGCTGGA
GCCCTGCAGAGGAGGCCCAGGGTGCATGGCATGGGGCCCAGGCAAGGCCATCGCCTTGGTGTGGGATTGGGATGGA
GCAGGGAGGAGCACCCGGCCTGGCTTCCTCAGAGTTGAGTCAGCCCAGGTGAGATGCCCACGAGGGGCTGGGCAGG
CAACACAGTGGAGCCAGGACCCAGGGGCAGGCGGGGCACGGGGACAAGAGCCCCACGGGAGAGGGCACTGACAGGC
CAGCAAGGAGAGAAGCAGGCTGTTATACTAGGACTCTGAAAGGAACTGGGAAGACCACTGTCTGTTCCAAAAGAA
AGGAAAAACCTGTGGCCTTTAGGGAATTCAAAAAAAA

8.5 Sequences: Transamidase subunits UniProt

Sequences were retrieved July 2018

>sp|Q92643|PIGK_HUMAN GPI-anchor transamidase OS=Homo sapiens GN=PIGK PE=1 SV=2 MAVTDS
LSRAATVLATVLLLSFGSVAASHIEDQAEQFFRSGHTNNWAVLVCTSRFWFNYRHVANTLSVYRSVKRLGIPDSHIV
LMLADDMACNPRNPKPATVFSHKNMELNVYGDDVEVDYRSYEVTVENFLRVLTGRIPPSTPRSKRLLSDDRSNILIY
MTGHGGNGFLKFQDSEEITNIELADAFEQMWQKRRYNELLFIIDTCQGASMYERFYSPNIMALASSQVGEDSLSHQPD
PAIGVHLMDRYTFYVLEFLEEINPASQTNMNDLFQVCPKSLCVSTPGHRTDLFQRDPKNVLITDFFGSVRKVEITTETI
KLQQDSEIMESSYKEDQMDEKLMEPLKYAEQLPVAQIIHQKPKLKDWHPPGGFILGLWALIIMVFFKTYGIKHMKFIF

>sp|Q96S52|PIGS_HUMAN GPI transamidase component PIG-S OS=Homo sapiens GN=PIGS PE=1 SV=3
MAAAGAAATHLEVARGKRAALFFAAVAIVLGLPLWWKTTETYRASLPYSQISGLNALQLRLMVPVTVVFTRESVPL
DDQEKLPFTVVHEREIPLKYKMKIKCRFQKAYRRALDHEEEALSSGSVQEAEAMLDEPQEQAEGSLTVYVISEHSSLLP
QDMMSYIGPKRTAVVRGIMHREAFNIIGRRIVQVAQAMSLTEDVLAAALADHLPEDKWSAEKRRPLKSSLGYEITFSL
LNPDPKSHDVYWDIEGAVRRYVQPFLNALGAAGNFSVDSQILYYAMLGVNPRFDSASSSYYLDMHSLPHVINPVESR
LGSSAASLYPVLNFLLYVPELAHSPLYIQDKDGAPVATNAFHSPRWGGIMVYNVDSKTYNASVLPVRVEVDMVRV
MEVFLAQLRLLFGIAQPQLPPKCLLSGPTSEGLMTWELDRLLWARSVENLATATTTLTSLAQLLGKISNIVIKDDVASE
VYKAVAAVQKSAEELASGHLASAFVASQEAVTSSELAFFDPSLLHLLYFPDDQKFAIYIPLFLPMAVPILLSLVKIFLET
RKSWRKPEKTD

>sp|Q969N2|PIGT_HUMAN GPI transamidase component PIG-T OS=Homo sapiens GN=PIGT PE=1 SV=1
MAAAMPLALLVLLLLGPGGWCLAEPPRDSLREELVITPLPSGDVAATFQFRTRWDSELQREGVSHYRLFPKALGQLIS
KYSLRELHLSFTQGFWRTRYWGPPFLQAPSGAELWVWFQDTVTDVDKSWKELSNVLSGIFCASLNFIDSTNTVTPTA
SFKPLGLANDTDHYFLRYAVLPREVVCTENLTPWKKLLPCSSKAGLSVLLKADRLFHTSYHSQAVHIRPVCRNARCTS
ISWELRQTLSVVFDAFITGQGKKDWSLFRMFSRTLTEPCPLASESRVYVDITTYNQDNETLEVHPPPTTTYQDVILGT
RKTYAIYDLLDTAMINNSRNLNIQLKWKRPPENEAPPVPFLHAQRYVSGYGLQKGELSTLLYNTHPYRAFPVLLLDTV
PWYLRLYVHTLTITSKGKENKPSYIHYQPAQDRLQPHLLEMLIQLPANSVTKVSIQFERALLKWTEYTPDPNHGFYVS
PSVLSALVPSMVAAKPVDWEESPLFNSLFPVSDGSNYFVRLYTEPLLVNLPTPDFSMPYNVICLTCTVVAVCYGSFY
NLLTRTFHIEEPRTGGLAKRLANLIRRARGVPPL

>sp|Q9H490|PIGU_HUMAN Phosphatidylinositol glycan anchor biosynthesis class U protein OS=Homo sapiens GN=PIGU PE=1 SV=3 MAAPLVLVLVVAVTVRAALFRSSLAEFISERVEVVSPLSSWKRVVEG
LSLLDLGVSPYSGAVFHETPLIIYLFHFLIDYAELVFMITDALTAIALYFAIQDFNKVVFKKQKLLLELDQYAPDVAELIR
TPMEMRYIPLKVALFYLLNPYTILSCVAKSTCAINNTLIAFFILTTIKGSAFLSAIFLALATYQSLYPLTLFVPGLLYLLQR
QYIPVKMKSKAFWIFSWEYAMMYVGSLVVIICLSFFLLSSWDFIPAVYGFILSVPDLTPNIGLFWYFFAEMFEHFSLFF
VCVFQINVFFYTIPLAIKLKEHPIFFMFIQIAVIAIFKSYPTVGDVALYMAFFPVWNHLYRFLRNIFVLTCIIIVCSLLFPV
LWHLWIYAGSANSNFFYAITLTFNVGQILLISDYFYAFLRREYYLTHGLYLTAKDGTEAMLVLK

>sp|O43292|GPAA1_HUMAN Glycosylphosphatidylinositol anchor attachment 1 protein OS=Homo sapiens GN=GPAA1 PE=1 SV=3 MGLLSDPVRRRALARLVLRLNAPLCVLSYVAGIAWFLALVFPPLTQRTYMSENA
MGSTMVEEQFAGGDRARAFARDFAAHRKKSGALPVAWLERTMRSVGLEVYTQSFSRKLPFPDETHERYMVSGTNV
YGILRAPRAASTESLVLTVPCGSDSTNSQAVGLLLALAAHFRGQIYWAKDIVFLVTEHDLLGTEAWLEAYHDVNVTG
MQSSPLQGRAGAIQAAVALELSSDVVTSLDVAVEGLNGQLPNLDLLNLFQTFCQKGGLLCTLQGKLQPEDWTSLDGPL
QGLQTLLLMVLRQASGRPHGSHGLFLRYRVEALTLRGINSFRQYKYDLVAVGKALEGMFRKLNHLLERLHQSFFLYLL
PGLSRFVSIGLYMPAVGFLLLVLGLKALELWMQLHEAGMGLEEPGGAPGPSVPLPPSQGVGLASLVAPLLISQAMGLA
LYVLPVLGQHVATQHFPVAEAEAVVLTLLAIYAAGLALPHNTHRVVSTQAPDRGWMALKLVALIYLALQLGCIALTN
FSLGFLLATTMVPTAALAKPHGPRTLYAALLVLTSPAATLLGSLFLWRELQEAPLSLAEGWQLFLAALAQGVLEHHTY
GALLFPLLSLGLYPCWLLFWNVLFWK

9 Abbrevations

BZH	Heidelberg University Biochemistry Center
Cas9	CRISPR associated protein 9
Chol	cholesterol
COPI	coatomer protein I
COPII	coatomer protein II
CRISPR	clustered regularly interspaced short palindromic repeats
CuAAC	copper-catalysed azide-alkyne cycloaddition
CNBr	cyanogen bromide
DNA	deoxyribonucleic acid
ER	endoplasmic reticulum
ERES	ER-exit sites
EtNP	ethanolaminephosphate
ERAD	ER-associated degradation
FBS	fetal bovine serum
GlcN	glucosamine
GPAA1	GPI attachment 1 protein
GPI	glycosylphosphatidylinositol
GPI-AP	GPI-anchored protein
GPL	glycerophospholipid
GRAVY	grand average hydropathy
GM3	monosialodihexosylganglioside
IP	immunoprecipitation
LB medium	Luria-Bertani medium
m/z	mass-to-charge ratio
Man	mannose
MPD	mannose-P-dolichol
MSP	membrane scaffold protein
NCBI	national center for biotechnology information
HDR	homology directed repair
NHEJ	non-homologous end joining
NHS	N-hydroxysuccinimide
pac	photoactivatable and clickable
PA	Phosphatidic acid
PBS	phosphate-buffered saline
PC	phosphatidylcholine
PE	phosphatidylethanolamine
PGAP	GPI inositol-deacylase
PS	phosphatidylserine
PI	Phosphatidylinositol
PIG	PI-glycan biosynthesis class protein
RG	research group
(g)RNA	(genomic) ribonucleic acid
RT	room temperature
S1PL	sphingosine-1-phosphate lyase
SDS-PAGE	sodium dodecyl sulfate polyacrylamide gel electrophoresis
SMA	styrene-maleic acid
SMALP	SMA lipid particles
SP	sphingolipids
Sph	sphingosine

ST	sterols
TMD	transmembrane domain
UTR	untranslated region
UV	ultraviolet